

**EXTRACTS FROM THE PRAIRIE PLANT *SYMPHORICARPOS*  
*OCCIDENTALIS* OR THE NATURAL PRODUCT, PHEOPHORBIDE A, INDUCE  
LIGHT-DEPENDENT VACUOLATION OF HUMAN CELLS**

**JAN TUESCHER**  
**Bachelor of Science, University of Lethbridge, 2016**

A Thesis  
Submitted to the School of Graduate Studies  
of the University of Lethbridge  
in Partial Fulfilment of the  
Requirements for the Degree

**MASTER OF SCIENCE**

Department of Biological Sciences  
University of Lethbridge  
LETHBRIDGE, ALBERTA, CANADA

© Jan Tuescher, 2018

EXTRACTS FROM THE PRAIRIE PLANT *SYMPHORICARPOS OCCIDENTALIS* OR  
THE NATURAL PRODUCT, PHEOPHORBIDE A, INDUCE LIGHT DEPENDENT  
VACUOLATION OF HUMAN CELLS

JAN TUESCHER

Date of defence: November 21, 2018

Dr. Roy. Golsteyn Thesis Supervisor	Associate Professor	Ph.D.
--	---------------------	-------

Dr. Nehalkumar Thakor Thesis Examination Committee Member	Assistant Professor	Ph.D.
--	---------------------	-------

Dr. Steven Mosimann Thesis Examination Committee Member	Associate Professor	Ph.D.
--	---------------------	-------

Dr. Locke Spencer External Examiner University of Lethbridge Lethbridge	Associate Professor	Ph.D.
--	---------------------	-------

Dr. Steve Wiseman Chair, Thesis Examination Committee	Associate Professor	Ph.D.
--	---------------------	-------

## ABSTRACT

In this thesis, we investigate the prairie plant species *Symphoricarpos occidentalis* for compounds of biological interest. We have characterized the effects of *S. occidentalis* extracts in different human cell lines by phenotypic assays and found that they induce a light dependent vacuolation of the endoplasmic reticulum and the nuclear envelope. Vacuolated cells show an intense lamin A/C signal, in particular at the location of the nuclear envelope derived vacuole. We found that vacuolation appeared independent of protein synthesis, vacuolated cells were alive at 16 h, and light co-treatment increased extract toxicity 10-fold by 96 h. Spectral analyses and phenotypic screening showed that the cyclic tetrapyrrole compound, Pheophorbide a, had a similar effect on human cells. Insight into cytoplasmic vacuolation might be beneficial as a tool to study nuclear envelope organization and contribute to the understanding of lamin-related diseases, such as Pelger-Huët anomaly.

## ACKNOWLEDGEMENTS

I would like to thank my supervisor Dr. Roy Golsteyn for his guidance and support throughout my M. Sc. I am extremely grateful for the opportunities I have been given and for his encouragement, knowledge and advice throughout my Master's degree. I am thankful to my committee members Dr. Steven Mosimann and Dr. Nehalkumar Thakor, who have provided me with useful advice to improve my project and dedicated their time to help me achieve this precious opportunity. Special thanks go to Dr. Raymond Andersen and Dr. Locke Spencer for their collaboration, interest and work on my project. I also thank Dr. Steve Wiseman for accepting to be the thesis examination chair.

I would also like to thank the members of the Department of Biological Sciences for the friendly, supportive and encouraging conversations, as well as providing volunteer opportunities to give back to the University community. I am grateful to Dr. Nehalkumar Thakor, Dr. Brent Selinger, Dr. Hans-Joachim Wieden, Dr. Andy Hudson and Bruce McMullin for sharing their knowledge, equipment and supplies.

My research has also greatly benefitted from the support and advice of past and present lab members, including Dr. Sophie Kernéis, Alessandra Bosco, Layla Molina, Dani Kalsbeek and Chad Beck.

I would not have been able to accomplish this goal without moral support, motivation, kindness and motivation of friends and family, including my parents Hanspeter and Marie-Louise Tüscher. I want to thank especially Colyn Cleland and Reid Stoyberg for providing me with many stories to share and laugh about. Finally, I would like to thank Ashley Henrickson, for her unconditional love, patience and support.

## TABLE OF CONTENTS

ABSTRACT .....	iii
ACKNOWLEDGEMENTS .....	iv
TABLE OF CONTENTS .....	v
LIST OF FIGURES .....	viii
LIST OF ABBREVIATIONS .....	x
CHAPTER 1: General Introduction .....	1
1.1 Natural products as the source of bioactive compounds .....	1
1.2 Natural products in plants .....	2
1.3 Investigating the Canadian prairie plant species <i>Symphoricarpos occidentalis</i> .....	4
1.3.1 Canadian prairie plant species .....	4
1.3.2 The plant species: <i>Symphoricarpos occidentalis</i> .....	5
1.4 Type of assay: Phenotypic screening against human cancer cells .....	7
1.5 Plant photosensitizers .....	9
1.5.1 Plant photosensitizers .....	9
1.5.2 Chlorophyll and chlorophyll derivatives in plants .....	10
1.6 Photophysics and photochemistry of photosensitizers .....	11
1.6.1 Molecular bonding and absorption spectroscopy of cyclic tetrapyrroles .....	11
1.6.2 Photosensitizer fluorescence .....	13
1.6.3 Photosensitizer photoactivity .....	14
1.7 Macromolecule targets of photosensitizers .....	15
1.7.1 Proteins .....	16
1.7.2 Lipids .....	17
1.8 Subcellular localization and photodamage .....	18
1.8.1 Mitochondria .....	20
1.8.2 Lysosomes .....	21
1.8.3 Endoplasmic reticulum .....	22
1.8.4 Nuclear envelope .....	24
1.9 Cytoplasmic vacuolation of human cells .....	25
1.9.1 Vacuolation of the endoplasmic reticulum .....	26
1.9.2 Vacuolation of the nuclear envelope .....	28
1.10 Research aims and objectives .....	30
CHAPTER 2 - Materials and Methods .....	35
2.1 Collection of plants .....	35
2.2 Preparation of plant extracts .....	35
2.3 Cell culture .....	36
2.4 Light irradiation .....	37
2.5 Cell viability assay .....	37
2.6 Light microscopy .....	38
2.7 Fluorescence microscopy .....	39
2.8 Immunofluorescence microscopy .....	39
2.9 Fluorescence intensity analysis .....	40
2.10 Absorbance and fluorescence spectral scanning .....	40
2.11 Optical filters .....	41
2.12 Molecular structures .....	41

2.13	Statistics.....	42
CHAPTER 3 - Extracts prepared from <i>S. occidentalis</i> or the cyclic tetrapyrrole, Pheophorbide a, induce vacuolation of the endoplasmic reticulum and the nuclear envelope upon exposure to ambient light .....		
3.1	Introduction .....	43
3.2	Results .....	46
3.2.1	Extracts from <i>S. occidentalis</i> leaves are cytotoxic to the HT-29 cell line.....	46
3.2.2	Characterization of morphological changes induced by treatment with <i>S. occidentalis</i> extracts .....	47
3.2.3	The vacuolated phenotype occurs in different cell lines .....	49
3.2.4	Cells develop a vacuolated phenotype after imaging at room conditions .....	49
3.2.5	U2OS cells acquire vacuoles in a concentration and ambient incubation duration-dependent manner when treated with PP-630-F .....	50
3.2.6	The vacuolated phenotype requires co-treatment with light .....	52
3.2.7	Characterization of the photoinduction event in PP-630 treated cells .....	53
3.2.8	Incubation at ambient light increases cytotoxicity of PP-630 against human cells.....	55
3.2.9	Vacuolated cells are alive as determined by propidium iodide impermeability.....	56
3.2.10	PP-630 and ambient light-induced vacuoles are not acidic or lipid droplets ....	56
3.2.11	Identification of a photosensitizing compound, Pheophorbide a .....	58
3.2.12	Co-treatment of Pheophorbide a and ambient light induces a vacuolated phenotype similar to <i>S. occidentalis</i> extracts .....	58
3.2.13	Absorption and fluorescence spectral scans of <i>S. occidentalis</i> leaf extracts show similar spectra to Pheophorbide a. ....	59
3.2.14	Perinuclear origin of vacuolation .....	60
3.2.15	Pheophorbide a and PP-630 emit fluorescence and localize to the perinuclear area .....	61
3.2.16	Perinuclear vacuolation is different from a known vacuole-inducing compound, cyclosporine A.....	63
3.2.17	The vacuolated phenotype shows a dispersed, vacuolated endoplasmic reticulum.....	64
3.2.18	The vacuolated phenotype is not inhibited by translation inhibition .....	65
3.2.19	The vacuolated phenotype originates mainly outside of the endoplasmic reticulum.....	66
3.2.20	Perinuclear vacuolation induces an increase in lamin A/C signal at the nuclear lamina .....	67
3.3	Discussion.....	69
CHAPTER 4 – Comparison of the wavelengths and radiant exposures required to induce vacuolation in <i>S. occidentalis</i> extract or Pheophorbide a treated cells .....		
4.1	Introduction .....	106
4.2	Results .....	108
4.2.1	Identification of vacuole-inducing sections of the ambient electromagnetic spectrum in cells treated with PP-630 or Pha.....	108
4.2.2	Light specific to 408 nm or 660 nm induces vacuoles in cells treated with either <i>S. occidentalis</i> leaf extract or Pheophorbide a.....	109
4.3	Discussion.....	110
CHAPTER 5 - General discussion.....		
		118

5.1	The presence of phototoxic cyclic tetrapyrroles in <i>S. occidentalis</i> extracts .....	119
5.2	The ER and nuclear envelope are subcellular targets of <i>S. occidentalis</i> and Pheophorbide a.....	120
5.3	Photodamage to structural proteins of the nuclear envelope and mechanic stress induces vacuolation of the nuclear envelope .....	122
5.4	Photosensitizers as a molecular tool to study cytoplasmic vacuolation, Pelger-Huët anomaly and Greenberg skeletal dysplasia, or cell death .....	124
5.5	Conclusion.....	128
	REFERENCES .....	130

## LIST OF FIGURES

Figure 1.1 A typical absorption spectrum of a cyclic tetrapyrrole photosensitizer. ....	32
Figure 1.2 A simplified Jablonski diagram showing typical changes in molecular electronic states associated with excitation of photosensitizers.....	33
Figure 1.3 Structures of selected photosensitizers that localize preferentially or partially to the ER and of the photosensitizer used in this thesis, Pheophorbide a. ....	34
Figure 3.1. Scheme for the extraction of <i>S. occidentalis</i> leaves with different solvents and the PP abbreviations used throughout this thesis. ....	80
Figure 3.2. Extracts prepared from <i>S. occidentalis</i> leaves are toxic to HT-29 cells. ....	81
Figure 3.3. <i>S. occidentalis</i> leaf extracts induce phenotypic changes in human cells.....	82
Figure 3.4. Induction of an aberrant morphologies in HT-29 cells is retained in the DCM extract in a sequential extraction of <i>S. occidentalis</i> leaves with 75% EtOH, HEX and DCM. ....	83
Figure 3.5 <i>S. occidentalis</i> leaf extract induces a vacuolated phenotype in different cell lines. ....	84
Figure 3.6. Vacuolation is induced in <i>S. occidentalis</i> leaf extract treated cells after cells have been imaged by phase contrast microscopy. ....	85
Figure 3.7. Vacuolation of cells is dependent on the concentration of <i>S. occidentalis</i> leaf extract and duration of incubation at room conditions. ....	86
Figure 3.8. Cells acquire vacuoles by co-treatment with PP-630-F and ambient light. ....	87
Figure 3.9. Vacuolation requires <i>S. occidentalis</i> leaf extract treatment prior to ambient light exposure.....	88
Figure 3.10. Co-treatment with <i>S. occidentalis</i> leaf extracts and light increases extract toxicity. ....	89
Figure 3.11. Vacuolated cells are alive as determined by staining with the membrane-impermeable dye propidium iodide. ....	90
Figure 3.12. <i>S. occidentalis</i> leaf extract and light-induced vacuoles are not acidic vesicles as determined by AO staining.....	91
Figure 3.13. <i>S. occidentalis</i> leaf extract and light-induced vacuoles are not lipid droplets as determined by Nile red staining.....	92
Figure 3.14. The structure of Pheophorbide a.....	93
Figure 3.15. Treatment with Pheophorbide a induces a vacuolated phenotype similar to <i>S. occidentalis</i> leaf extracts.....	94
Figure 3.16. <i>S. occidentalis</i> leaf extracts show a similar absorption spectrum to Pheophorbide a.....	95
Figure 3.17. Onset of vacuolation in <i>S. occidentalis</i> leaf extract or Pha and light occurs at the perinuclear area. ....	96
Figure 3.18. Fluorescence spectra of PP-630-F and Pheophorbide a. ....	97
Figure 3.19. <i>S. occidentalis</i> leaf extract and Pha fluorescence accumulates at the perinuclear location and vacuolation originates mainly from outside the fluorescence. ....	98

Figure 3.20. <i>S. occidentalis</i> leaf extract and Pha vacuolation originates mainly from outside the fluorescence. ....	99
Figure 3.21. Onset of vacuolation in cells treated with either <i>S. occidentalis</i> leaf extract or Pheophorbide a and light is different from cyclosporine A. ....	100
Figure 3.22. <i>S. occidentalis</i> leaf extract and light-induced vacuolated cells show a dispersed endoplasmic reticulum. ....	101
Figure 3.23. Inhibition of protein synthesis does not prevent vacuole formation in cells treated with <i>S. occidentalis</i> leaf extract or Pha and light. ....	102
Figure 3.24. Perinuclear vacuoles originate mainly from outside the endoplasmic reticulum. ....	103
Figure 3.25. Intense lamin A/C staining occurs at the location of the perinuclear vacuoles. ....	104
Figure 3.26. Intense lamin A/C staining occurs at the location of the perinuclear vacuoles. ....	105
Figure 4.1. Transmission spectra of various filters used in the identification of vacuole-inducing sections of the ambient light spectrum. Ambient.....	115
Figure 4.2. Identification of vacuole-inducing sections of the ambient light spectrum in cells treated with either <i>S. occidentalis</i> leaf extract or Pha.....	116
Figure 4.3. Light specific to 408 nm or 660 nm induces vacuoles in cells treated with either <i>S. occidentalis</i> leaf extract or Pheophorbide a. ....	117

## LIST OF ABBREVIATIONS

A172	Human glioblastoma cell line
A549	Human lung adenocarcinoma cell line
ABCB6	ATP-binding cassette transporter member 6
AO	Acridine orange
ATP	Adenosine triphosphate
ATPase	Adenosine triphosphatase
BAPTA-AM	1,2-bis(o-aminophenoxy)ethane-N,N,N',N'-tetraacetic acid acetoxymethyl ester
BSA	Bovine serum albumin
CAD	Cationic amphiphilic drugs
CHX	Cycloheximide
CPT	Camptothecin
CsA	Cyclosporine A
DCM	Dichloromethane
DMEM	Dulbecco's Modified Eagle Medium
DMSO	Dimethyl sulfoxide
DNA	Deoxyribonucleic acid
ER	Endoplasmic reticulum
EtOH	Ethanol
FBS	Fetal bovine serum
FR	Far red
HeLa	Human cervical adenocarcinoma cell line
HEPES	4-(2-hydroxyethyl)-1-piperazineethanesulfonic acid
HPPH	2-[1-hexyloxyethyl]-2-devinyl pyropheophorbide-a
HT-29	Human colorectal adenocarcinoma cell line
LED	Light emitting diode
LINC	Linker of nucleoskeleton and cytoskeleton
M059K	Human glioblastoma cell line
MDA-MB-231	Human breast medullary adenocarcinoma cell line
MEM-NEAA	Modified Eagle Medium non-essential amino acids
MTT	3-((4,5)-dimethylthiazol-2-yl)-2,5-diphenyl-tetrazolium bromide
NPe6	mono-L-aspartyl chlorin e6
Pha	Pheophorbide a
PBS	Phosphate buffered saline
PI	Propidium iodide
ROS	Reactive oxygen species
S <sub>0</sub>	Ground state
S <sub>1</sub>	First excited singlet state
S <sub>2</sub>	Second excited singlet state
SDS	Sodium dodecyl sulphate
T <sub>1</sub>	First excited triplet state
U2OS	Human osteosarcoma cell line
U87 MG	Human glioblastoma cell line

UV  
WI-38

Ultraviolet  
Human non-cancerous lung fibroblastic cell line

## CHAPTER 1: General Introduction

This thesis is about the effects of extracts prepared from the prairie plant *Symphoricarpos occidentalis* on human cells. We found that these extracts induce the formation of cytoplasmic vacuoles upon exposure to light. We then used different assays to determine that these vacuoles originate from the endoplasmic reticulum (ER), whereas a striking, large perinuclear vacuole originates from the nuclear envelope. We also showed that *S. occidentalis* extracts induce intense staining of lamin A/C protein, particularly at the nuclear location of the perinuclear vacuole. By spectral analysis and morphological screening, we then identified that the cyclic tetrapyrrole, Pheophorbide a, has a similar vacuolation photoactivity. Using the vacuolated morphology as a bioassay, we then identified specific wavelengths that can induce vacuolation. Here I provide a review of the discovery of compounds with biological activity from plants, the sensitization of human cells to light with photoactive compounds, and the vacuolation of human cells.

### 1.1 Natural products as the source of bioactive compounds

All organisms produce a vast number of organic compounds that enable them to live, grow and reproduce. These organic compounds are termed natural products and include an organisms' primary and secondary metabolites. Primary metabolites are considered fundamental to growth, whereas secondary metabolite describes natural products that are not directly required for growth but contribute to organism survival through their biological effect on other organisms (Dewick, 2009). Secondary metabolites may be produced as a result of adaptation of an organism to its environment under abiotic stress, or as a defence

mechanism under biotic stress to assist in survival from predation or infection (Maplestone et al., 1992; Dewick, 2002).

Due to interactions between organisms and evolutionary pressures, organisms have developed structurally diverse compounds that interact with targets in competing organisms. The inherent advantage of these compounds over synthetic compounds is that they often show properties that are also desirable for pharmaceutical drugs, such as improved cell penetration or interaction with proteins (Lee and Schneider, 2001; Feher and Schmidt, 2003b; Feher and Schmidt, 2003a). For example, many effective drugs represent naturally occurring metabolites and emulate native substrate binding (Hajduk et al., 2005; Dobson et al., 2009). As such, the investigation of organisms for natural products is a valuable approach to discovering compounds with new biological activities and has resulted in the development of many clinically successful drugs, such as penicillin or the anticancer drug Taxol® (Mann, 2000; Newman and Cragg, 2016).

## **1.2 Natural products in plants**

Historically plants have been used for many centuries by humans for their medicinal properties against a wide range of human diseases, and they are still used today in traditional treatments (Newman et al., 2000; Cordell and Colvard, 2012). Whereas plants were used initially for medicinal purposes in many different ways, such as eaten or applied as a lotion, the discovery and isolation of several compounds in the early 1800s set the stage for the notion of pure compounds as active drugs, such as morphine from *Papaver somniferum* L. (opium poppy) or salicin from *Salix alba* (willow tree) (Serturmer, 1805; Hedner and Everts, 1998; Dias et al., 2012). Over the last two centuries, natural products and their derivatives and mimics have contributed significantly to the development of pharmaceuticals. A recent

review on natural products as sources of new drugs showed that of the 1211 small-molecule approved drugs between 1940 to 2014, 65% were either natural products, a derivative, or inspired therefrom, a proportion that rises to 75% in the area of cancer (Newman and Cragg, 2016). Examples include the anticancer compounds paclitaxel, isolated from the Pacific Yew Tree *Taxus brevifolia*, the *vinca* alkaloids, vinblastine and vincristine, isolated from the Madagascar periwinkle *Catharanthus roseus*, or camptothecin, isolated from the Happy Tree, *Camptotheca acuminata* (Newman and Cragg, 2016). The discovery of natural products has also provided us with tools to study biological mechanisms, such as the spindle assembly checkpoint by taxol or the *vinca* alkaloids (Musacchio and Salmon, 2007; Matson and Stukenberg, 2011).

There is clear evidence that plants are a source of compounds with novel biological effects. However, it has been suggested that of the estimated 250,000 to 500,000 existing plant species, only 6% have been investigated pharmacologically and only 15% phytochemically (Hostettmann and Marston, 2002; Cragg and Newman, 2013; Ngo et al., 2013). It has also been suggested that up to 23,490 new chemical entities with new mechanisms of action may still to be discovered, although these estimates rely on the number of discovered drugs to date, the use of a certain natural product by multiple plant species, and the number of plants that have been screened to date, the latter two of which are difficult to estimate (Miller, 2011). Furthermore, ethnopharmacological information about traditional uses of plants can sometimes provide hints about species that may harbour compounds for therapeutic use. For example, an analysis of 122 plant-derived therapeutic drugs showed that 80% of them had an ethnomedical use that was identical or related to the current use of the drug (Fabricant and Farnsworth, 2001).

These facts led us to believe that organisms are an excellent source for the discovery of compounds with novel biological activities. Furthermore, plants are an accessible source of natural products, have historically been the source of diverse and effective compounds with biological activities, and many plants remain to be investigated for such compounds.

### **1.3 Investigating the Canadian prairie plant species *Symphoricarpos occidentalis***

One approach to discover previously unknown compounds or compounds with previously unknown biological activities from plants is to investigate species that have either been largely untested due to small distribution or that have been reported as toxic with little or no scientific information of the bioactive compound.

#### *1.3.1 Canadian prairie plant species*

Canada is a country with 15 terrestrial ecozones and Alberta's ecozones are mainly the prairies and boreal plains, as well as small portions of the montane cordillera, taiga plains, taiga shield and boreal shield (Group, 1996; Marshall et al., 1999). Despite extensive research into plant natural products worldwide, the Alberta ecological zones have rarely been investigated for plants with bioactive secondary metabolites (Cho and Martin, 1971; Kernéis et al., 2015; Bosco, 2017). Plants in the Albertan prairies have coevolved with both abiotic and biotic stresses, such as the prevalence of a deep snowpack in the spring that shortens the growing season, or the presence of grazing herbivores, respectively (Beaubien and Hamann, 2011). These factors increase competition for survival between plant species, which contributes to the production of secondary metabolites (Kliebenstein, 2004; Rosenthal and Berenbaum, 2012; Brunetti et al., 2013). Furthermore, prairie plants have been used by Indigenous peoples of Canada for the treatments of various diseases and maladies (Uprety et al., 2012). For example, Bos et al. recently screened a library of 35 Canadian medicinal plant

extracts for anticancer activities, including species that are native to the Canadian prairies, and discovered that 11 were potent inducers of cell death (Bos et al., 2016). Combined, this information indicates that Alberta prairie plant species likely harbour an abundance of diverse compounds with biological activities. To support this hypothesis further, native prairie plants of the genus *Thermopsis* and *Gaillardia*, which are toxic to herbivores and humans and are used in traditional medicine, contained anticancer activities when extracts prepared from plant species of these genera were tested against human cells (McGrath-Hill and Vicas, 1997; Pahl and Smreciu, 1999; Kernéis et al., 2015; Bosco, 2017). Hence, these observations and the abundance of untested plant species in Canada suggests that investigating prairie plant species could lead to the discovery of compounds with novel biological activities.

### 1.3.2 *The plant species: Symphoricarpos occidentalis*

We selected the prairie plant species, *Symphoricarpos occidentalis*, also known as Snowberry, for investigation. *S. occidentalis* is a species of the small *Symphoricarpos* genus in the Caprifoliaceae (Honeysuckle) family and is native to much of North America and is found east of the Rocky Mountains (Moss, 1932; Looman and Best, 1979; Kuijt, 1982; Tannas, 2003). *S. occidentalis* is mainly found throughout bush areas of the Alberta prairies, valley slopes, and the Cypress Hills, as well as in rocky and sandy woodlands (Looman and Best, 1979; Moss and Packer, 1983). *Symphoricarpos* species show resistance to browsing by livestock due to their low palatability compared to other shrubs, and it also reduces forage production on the most productive sites by outcompeting many other plant species and creating a grazing barrier (Pelton, 1953; Lesperance et al., 1970). *Symphoricarpos* species have been reported to tolerate environmental stresses well and showed resistance to common methods of eradication, such as cutting or fire (Pelton, 1953; Anderson and Bailey, 1979).

*Symphoricarpos* species have been used to treat a variety of external and internal maladies by Indigenous peoples of Canada; decoctions of stems, leaves and/or fruits were drunk as a diuretic, for urinary and kidney problems, pregnancy and labour-related pains, and teething, whereas the whole plant was crushed, boiled and applied for sore eyes and to treat skin rashes (Kuhnlein and Turner, 1991; Moerman, 1998; Keane, 2003; Uprety et al., 2012). Berries and leaves of this plant are also known to be mildly toxic and consumption of such has been reported to cause mild toxicity when ingested (Amyot, 1885; Chavant et al., 1975; Lewis, 1979; Bunjes, 2004).

Investigations into the chemical profile of *Symphoricarpos* species have identified a large diversity of compounds with potential biological activities, including flavonoids, coumarins, alkaloids, phenolic acids and iridoids (Raffauf, 1970; Smolenski et al., 1974; Szauffer et al., 1978; Hegnauer, 1989). For example, iridoids have been suggested to play an important role in plant defence against both herbivores and pathogens and cytotoxic iridoids have been isolated from the leaves of other species in the family Caprifoliaceae (Bowers et al., 1991; Wang et al., 2003; Whitehead and Bowers, 2013). Furthermore, the alkaloid chelidone, which is toxic to human cells, was previously isolated from the leaves of the closely related species, *Symphoricarpos albus*, although the concentration in the plant was suggested to be too low (0.0013%) to cause any toxicity (Szauffer et al., 1978; Hegnauer, 1989; Kemény-Beke et al., 2006). Previous plant screening experiments for toxicity included *S. albus* berry extracts, which were found to have low toxicity against either a leukemia cell line (CCRF-CEM; non-toxic at 10 µg/ml), mice or rats (LD50s:  $\geq 225$  mg/kg body weight), or brine shrimp (LC50:  $>1,000$  µg/mL)(Chavant et al., 1975; Deeg et al., 2012; Karchesy et al., 2016; Barnaby et al., 2018). In plant screenings for anti-microbial, anti-fungal, and anti-

viral properties, *S. albus* leaf extracts were reported by one group to contain some anti-microbial activity ( $> 1,000 \mu\text{g/mL}$ ) against standard Gram-positive and Gram-negative strains (McCutcheon et al., 1992; McCutcheon et al., 1995; McCutcheon et al., 1997; Szauffer-Hajdrych and Goslinska, 2004).

This information shows that the prairie plant, *S. occidentalis*, is native to the Alberta prairies, has been used as a medicinal plant and was reported as toxic. Furthermore, dominant growth of *S. occidentalis*, avoidance by grazing herbivores and the indication of compounds with potential bioactivities in this plant, indicates that *S. occidentalis* leaves possibly harbour compounds of biological interest. Moreover, preliminary investigations with extracts prepared from *S. occidentalis* leaves in our laboratory showed a toxic effect against human cells, which validated further investigation of this plant species.

#### **1.4 Type of assay: Phenotypic screening against human cancer cells**

One approach to discover natural products with biological activities against human cells is that of phenotypic assays or phenotypic drug discovery. These are powerful assays to test compounds in relatively complex biological systems (e.g. representative of a disease or biology) without prior knowledge of the identity of a specific drug target or a hypothesis about the compound's role in treating a disease (Lee and Berg, 2013). Phenotypic assays were one the first methods of drug discovery and significantly contributed to the discovery of first-in-class small-molecule drugs, responsible for 28 out of 45 drugs approved by the United States Food and Drug Administration between 1999 and 2008 (Swinney and Anthony, 2011). Phenotypic assays frequently use cell-based assays, such as morphological changes, viability and proliferation, migration or invasion, secretion, or synthesis of a product (Zheng et al., 2013). In comparison to target-based approaches, phenotypic screening against human

cancer cells has several advantages, including consideration of the bioavailability of cellular targets, elimination of cell-impermeable compounds, or detection of synergism between compounds or with environmental factors, such as the interaction between a compound and light irradiation, for example (Cos et al., 2006; Rautio et al., 2008; Zheng et al., 2013). Phenotypic assays have been more successful historically than target-based approaches when measured by the number of first-in-class medicines produced (Swinney and Anthony, 2011; Moffat et al., 2017). In contrast, target-based approaches are successful for follower drugs, which are compounds in the same class as the initially approved drug (Swinney and Anthony, 2011).

We chose to screen *S. occidentalis* plant extracts initially in human cells by detection of morphological changes. Observation of morphological changes are a powerful approach to screen for the potential biological activity of a compound. Scientists have long relied on accurate descriptions and observations of cells in response to treatment or conditions. John Kerr reported in 1965 that “after ischemia, some hepatocytes looked as small masses of cytoplasm containing condensed nuclear chromatin” to describe what came to be known as apoptotic cells (Kerr, 1965). Other reports include microscopic observations of cytoplasmic vacuoles in cells undergoing physiological and pathological lysis or large numbers of rounded cells in a cell population treated with paclitaxel, which were later found to represent autophagy or a mitotic arrest, respectively (Novikoff and Essner, 1962; Jordan et al., 1993). In these cases, the morphological change observed provided a hint about the underlying mechanism, demonstrating the power and usefulness of morphological observations of treated cells.

## 1.5 Plant photosensitizers

By the phenotypic approach described above, we observed that *S. occidentalis* leaf extract-treated cells developed large, cytoplasmic vacuoles, which only occurred upon exposure to light. We also found that the cyclic tetrapyrrole molecule, Pheophorbide a, had a similar photoactivity. To understand how light can interact with compounds to induce a biological effect, an understanding of a group of compounds termed photosensitizers is required, as well as their presence in plants.

### 1.5.1 Plant photosensitizers

Photosensitizers are compounds that absorb energy from ultraviolet-visible light and can induce chemical changes in other compounds by photophysical and photochemical processes (Castano et al., 2004). These compounds may be used to an organisms' advantage, such as the parasitization of plant leaves by the fungal genus *Cercospora* (photosensitizer: cercosporin), or as defense mechanisms by plants, such as the photosensitizer sanguinarine by bloodroot (*Sanguinaria canadensis*) or the photosensitizer hypericin by St. John's-wort (*Hypericum perforatum*) (Pace, 1942; Daub, 1982; Arnason et al., 1992). Another group of photosensitizers are the cyclic tetrapyrroles, which is a class of molecules that contain four connected pyrrole or pyrrole-like rings. Plant cyclic tetrapyrroles include chlorophyll and intermediates in chlorophyll metabolism, such as pheophorbides, pheophytins, chlorophyllides, protoporphyrins and their derivatives (Brandis et al., 2006). Notably, these cyclic tetrapyrroles make up the largest portion of natural photosensitizers investigated for therapeutic treatments and they have also been investigated as molecular tools, such as for *in vivo* visualization of tumorigenic tissue based on their fluorescent properties (Nyman and Hynninen, 2004; Celli et al., 2010).

### *1.5.2 Chlorophyll and chlorophyll derivatives in plants*

Chlorophyll biosynthesis is composed of the initial formation of protoporphyrin IX from eight molecules of aminolaevulinic acid and the metabolism of subsequent tetrapyrrole intermediates to chlorophyll (Eckhardt et al., 2004). Conversely, chlorophyll breakdown occurs by destruction of the conjugated system delocalized  $\pi$  electrons, which is responsible for the photophysical and photochemical properties of cyclic tetrapyrroles, and is completed with the disposal of non-fluorescent chlorophyll catabolites inside the plant vacuole (Hörtensteiner and Kräutler, 2011). General intermediates of chlorophyll breakdown are pheophytin a, chlorophyllide a and pheophorbide a, that derive from the demetallation and/or dephytylation of chlorophyll (Hörtensteiner and Kräutler, 2011). Pheophorbide a is the last phototoxic intermediate in chlorophyll breakdown and is either converted into non-toxic non-fluorescent chlorophyll catabolites or can undergo further reactions, such as the conversion to pyropheophorbide a (Shioi et al., 1996).

Notably many intermediates and other phototoxic tetrapyrrole derivatives have previously been isolated from different plant species and suggested to have physiological roles (Shioi et al., 1996; Stermitz et al., 2000; Wongsinkongman et al., 2002; Chan et al., 2006; Tan et al., 2011; Sowemimo et al., 2012). For instance, Hörtensteiner and Kräutler reviewed chlorophyll breakdown in higher plants and indicated that many cyclic tetrapyrrole derivatives have not yet been assigned clear roles and suggested that they could have physiological roles, such as in response to biotic and abiotic stresses (Hörtensteiner and Kräutler, 2011). Similarly, others found that the overexpression of numerous enzymes involved in chlorophyll breakdown or modification, including Pheophorbide a oxygenase, stay-green, pheophytinase or chlorophyllase, are highly up-regulated under abiotic stress or in response to parasitisation (Greenberg et al., 1994; Ishikawa et al., 2001; Mach et al., 2001;

Pružinská et al., 2003; Kariola et al., 2005; Quinn et al., 2014). The intermediate metabolite Pha has also been shown upregulated during parasitization to mediate reactive oxygen species signalling, which leads to a systemic plant defence response (Griebel and Zeier, 2008). Specific to herbivory, Hu et al. suggested that chlorophyllase catabolizes chlorophyll into the toxic derivative chlorophyllide a specifically during leaf damage that occurs during chewing by herbivores and suggested that it deters feeding (Hu et al., 2015).

## **1.6 Photophysics and photochemistry of photosensitizers**

In this thesis, we examine the presence of cyclic tetrapyrroles in plant extracts by spectroscopic analyses, localize the extract and Pha in human cells by fluorescence microscopy and examine the effects that occur upon exposure of cell extract or Pha treated cells to light. To understand how cyclic tetrapyrroles can be detected in plant extracts or visualized in cells and to understand how photosensitizers absorb light and damage neighbouring molecules, an introduction of their photophysics and photochemistry is required.

### *1.6.1 Molecular bonding and absorption spectroscopy of cyclic tetrapyrroles*

Covalent bonding occurs with the overlap of two “head on” atomic orbitals and results in the formation of a stable low-energy sigma bond ( $\sigma$ ) that is filled with electrons and an unfilled and unstable, high-energy sigma anti-bond ( $\sigma^*$ ). Pi bonds ( $\pi$ ) and pi anti-bonds ( $\pi^*$ ), are covalent bonds that result from a “lateral overlapping” of atomic orbitals and are found in higher than single bonds (double, triple, etc.). A further non-bonding orbital (n) can also be occupied by electrons, such as lone pairs or electrons that are not contributing to  $\sigma$ - or  $\pi$ -bond formation.

In general, bonds from lowest to highest orbital are noted as  $\sigma < \pi < n < \pi^* < \sigma^*$ , with the stable  $\sigma$ ,  $\pi$  and  $n$ -orbitals occupied by electrons and anti-bonding orbitals devoid of electrons. Absorption of energy from radiation can promote electrons into a higher orbital if the energy corresponds to the energy difference between an occupied (bonding) and an unoccupied (antibonding) orbital. Since wavelength and energy are inversely related, shorter wavelengths can promote a bigger electron jump, whereas higher wavelengths can promote a smaller electron jump to an antibonding orbital. Wavelengths with energy higher than approximately 6.2 eV (<200 nm) are required for large jumps, such as from  $\sigma$  to  $\sigma^*$  or  $n$  to  $\sigma^*$ , whereas wavelengths above 200 nm can promote smaller jumps, such as  $\pi$  or  $n$  to  $\pi^*$  (Nilapwar et al., 2011).

Delocalization of  $\pi$ -electrons allows for conjugation of the  $\pi$  bonds, which is the interaction of two double bonds separated by a single bond in a molecule. Delocalization results in a greater space for electron moving, which results in a lower total energy, a greater binding energy and smaller energy differences between  $\pi$  and  $\pi^*$  orbitals (Krygowski and Stępień, 2005). Hence, molecules with a large delocalization system can absorb light at higher wavelengths, which can be used uniquely for their identification. For example, cyclic tetrapyrroles often absorb light between 600-800 nm, which can be used for spectral identification in chromatographic separations of plant tissue (Mangos and Berger, 1997).

A compound's absorption can be determined by passing a beam of a specific wavelength through a solution of this compound and measuring the number of photons that are not absorbed. The absorption spectrum of cyclic tetrapyrroles shows several characteristic electron transitions: The B band or Soret band in the near-UV region between ~380–420 nm and several smaller Q-bands in the visible region between ~500–800 nm (Figure 1.1). These

bands represent wavelengths that can induce  $\pi$  to  $\pi^*$  electron transitions of the delocalized  $\pi$ -electrons in the cyclic tetrapyrrole ring (Gouterman, 1959, 1961). The excitation of electrons from the ground state ( $S_0$ ) to occupation of the  $\pi^*$ -orbital gives rise to the various excited states of a photosensitizer ( $S_1$ ,  $S_2$ , etc.). Excitation usually occurs to a higher vibrational level of the excited state, from which electrons relax rapidly to the lowest vibrational level of the excited electronic state in a process termed “vibrational relaxation”. As shown in Figure 1.1 and Figure 1.2, transition to the first excited state ( $S_1$ ) in cyclic tetrapyrroles is elicited by the Q bands and the strong transition to the second excited state ( $S_2$ ) is elicited by the Soret band. In the chlorin group of cyclic tetrapyrroles, which includes chlorophyll and its derivatives, the Soret band is weakened and the most red-shifted peak is significantly increased. For example, the chlorophyll derivative Pha shows a typical chlorin absorption spectrum shown in Figure 1.1: a Soret band around 400 nm and Q-bands between 500 and 700 nm (Roeder et al., 1990; Eichwurz et al., 2000).

### 1.6.2 Photosensitizer fluorescence

In its ground state ( $S_0$ ) a photosensitizer contains two electrons with opposite spins. Upon absorption of light with the appropriate energy, an electron is promoted into an excited singlet state  $S_x$  (with  $x = 1, 2, 3, \dots$  in the order of increased energetic state), which is energetically less preferable than  $S_0$  and very short-lived (nanoseconds) (Figure 1.2). If electrons are promoted into a higher-energy excited singlet state, such as  $S_2$  elicited by the Soret band, they rapidly fall to the lowest vibrational level of that state (e.g.  $S_2$  or  $S_3$ ) by vibrational relaxation and heat dissipation, and subsequently to the lowest-energy singlet excited state ( $S_1$ ) by internal conversion. Return to  $S_0$  occurs by several mechanisms: directly by emission of light (fluorescence) or further internal conversion/heat dissipation; or

indirectly by intersystem crossing into a relatively long-lived triplet state photosensitizer ( $T_1$ ). Most cyclic tetrapyrroles, such as Pha, show a fluorescence emission between 650-700 nm upon excitation at the Soret- or Q-bands (Roeder and Wabnitz, 1987). These fluorescence properties of photosensitizers allow their subcellular localization using fluorescence microscopy. For example, Kessel et al. showed that subcellular localization is crucial to assess photosensitizer phototoxicity and that co-localization with fluorescent probes can be used to characterize sites of photodamage (Kessel et al., 1997; Kessel, 2004).

### *1.6.3 Photosensitizer photoactivity*

From the  $T_1$  state, transition to  $S_0$  occurs either by emission of phosphorescence (unfavoured) or either by electron transfer/hydrogen abstraction with another compound (Type I) or transfer of energy (Type II) to a neighbouring compound (Figure 2) (Foote, 1991; Baptista et al., 2017). It is by these chemical reactions with other species that photosensitizers are thought to induce direct and indirect damage to other compounds and a high quantum efficiency for the  $S_1$  to  $T_1$  transition is thought to increase a photosensitizers' phototoxic effect (Takemura et al., 1989). In the Type I reaction, the photosensitizer reacts directly with a substrate by hydrogen atom abstraction or electron transfer reactions and produces radical anions or cations in both the photosensitizer and the substrate. In the presence of oxygen, these radicals can further react to produce reactive oxygen species, whereas direct electron transfer to molecular oxygen can produce superoxide anions and subsequently hydrogen peroxide that easily passes through biological membranes and can induce cell death (Sharman et al., 2000). The Type II reaction is described as the transfer of energy to molecular oxygen in its triplet ground state ( $^3O_2$ ), which produces the very reactive singlet

oxygen ( $^1\text{O}_2$ ) that can react with macromolecules in the immediate vicinity of its generation to produce oxidized macromolecules.

Both types of reactions have been well described and are thought to occur in parallel when photosensitizers are irradiated with light. However, prediction of the type of reaction that predominates upon irradiation of a photosensitizer is difficult and has been a continuous topic of discussion that considers the biological environment, such as oxygen concentration or solvent polarity, and photosensitizer characteristics, including its photochemical properties, subcellular localization or macromolecule interaction (Foote, 1991; Sharman et al., 2000; Garcia-Diaz et al., 2016; Baptista et al., 2017). Since the substrate and oxygen compete for photosensitizer interaction, it suggested that Type I processes generally predominate under high substrate and low oxygen concentrations and vice versa for Type II processes (Ochsner, 1997; Fuchs and Thiele, 1998). For example, proximity or binding to macromolecules supports direct damage to macromolecules by Type I processes. This was specifically demonstrated with benzochlorin derivatives that do not form singlet oxygen species yet efficiently photosensitize human cells, likely due to proximity and/or binding to important biological macromolecules (Skalkos et al., 1994).

## **1.7 Macromolecule targets of photosensitizers**

In this thesis, we examine the localization and damage that occurs upon exposure of plant extract- or Pha-treated human cells to light. We found that these treatments likely induce damage to the membranes of the ER and nuclear envelope, resulting in their vacuolation. Understanding our results requires an understanding of the subcellular localization and molecular targets of photosensitizers. Most photosensitizers readily incorporate into subcellular membranes due to their hydrophobic nature and exert damage

by Type I and Type II processes, which mainly targets lipids and structural membrane-associated proteins. As described, the ratio of these processes is dependent on numerous factors, including photosensitizer photochemistry and photosensitizer environment, which affect the type and extent of macromolecule damage.

### *1.7.1 Proteins*

Kinetic data shows that proteins are a major target of photosensitizer generated singlet oxygen, especially the amino acids tryptophan, histidine, tyrosine, methionine, and cysteine (Wilkinson et al., 1995; Davies, 2004). Several photoproducts can form as a result of oxidative damage to amino acids, including sulfoxides, endoperoxides, disulfides or tyrosine dimers. Immediate protein photooxidation products can be resolved by reaction with antioxidants, such as glutathione, or by transfer to other proteins or macromolecules that cells may upregulate to resolve oxidative stress (Di Mascio et al., 1990). Oxidative protein damage that is not resolved immediately can result in multiple effects, including local or global unfolding, backbone fragmentation, covalent crosslinking and protein aggregation (Davies and Dean, 1997). Crosslinking of proteins is thought to occur as a secondary reaction between photooxidation products, such as disulfide cross-links between two thiol radicals, 2,2-biphenyl cross-links between two tyrosyl radicals, or cross-links by the reaction of two carbon-centred radicals (Berlett and Stadtman, 1997). The formation of damaged or modified proteins due to photooxidation has a wide range of effects on their properties and function, including increased susceptibility to changes in conformation or unfolding, or increased resistance of the oxidized protein to proteolytic enzymes (Davies, 2004).

Although global crosslinking is often observed after photodamage, crosslinking of specific proteins has previously been reported, such as the covalent polymerization and

aggregation of lamin proteins (Lavie et al., 1999; Chiarini et al., 2008; Singla et al., 2013; Maitra et al., 2015). Lamins are a major component of the nuclear lamina that is present below the inner nuclear membrane and forms part of the nuclear envelope (Dechat et al., 2008). Specifically, lamins were found to aggregate covalently into 210 and 244 kilodalton protein aggregates in response to photodamage with the ER localizing compounds protoporphyrin IX, hypericin or calphostin C (Lavie et al., 1999; Chiarini et al., 2008; Singla et al., 2013; Maitra et al., 2015). Cell death was also noted to follow lamin protein aggregation. The reason these photosensitizers induced specific lamin crosslinking and aggregation remains unknown. These observations are related to our results, as we observed the accumulation of lamin protein upon irradiation of human cells treated with *S. occidentalis* plant extracts or Pha.

### 1.7.2 Lipids

Most of the cyclic tetrapyrroles exert their photoactivity after preferential association with membranes, making lipids and membrane-associated proteins a major target for photodamage (Ricchelli, 1995; Lavi et al., 2002). In particular, unsaturated fatty acids are major targets because the low carbon-hydrogen bond energies in methylene groups allows allylic hydrogen atoms to be readily abstracted by photogenerated radicals and reactive oxygen species (Guéraud et al., 2010). This leads to the formation of phospholipid radical species that can further react with oxygen to form peroxy radicals. These lipid radicals may then perpetuate the radical damage by abstracting hydrogen atoms from neighbouring molecules to stabilize themselves and further propagate the lipid peroxidation until terminated either by radical-radical reactions forming non-radical phospholipid products or by antioxidants, such as  $\alpha$ -tocopherol (Buettner, 1993; Guéraud et al., 2010). Oxidative

damage to unsaturated lipids has significant effects on numerous parameters of membranes including intermolecular lipid packing, membrane fluidity, permeability or thermotropic phase properties (Girotti, 1998; Jacob and Mason, 2005; Bacellar et al., 2018). The consequences of lipid peroxidation also include the secondary modifications of membrane proteins, such as the covalent adduct formation between proteins and lipid peroxidation-derived aldehydes (Spickett et al., 2010; Pizzimenti et al., 2013).

Cyclic tetrapyrrole photosensitizers are known to produce singlet oxygen species and induce lipid peroxidation. Relevant to this thesis, photoactivated Pha has been shown to produce singlet oxygen species when incorporated into different lipid membrane environments, such as liposomes, erythrocyte ghost cells or human cells (Roeder et al., 2000; Schlothauer et al., 2008). Furthermore, Rapozzi et al. showed that the photodynamic effect of Pha in human cells includes the formation of lipid peroxides and the activation of an oxidative stress response (Rapozzi et al., 2009).

## **1.8 Subcellular localization and photodamage**

In this thesis, we examine the localization of *S. occidentalis* extracts or Pha in human cells and examine the cellular response to photodamage. We observed the accumulation of fluorescence to the perinuclear area prior to irradiation and to the membranes of the ER and nuclear envelope derived cytoplasmic vacuoles. To understand our results, an understanding of the subcellular localization of photosensitizers is required as the photoactivity of photosensitizers largely depends on their photodamage target, such as protein or lipids, which again largely depends on the subcellular localization of a photosensitizer (Berg and Moan, 1994; Henderson et al., 1997; MacDonald et al., 1999).

The uptake of photosensitizers is largely determined by their size, hydrophobicity, charge and structural asymmetry. General findings have shown that hydrophobic photosensitizers are taken up by passive diffusion across the plasma membrane, whereas hydrophilic photosensitizers enter cells by endocytosis (Kelbauskas, 2002; Ben-Dror, 2006). Owing to the large size of their macrocycle, cyclic tetrapyrrole photosensitizers tend to dimerize and aggregate in aqueous solutions. For example, Pha exists in a monomer-dimer equilibrium up to a concentration of 30  $\mu\text{M}$  and as higher aggregates above this concentration (Eichwurz et al., 2000). These aggregates are thought to be taken up by endocytosis and subsequently disaggregate in the cell interior depending on the extent of aggregation. For example, Kelbauskas showed that lipophilic pyropheophorbide-a derivatives, by attachment of long alkyl side chains, were less likely to disaggregate after cellular uptake, whereas MacDonald et al. showed that highly aggregated pyropheophorbide-a derivatives are sequestered in lysosomes and disaggregated monomers are mainly localized in the mitochondria (MacDonald et al., 1999; Kelbauskas, 2002).

Cyclic tetrapyrrole photosensitizers are thought to localize mainly to the membranes of mitochondria, ER or lysosomes, although the nuclear envelope has also been suggested as a target. However, this localization can vary widely between compounds with similar basic structures or physicochemical characteristics or with extracellular photosensitizer concentration (Henderson et al., 1997; MacDonald et al., 1999). The photosensitizer used in this thesis, Pha, has been suggested to localize to the mitochondria by colocalization studies with fluorescent mitochondrial probes (Lee et al., 2004; Tang et al., 2009a; Bui-Xuan et al., 2010; Hoi et al., 2012).

### *1.8.1 Mitochondria*

Mitochondria are the main organelles responsible for the production of energy and regulation of cellular metabolism. Mitochondria are composed of an outer mitochondrial membrane that surrounds the inner membrane and creates a small intermembrane space in between. The inner mitochondrial membrane is extensively folded into cristae and contains many proteins responsible for ATP synthesis, as well as a large percentage of cardiolipin, a phospholipid that binds to cytochrome c. Damage to mitochondrial membranes, such as cardiolipin oxidation or outer membrane permeabilization, can lead to the release of cytochrome c and other proapoptotic factors from the intermembrane space into the cytoplasm and initiation of apoptosis (Ott et al., 2007).

Mitochondrial localization and photodamage by photosensitizers has been extensively researched. Early research suggested that mitochondria are often sites of photodamage for cationic, hydrophobic photosensitizers, such as hematoporphyrin derivative or benzoporphyrin derivative, due to the influence of the mitochondrial membrane potential and the lipid bilayer of the membrane (Coppola et al., 1980; Dummin et al., 1997; Runnels et al., 1999; Hoye et al., 2008). There is some evidence that certain photosensitizers bind to proteins whereas others associate with the lipid domains. For example, Dellinger et al. showed that polar hematoporphyrin localizes preferentially to protein-rich areas of the inner membrane, whereas the less polar protoporphyrin IX is found in the lipid membrane bilayer (Dellinger et al., 1994). Furthermore, certain cyclic tetrapyrrole protein targets in the mitochondria have since been suggested including the 2-oxoglutarate carrier, a transporter of endogenous porphyrins such as heme and the heme precursors; the mitochondrial ATP-binding cassette transporter ABCB6, which can confer photodynamic therapy resistance; and

the peripheral benzodiazepine receptor, which is thought to contribute to cell death when inhibited by photodynamic therapy (Verma et al., 1998; Kabe et al., 2006; Krishnamurthy et al., 2006).

Mitochondrial photodamage is correlated with rapid induction of the mitochondrial outer membrane permeabilization, mitochondrial membrane depolarization, degradation of mitochondria-associated Bcl-2, cytochrome c-release and activation of caspase-3, -6 and -7 within minutes after photodynamic therapy (Mroz et al., 2011). Relevant to this thesis, these observations have previously been made in cells treated with Pha, which induced apoptosis upon photoirradiation (Lee et al., 2004; Radestock et al., 2007; Tang et al., 2009a; Bui-Xuan et al., 2010; Hoi et al., 2012). However, the photooxidation reactions in the mitochondria that ultimately lead to these events remain to be described completely. They are thought to include photooxidation and degradation of critical antiapoptotic proteins, peroxidation of cardiolipin, and increase of mitochondrial membrane permeability (Buytaert et al., 2007). Notably, photosensitizers localizing to non-mitochondrial membranes, such as mono-L-aspartyl chlorin e6 (NPe6; lysosomes) or hypericin (ER), can also induce cell death by activation of cellular pathways or responses that ultimately converge on the mitochondria (Reiners et al., 2002; Buytaert et al., 2006b).

### *1.8.2 Lysosomes*

Lysosomes are spherical vesicles involved in various cell processes, including secretion, plasma membrane repair, signalling and energy metabolism (Settembre et al., 2013). Furthermore, these organelles contain hydrolytic enzymes, which can degrade and recycle extracellular material by fusion with endosomes and intracellular material by fusion with autophagosomes.

Lysosomes are intracellular targets for a number of photosensitizers, such as NPe6 (Reiners et al., 2002). It has been shown that photosensitizers with a net ionic character, particularly with a net charge of  $-2$  or greater, and with greater degrees of aggregation are taken up generally by endocytosis and accumulate in lysosomes (Woodburn et al., 1991; MacDonald et al., 1999). Although these photosensitizers often show a lower phototoxicity, they can still induce cell death after membrane lysis or permeabilization and redistribution of the photosensitizer (Berg et al., 1991; Berg and Moan, 1994; MacDonald et al., 1999). Furthermore, lysosomal damage has also been shown to release cathepsins, which cleave the pro-apoptotic Bid and lead to the induction of mitochondrial-mediated apoptosis (Reiners et al., 2002).

### *1.8.3 Endoplasmic reticulum*

The ER is a netlike labyrinth of tubules and flattened sacs that extend from the outer nuclear membrane into the cytosol and account for approximately 50% of the total membrane surface. The ER has a central role in lipid and protein biosynthesis, as well as  $\text{Ca}^{2+}$  sequestration, storage and release. The ER synthesizes most secreted and transmembrane proteins and cells can rapidly adjust their protein-folding capacity and protein flux in response to cell differentiation, environmental conditions and the physiological state of the cell (Walter and Ron, 2011).

Subcellular localization to the ER has not received as much interest as photosensitizer localization to other organelles in the past. Notably, a number of photosensitizers have been assigned ER-localization after initial localization studies focused on the mitochondria, such as the clinical photodynamic therapy drug Verteporfin (benzoporphyrin derivative), Photofrin (hematoporphyrin derivative) or Foscan (HPPH) (Runnels et al., 1999; Granville

et al., 2001; Takeuchi et al., 2003; Saenz et al., 2017). For instance, meta-tetra(hydroxyphenyl)chlorin (mTHPC) is a successful second-generation photosensitizer and was discovered post-clinical approval to localize mainly to the ER, which was also contrary to the belief in mitochondria localizing action (Teiten et al., 2003a). Further support for the ability of ER localizing photosensitizer to be efficient photosensitizers was demonstrated with redaporfin, a promising photodynamic therapy agent that has completed Phase II clinical trials (NCT02070432) and induces significant ER stress as its main mode of action, as indicated by the phosphorylation of eukaryotic translation initiation factor 2-alpha (eIF2 $\alpha$ ) or the exposure of calreticulin at the cell surface (Gomes da Silva et al., 2018). Other examples of ER localizing photosensitizers are the cyclic tetrapyrrole derivatives chlorin p6, HPPH and MPPa, DH-II-24, or the naturally occurring anthraquinone derivative hypericin (Sun and Leung, 2002; Ritz et al., 2008; Begum et al., 2009; Lim et al., 2009). The structures of these ER-localizing compounds and of the photosensitizer used in this thesis, Pheophorbide a, are shown in Figure 1.3.

ER photodamage induces a rapid depletion of ER Ca<sup>2+</sup> stores, which was suggested to occur partially by photoinactivation of the sarco/endoplasmic reticulum Ca<sup>2+</sup>-ATPase and by photodamage and by permeation of the ER membrane bilayer (Buytaert et al., 2006a). This Ca<sup>2+</sup> depletion is thought to be specific to ER photodamage as demonstrated with the ER-specific photosensitizers hypericin or redaporfin but it can also be observed with photosensitizers that partially localize to the ER, such as the cyclic tetrapyrrole verteporfin, hematoporphyrin derivative and DH-II-24 (Tajiri et al., 1998; Granville et al., 2001; Ritz et al., 2008; Yoo et al., 2009; Gomes da Silva et al., 2018). The photosensitizer used in this thesis, Pha, has also been reported to increase cytoplasmic Ca<sup>2+</sup> levels (Inanami et al., 1999).

In addition to  $\text{Ca}^{2+}$  release, ER photodamage also induces oxidative stress conditions that can irreversibly damage proteins synthesized at the ER and deregulate protein homeostasis (Gomes da Silva et al., 2018; Kessel, 2018). Protein homeostasis is achieved by a coordination between the unfolded protein response, which regulates expression of genes that mediate ER homeostasis, such as protein folding chaperones, and the endoplasmic-reticulum-associated protein degradation pathway, which degrades irreversibly misfolded proteins by delivering them to the proteasome (Smith et al., 2011; Tabas and Ron, 2011). This system clears mildly oxidized and misfolded proteins, but excessive unfolding can overburden it. In addition, ER photodamage has also been shown to inhibit proteasomes, which prevents endoplasmic-reticulum-associated protein degradation, further promotes accumulation of misfolded proteins and potentiates the toxic effects of ER localizing photosensitizers (Szokalska et al., 2009). Extensive photodamage to the ER may lead to irreversible protein aggregation of many cellular proteins and combined with  $\text{Ca}^{2+}$  depletion from the ER can lead to cell death (Tabas and Ron, 2011).

#### *1.8.4 Nuclear envelope*

The nuclear envelope consists of two closely juxtaposed membranes, termed inner nuclear membrane and outer nuclear membrane, which encapsulate the nuclear lamina and chromatin. The outer membrane is contiguous with the ER, whereas the inner membrane faces the nucleoplasm and connects to proteins making up the nuclear lamina, such as A- and B-type lamins. The nuclear membrane is tethered together by integral membrane proteins, such as the Sun proteins or nesprins, which also function to link the nucleoskeleton and cytoskeleton (LINC complex) (Crisp et al., 2006b). The nuclear envelope is continuously

remodelled during the cell cycle and is important for various cellular processes, such as regulation of gene expression or nuclear positioning and migration (Hetzer et al., 2005).

Early photosensitizer localization studies showed that the nuclear envelope may be an important target of photosensitizers. Specifically, different oligomer mixtures of hematoporphyrin derivative (Photosan III, Photofrin II) or hematoporphyrin derivative enriched with monomers were shown to localize preferentially to the nuclear envelope in a ‘patchy’, discontinuous pattern (Tatsuta et al., 1984; Krammer et al., 1993). Furthermore, Krammer et al. noted photoinduced separation and swelling of the nuclear envelope and subsequent cell death and suggested that the nuclear envelope as an important target of photodynamic processes (Krammer et al., 1993). A subsequent study with Photofrin also showed that the most intensive signal is observed at the nuclear envelope but concluded that intracellular localization of Photofrin remained unclear and contradictory (Saczko et al., 2007).

## **1.9 Cytoplasmic vacuolation of human cells**

In this thesis, we examine the vacuolation of the ER and nuclear envelope in human cells co-treated with *Symphoricarpos occidentalis* extracts or Pha and light. To understand our results, an understanding of cytoplasmic vacuolation in human cells is required.

Vacuoles are commonly observed in plants and fungi, where they serve specific purposes (Klionsky et al., 1990; Wink, 1993). By contrast, most animal cells do not contain vacuoles as organelles and their appearance is an unusual phenomenon that occurs as an adaptive response to limit damage by toxins (Henics and Wheatley, 1999; Shubin et al., 2016). Vacuolation of human cells can be either transient or irreversible (Henics and Wheatley, 1999; Chen et al., 2013; Shubin et al., 2016). For example, certain compounds

containing a lipophilic group and a basic amine, termed cationic amphiphilic drugs, can become trapped and accumulated in lysosomes, which induces an osmotic influx and expansion of the compartment that is reversible upon removal of the compound (Anderson and Borlak, 2006). In contrast, compounds causing excessive protein misfolding and ER stress can induce an irreversible dilation of the ER (Kar et al., 2009; Wang and Chen, 2012; Ram and Ramakrishna, 2014; Jeong et al., 2015; Wang et al., 2017).

### *1.9.1 Vacuolation of the endoplasmic reticulum*

Although vacuolation of the ER had been observed prior, in 2000 Sperandio *et al.* specifically described a type of cell death that was accompanied by the vacuolation of the ER and termed it paraptosis (Sperandio et al., 2000). Since then, a number of other genetic, physiological or pharmacological toxic agents have been reported to induce cytoplasmic vacuolation of the ER and paraptotic cell death. This includes oxidative stress (Yung et al., 2007; Lena et al., 2010; Barilli et al., 2014; Wei et al., 2015), overexpression of several receptors (Castro-Obregon et al., 2002; Sanchez et al., 2002; Wang et al., 2004), growth factor stimulation (Fombonne et al., 2004; Fombonne et al., 2006), viral infections (Monel et al., 2017), heme accumulation (Petrillo et al., 2018) or photodynamic therapy (Kaul and Maltese, 2009; Gomes da Silva et al., 2018; Kessel, 2018). These toxic agents elicit a number of cellular events, including the perturbation of protein and ion homeostasis, the induction of ER stress, and the generation of reactive oxygen species (ROS), which are suggested to act in a feed-forward self-amplified loop (Yoon et al., 2012). It has been suggested that protein accumulation inside the ER and osmotic deregulation of the ER subsequently induce an osmotic influx of water into the ER, leading to its unfolding and vacuolation (Mimnaugh et al., 2006; Yoon et al., 2014c).

Perturbation of protein homeostasis by vacuole-inducing compounds has been shown to occur mainly through the induction of misfolded and/or unfolded proteins in the ER and inhibition of the ER-associated degradation system by proteasomal inhibition. The former may occur by several mechanisms, such as the disruption of sulfhydryl homeostasis, protein oxidation by reactive oxygen species or inhibition of protein folding chaperones (Yoon et al., 2014b; Jeong et al., 2015; Kim et al., 2017). A number of authors have shown that co-inhibition of protein folding chaperones and proteasomal degradation is sufficient to induce ER vacuolation and suggested that the increasing protein concentration in the ER contributes to an osmotic influx of water and dilation of the ER (Mimnaugh et al., 2006; Yoon et al., 2012; Yoon et al., 2014c; Yumnam et al., 2015; Xue et al., 2018). Others have shown that both ER  $\text{Ca}^{2+}$  depletion and influx into mitochondria were crucial to vacuolation and precede the accumulation of misfolded proteins, although solely inducing the depletion of  $\text{Ca}^{2+}$  from the ER by specific inhibition of the sarcoendoplasmic reticulum calcium transport ATPase only induced a few vacuoles or no vacuoles in different experiments (Yoon et al., 2012; Ram and Ramakrishna, 2014; Yoon et al., 2014c; Xue et al., 2018).

ER vacuolation can sometimes be abrogated with  $\text{Ca}^{2+}$  or reactive oxygen species (ROS) scavengers, knockdown of ER and mitochondrial  $\text{Ca}^{2+}$  transporters, or inhibitors of transcription or translation (Yoon et al., 2012; Yoon et al., 2014b; Jeong et al., 2015). However, the effectiveness of these inhibitors varies between vacuole inducing compounds, scavengers and inhibitors, indicating a redundancy in vacuole inducing mechanisms. For example, protein synthesis inhibitors, such as cycloheximide, have been suggested to reduce ER vacuolation by decreasing ER protein folding load and reduce osmotic pressure (Jeong et al., 2015). In contrast, others have demonstrated that cycloheximide does not reduce ER

vacuolation and promoted paraptotic cell death in their experiments (Chen et al., 2008; Jeong et al., 2015; Venkatesan et al., 2016; Wang et al., 2017). A common observation among ER vacuole inducing compounds is the ineffectiveness of inhibitors of autophagy, apoptosis, necrosis or necroptosis to inhibit ER vacuolation, as well as the absence of staining for necrosis with the cell-impermeant chemical, propidium iodide, or for autophagy with lysosomal specific dyes, such as Acridine orange (AO) (Sun et al., 2010; Lee et al., 2015b; Kim et al., 2017).

Related to this thesis, ER vacuolation and subsequent cell death has recently been demonstrated with photosensitizers that specifically localize to the ER, including the cyclic tetrapyrrole derivative redaporfin or the anthraquinone hypericin, as well as photosensitizers partially localizing to the ER, such as the cyclic tetrapyrrole derivatives mTHPC, Photofrin and HPPH (Gomes da Silva et al., 2018; Kessel, 2018). The authors suggested that ER localization was required since non-ER localizing photosensitizers did not induce ER vacuolation. However, the mechanism underlying the induction of ER-derived vacuoles in response to ER photodamage has not been clearly described. ER-localizing photosensitizers that induce ER vacuolation are indicated in Figure 1.3.

### *1.9.2 Vacuolation of the nuclear envelope*

Related to the findings presented in this thesis, the nuclear envelope was previously identified as a target of photosensitizer localization (Section 1.8.4) and lamin proteins have been identified as a target of photodamage (Section 1.7.1). As described previously, early research on cyclic tetrapyrroles in the 1980s and 90s suggested that the nuclear envelope is an important target of certain photosensitizers, which resulted in the vacuolation of the nuclear envelope upon photoirradiation (Tatsuta et al., 1984; Krammer et al., 1993). More

recent scientific findings on nuclear envelope vacuolation and results presented in this thesis require an introduction of nuclear envelope vacuolation.

The nuclear envelope consists of two lipid bilayers, encloses the chromatin and connects to the nuclear lamina. Integral membrane proteins, such as Sun1, Sun2, or nesprins, span across the perinuclear space of the nuclear envelope, tethering the two membranes together as part of the LINC complex and connect mainly to lamin A/C in the nuclear lamina (Crisp et al., 2006a). The lamin B receptor is an inner nuclear membrane protein that connects the inner nuclear membrane to lamin B. Nuclear envelope vacuolation was reported in cells expressing various C-terminal truncations and mutations of the lamin B receptor, which are present in the human diseases Pelger-Huët anomaly or Greenberg dysplasia (Zwerger et al., 2010; Funakoshi et al., 2011; Giannios et al., 2017). The lamin B receptor forms higher oligomers and distinct microdomains in the nuclear envelope, and it interacts with both lamin B and chromosomes (Makatsori et al., 2004). The lamin B receptor modifications introduced by Zwerger et al. and others were also found to change its diffusional mobility, lead to its focal aggregation and cause an overload of the nuclear- and the ER-associated degradation system (Tsai et al., 2016; Giannios et al., 2017). Furthermore, in a follow up article to their original findings, Zwerger et al. 2010 concluded that the expression of the lamin B receptor mutants likely promoted an osmotic influx of water into the perinuclear space and the dissociation of proteins that generally confine the constraints of the nuclear envelope (LINC complex), which would subsequently result in a separation of the inner and outer nuclear membrane (Herrmann and Zwerger, 2010). Others have shown that the depletion of Sun proteins of the LINC complex can lead to focal expansions and vacuolation of the nuclear envelope in human HeLa cells and *Caenorhabditis elegans* body wall muscle cells. (Crisp et

al., 2006a; Cain et al., 2014). As these proteins play a role in maintaining an even spacing between the nuclear envelope membranes, the authors suggested that the mechanical pressures on the nucleus in cells depleted of Sun proteins were responsible for the nuclear envelope expansion.

### **1.10 Research aims and objectives**

One of the objectives of cell biology is to understand the basic mechanisms that drive human cells, including mechanisms by which cells respond to toxic stimuli. Natural products with novel biological activities may induce these response mechanisms by interaction with specific cell signalling pathways or disruption of cell homeostasis. Plants have been an abundant source for the discovery of natural products with novel biological activities. Canadian prairie plants have not been investigated extensively for natural products of biological interest. Thus, investigation of these plants may lead to the discovery of compounds with novel biological activities.

When I started this project, it had been observed that extracts prepared from *S. occidentalis* leaves were toxic to human cells and induced several morphological changes, an effect that was retained when plant extracts were subjected to chromatography. Literature information also suggests that *Symphoricarpos* species are toxic and contain several groups of compounds that may be of biological interest. Therefore, I chose to investigate further the effects of *S. occidentalis* on human cells.

To summarize, my objectives were:

1. To confirm the toxicity and morphological changes induced by *S. occidentalis* extracts on HT-29 cells by morphological screening and cell viability assays;

2. To determine whether this effect is a common biological phenomenon in other cell types and characterize the effect in a model cell line;
3. To identify potential compounds that cause the biological effect.

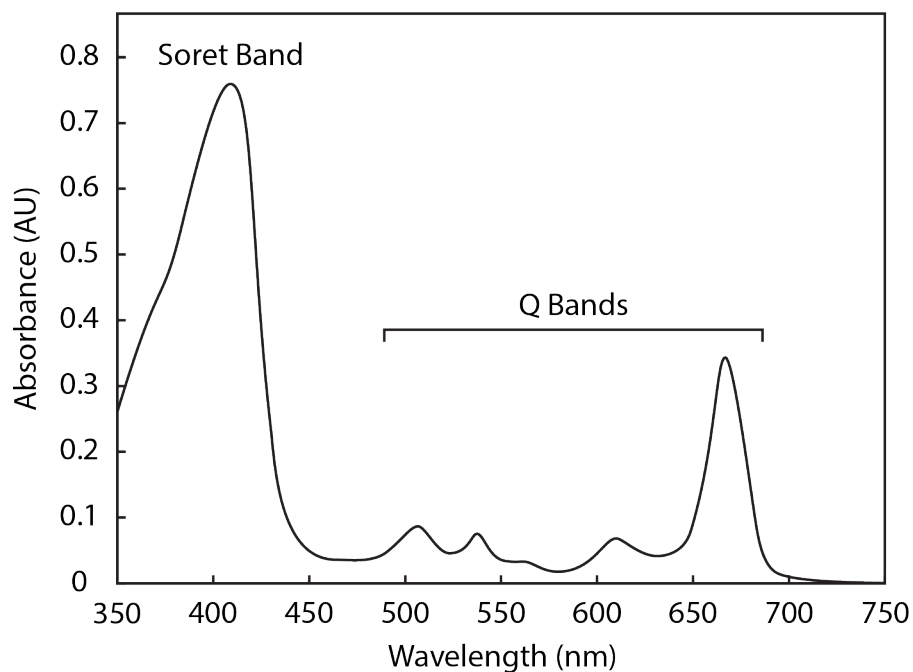


Figure 1.1 A typical absorption spectrum of a cyclic tetrapyrrole photosensitizer. Shown is the typical Soret-band and the four smaller Q-bands, which represent transitions to the second excited state ( $S_2$ ) and the first excited state ( $S_1$ ), respectively. The spectrum shown is of the chlorin cyclic tetrapyrrole, Pheophorbide a (Eichwurz et al., 2000).

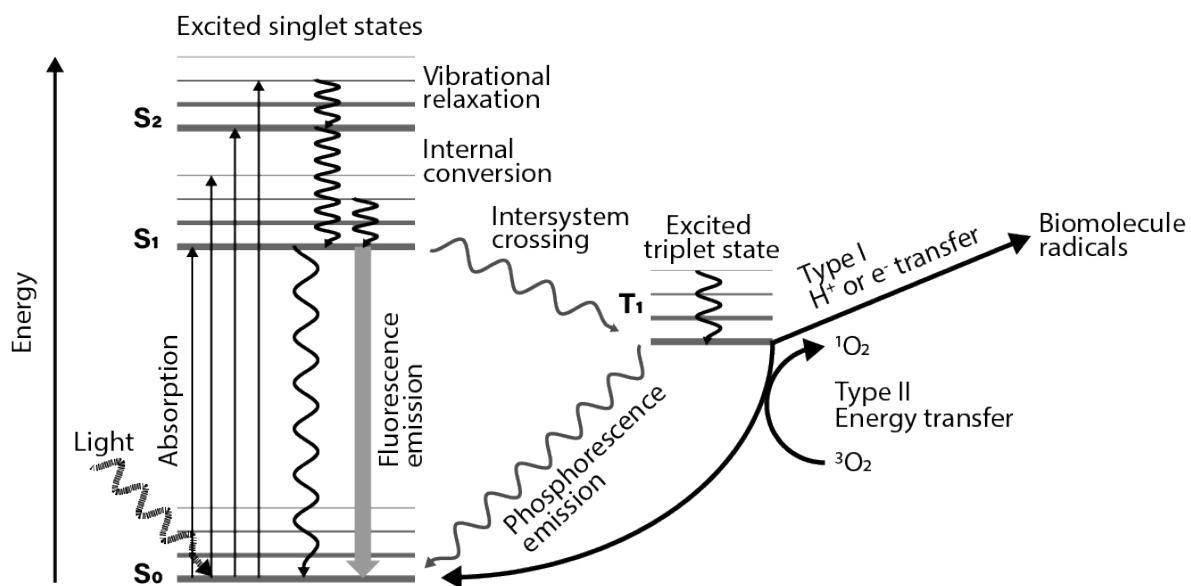


Figure 1.2 A simplified Jablonski diagram showing typical changes in molecular electronic states associated with excitation of photosensitizers. Energy absorbed from light can excite an electron in a compound from the ground state ( $S_0$ ) to an excited singlet state ( $S_1, S_2$ ). Electrons fall to the lowest vibrational level by internal conversion and subsequently to the ground state either directly by further internal conversion or emission of fluorescence, or indirectly by intersystem crossing to a triplet state ( $T_1$ ). From the  $T_1$  state, transition to  $S_0$  occurs either by emission of phosphorescence (unfavoured), or by electron transfer/hydrogen abstraction (Type I) or energy transfer (Type II) to molecular oxygen in its triplet ground state ( $^3O_2$ ) to produce singlet oxygen ( $^1O_2$ ). Adapted from (Abrahamse and Hamblin, 2016).

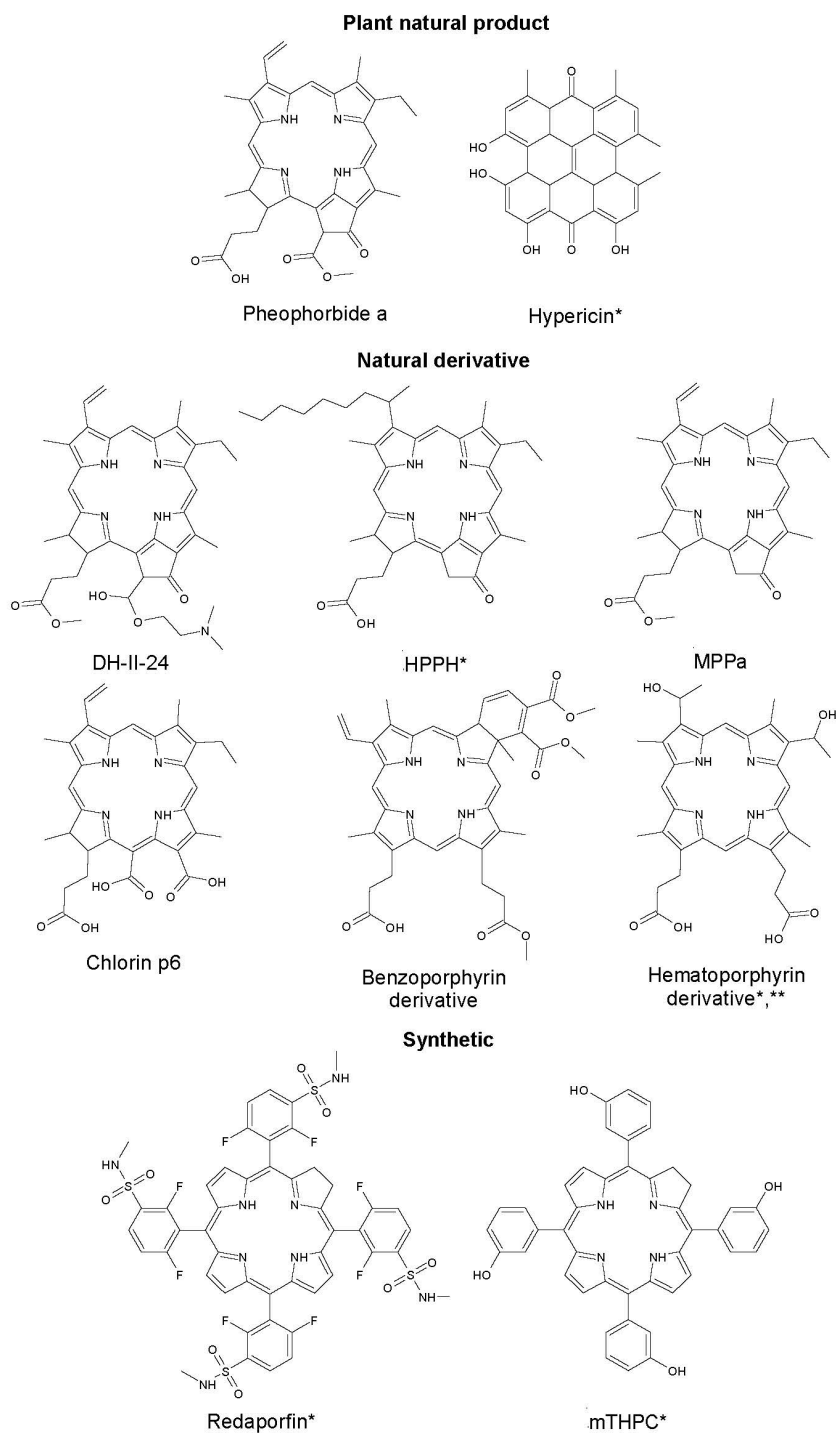


Figure 1.3 Structures of selected natural product, natural derivative and synthetic photosensitizers that localize preferentially or partially to the ER and of the photosensitizer used in this thesis, Pheophorbide a. Indicated are photosensitizers that were reported to induce vacuolation of the ER (\*) and nuclear envelope (\*\*). Benzoporphyrin- and hematoporphyrin derivative are of animal origin and the remaining natural photosensitizer derivatives are of plant origin. HPPH: 2-[1-hexyloxyethyl]-2-devinyl pyropheophorbide-a; MPPa: Pyropheophorbide-a methyl ester; mTHPC: meso-tetrahydroxyphenylchlorin.

## CHAPTER 2 - Materials and Methods

### 2.1 Collection of plants

*Symphoricarpos occidentalis* aerial plant parts were collected on the University of Lethbridge campus in summer 2017. Plant taxonomy was confirmed to species and voucher specimen Golsteyn#630 was provided to the University of Lethbridge Herbarium (Moss, 1932). Information including collection date, site description, associated species and location were stored with a voucher specimen. Plant tissue was collected for future genomic analysis and stored in 20% (w/w) silica gel (Fisher; S161-500) (Doležel et al., 2007). Following the harvest, plants were dried at a maximum temperature of 40°C for three or four days and flower heads, stems and leaves were separated and stored in paper bags at room temperature until use. Additional *Symphoricarpos* species aerial plant parts collected near Riley, AB were provided to the laboratory.

### 2.2 Preparation of plant extracts

Dried plant was prepared into a fine powder using a mechanical blender and a mortar and pestle. The powder was extracted overnight at room temperature in darkness under stirring with 10% ( $w_{\text{extract}}/v_{\text{solvent}}$ ) of either dichloromethane (DCM), 75% ethanol (EtOH) or water (H<sub>2</sub>O). The suspension was then filtered under vacuum (Whatman, No. 5) and the soluble fraction was dried with a rotary evaporator and by drying in a watch glass to give rise to the plant extract. Extracts were weighed, given a code number, and stored in the dark at room temperature until use. For sequential extractions, the insoluble plant material following an extraction was dried in a dark environment overnight at RT and then extracted with the next solvent in the same manner. The sequence of extraction was: 75% EtOH, n-hexane, DCM. To prepare stock solutions for biological assays, extracts were dissolved in dimethyl

sulfoxide (DMSO) to 50 mg/mL. Stock solutions were stored at -20°C in small aliquots to avoid freeze-thaw cycles.

### **2.3 Cell culture**

The human cell lines U2OS, A-172, U-87 MG, MDA-MB-231, A549 and M059K were maintained in Dulbecco's Modified Eagle Medium (DMEM)/F-12 (Gibco; 11320-082) supplemented with 10% (v/v) heat-inactivated fetal bovine serum (FBS) (Gibco; 12484028), 2 mM Modified Eagle Medium non-essential amino acids (MEM-NEAA) (Gibco; 11140050) and 15 mM HEPES (4-(2-hydroxyethyl)-1-piperazineethanesulfonic acid), pH 7.4. The HT-29 cell line was maintained in RPMI 1640 medium (Gibco; 21870-092) supplemented with 10% (v/v) heat-inactivated FBS (Gibco; 12484028) and 1.6 mM GlutaMAX (Gibco; 35050-061). The WI-38 cell line was maintained in DMEM/High glucose (Sigma; D6546) supplemented with 10% (v/v) heat-inactivated FBS (Gibco; 12484028), 2 mM MEM-NEAA (Gibco; 11140050), and 1.6 mM GlutaMAX (Gibco; 35050-061). Cells were grown at 37°C in 5% CO<sub>2</sub> and the media were changed every two-three days. HT-29 cells were plated at 1.0 x 10<sup>6</sup> cells/75 cm<sup>2</sup> flask and cultured for 48 h prior to treatment and the remaining cell lines were plated at 5.0 x 10<sup>5</sup> cells/75 cm<sup>2</sup> flask and cultured for 48 h prior to treatment. Following compounds were dissolved in dimethyl sulfoxide (DMSO; Sigma; D2438) and stored at -20°C: camptothecin (CPT) (10 mM; Sigma; 7689-03-4), nocodazole (200 µg/mL; Sigma; M1404-10MG), staurosporine (1 mM; Cayman Chemical; 81590), Lucifer yellow (1 mg/mL; Electron Microscopy Sciences, 17950), cycloheximide (10 mg/mL; Sigma; C6255), Cyclosporin A (10 mM; Cayman Chemical; 59865-13-3), nocodazole (200 mg/mL; Sigma; M1404) and Pheophorbide a (1 mg/mL; Cayman Chemical; 15664-29-6). DMSO was added as a solvent vehicle control.

## 2.4 Light irradiation

For ambient light incubations, treated cells were incubated in the cell culture room at approximately 2-meter distance of 4 fluorescent light bulbs. LED incubations were performed using LED emitters (LED Engin) specific to 408 nm (LZ4-00UB00-00U8) and 660 nm (LZ4-00R208) at a distance of 10 cm. Radiant exposure ( $\text{J}/\text{cm}^2$ ) was determined based on irradiation time (30 s) and radiant flux of the cell culture dish area ( $\text{W}/\text{cm}^2$ ). Radiant flux (W) was determined based on the typical normalized radiant flux over electrical current curves provided by LED Engin. Electrical current was measured using a power supply (Agilent E3615A) for the 408 nm (1000 mA) and the 660 nm (850 mA) LED at 15 V and 9 V, respectively. Radiant exposure was then regulated using Realterm (v. 2.0.0.70) software changing the LED duty cycle by pulse width modulation using a Teensy microcontroller board (SparkFun; DEV-13305) and a metal-insulator-semiconductor field-effect transistor (MOSFET) (ON Semiconductor; MTP3055VL). Instructions, the LED set-up and the code loaded onto the Teensy microcontroller board for pulse width modulation was kindly provided by Mr. Vince Weiler and Dr. Locke Spencer from the University of Lethbridge Department of Physics & Astronomy.

## 2.5 Cell viability assay

The cytotoxicities of CPT and of *S. occidentalis* extracts on HT-29 and U2OS cells were measured by the MTT (3-((4,5)-dimethylthiazol-2-yl)-2,5-diphenyl-tetrazolium bromide) assay (Sigma-Aldrich; M2128). HT-29 cells were plated at  $5 \times 10^5$  cells/96 well culture plate and cultured at  $37^\circ\text{C}$  for 48 h prior to treatment. U2OS cells were plated at  $2.5 \times 10^5$  cells/96 well culture plate and cultured at  $37^\circ\text{C}$  for 48 h prior to treatment. All treatments were performed in triplicate and experiments were performed three times. At 96

h, 20  $\mu$ L of MTT solution (5 mg/mL MTT in phosphate buffered saline (PBS) (137 mM NaCl, 3 mM KCl, 100 mM Na<sub>2</sub>HPO<sub>4</sub>, 18 mM KH<sub>2</sub>PO<sub>4</sub>) was added to the media in each well and the plates were incubated at 37°C for 3.5 h. The media were then aspirated and 100  $\mu$ L MTT solvent (4 mM HCl, 0.1% (v/v) IGEPAL (octylphenoxy polyethoxy ethanol), in isopropanol) was added to each well. Plates were placed on a shaker for 30 minutes in the dark and absorbance was measured at 590 nm using an Epoch microplate spectrophotometer (BioTek) operated by Gen 5.0 software. Data were normalized to 0.1% DMSO and nonlinear regression analysis was performed using log(inhibitor) versus normalized response using a variable slope calculated from the data. Cytotoxicity was reported in IC<sub>50</sub> concentrations; the concentration of the compound that reduced the absorbance of MTT by 50% by comparison to 0.1% (v/v) DMSO treated cells and the mean IC<sub>50</sub> values were calculated from three experiments.

## **2.6 Light microscopy**

HT-29 cells or all other cell lines were seeded at  $5.0 \times 10^4$  or  $2.5 \times 10^4$  cells per mL, respectively. Multi-well plates were prepared at 2, 1, or 0.5 mL per well for 6-, 12-, or 24-well plates, respectively, and incubated at 37°C for 48 h prior to treatment. Images were either captured with an Infinity 1 camera operated by Infinity Capture imaging software (Lumenera Corporation) on an Olympus CKX41 inverted microscope or a Cytation 5 cell imaging multi-mode reader (Biotek) operated by Gen 5 software (v 3.01). For time-lapse video microscopy, images were captured by phase contrast microscopy on a Cytation 5 imaging multi-mode reader (Biotek) operated by Gen 5 software (v 3.01) at 37°C and 5% CO<sub>2</sub>. Images were processed using Adobe Photoshop (CC 2015.0.0) or Image J software (ImageJ; 1.50f) and experiments were performed three times.

## **2.7 Fluorescence microscopy**

U2OS cells were plated on glass coverslips at  $0.5 \times 10^5$  cells/well in a 6 well culture plate or at  $2.5 \times 10^4$  cells/mL of media into 6-, 12-, or 24-well plates at 2, 1 or 0.5 mL/well, respectively, and incubated at 37°C for 48 h prior to treatment. Cells were incubated either with Acridine orange (Allied Chemical; 46005), Nile red (Sigma; 72485), or Propidium iodide (Invitrogen; P1304MP) at 1 µg/mL or 1X ER Cytopainter green (Abcam; 139481) for 15 minutes at 37°C. Nuclei were co-stained with 1 µg/mL Hoechst 33342 (Sigma; B2261) for 15 minutes at 37°C where indicated. To perform fluorescent localization of the plant extract or Pha, unstained cells were observed using a Texas Red filter cube (Biotek; 1225102; Ex:586/15; Em: 647/57). Cells were observed either on an Olympus BX41 microscope using either an Olympus 60x objective with 1.25 numerical aperture or on a Cytation 5 (Biotek) microscope using either an Olympus UPlanFL N 20x objective with 0.45 numerical aperture or an Olympus UPlanFL N 40x objective with 0.60 numerical aperture. Images were captured using an Infinity 3 camera operated by Infinity Capture imaging software (Lumenera Corporation) or Gen5 software (v 3.01) for the Olympus BX41 or Cytation 5 microscope, respectively. Images were prepared using either Adobe Photoshop (CC 2015.0.0) software or Image J software (ImageJ; 1.50f) and experiments were performed three times.

## **2.8 Immunofluorescence microscopy**

U2OS cells were plated into 6-, 12-, and 24-well plates at 2, 1 or 0.5 mL per well, respectively, and incubated at 37°C for 48 h prior to treatment. Treated cells were fixed at room temperature for 20 minutes in 3% (v/v) formaldehyde (Ted Pella Inc.) diluted in PBS. Fixation was quenched with 50 mM NH<sub>4</sub>Cl in PBS and cells were permeabilized for five minutes using 0.2% (v/v) Triton X-100 in PBS and blocked for 30 minutes with 3% (w/v)

BSA in PBS-T (0.1% (v/v) Tween-20 diluted in PBS). Cells were then incubated with primary antibody anti-lamin A/C (Santa Cruz; sc-6215; 1:150) diluted in 3% (w/v) BSA in PBS-T overnight at 4°C. After washing with PBS-T, cells were incubated for 1 h at room temperature with Alexa Fluor 488-conjugated anti-goat secondary antibody (Life Technologies; A11055; 1:150) diluted in 3% (w/v) BSA in PBS-T. Nuclei were then stained with 300 nM DAPI (4',6-diamidino-2-phenylindole) in PBS-T for 15 minutes. After washing with PBS-T, cells were imaged in PBS-T using a Cytation 5 (Biotek) microscope operated by Gen5 software (v 3.01). Images were prepared using either Adobe Photoshop (CC 2015.0.0) software or Image J software (ImageJ; 1.50f) and experiments were performed three times.

## **2.9 Fluorescence intensity analysis**

Images of treated U2OS cells stained with antibodies against lamin A/C were used to determine lamin A/C fluorescence intensity. Straight lines of 150 pixels in length were drawn across nuclei of 30 cells for each treatment and the lamin A/C fluorescence plot profiles were determined by measuring the intensity of each pixel using Image J software (ImageJ; 1.50f). Pixel intensity measurements were then normalized to the lowest and highest pixel intensity across all treatments. Measurements were grouped into intense or not intense staining based on the presence or absence of a lamin A/C peak in the plot profile, respectively. Mean plot profiles were prepared by calculating mean intensities of each pixel and standard deviations of three experiments.

## **2.10 Absorbance and fluorescence spectral scanning**

Absorbance and spectral analyses were performed on a Cytation 5 Cell Imaging Multi-Mode Reader (Biotek). Extracts or Pheophorbide a were dissolved at 500 µg/mL or

10 µg/mL in DMSO, respectively. AO was dissolved at 1 µg/mL in water. Readings were performed in clear, flat bottom and black wall polystyrene 96 well plates (Sigma; CLS3603). Absorbance readings were performed between 280-1000 nm and fluorescence readings were performed between (x+19 nm) to 700 nm, where x is the excitation wavelength. Readings were zeroed to DMSO or water for extracts and Pha or AO, respectively. Experiments were performed three times.

## 2.11 Optical filters

Transmission spectra of SCHOTT filters were plotted according to filter transmission data by SCHOTT. To obtain the transmission spectrum of the Leitz-Wetzlar K580 optical filter (> 580 nm), the filter absorbance was measured using an Ultrospec 2100 pro UV/Visible spectrophotometer (GE Healthcare) and the percent transmission calculated using

$$A = 2 - \log_{10}(\%T), \quad (2.1)$$

where A is the absorbance measured by the spectrophotometer and %T is the percent transmission (Thiers et al., 1959). Curves were prepared using the SCHOTT filter calculation tool in Microsoft Excel software (Biertümpfel, 2017).

## 2.12 Molecular structures

The chemical structures of benzoporphyrin derivative, hematoporphyrin derivative, chlorin p6, DH-II-24, HPPH, MPPa, mTHPC, hypericin, redaporfin and pheophorbide a were drawn in Chems sketch (ACD Labs; 2015.2.5) according to published literature (Nyman and Hynninen, 2004; Yoo et al., 2009; Abrahamse and Hamblin, 2016; Gomes da Silva et al., 2018).

### **2.13 Statistics**

Data and statistical analyses were performed using Prism 5 software (GraphPad; 5.04) and data were plotted as means from three separate experiments  $\pm$  standard errors of the means using Microsoft Excel 2010 software. Data and statistical analyses of fluorescence microscopy intensity data were plotted as mean plot profiles  $\pm$  standard deviation to show the deviation of intensity measurements in each sub-population of the selected cells. One-way ANOVA with Tukey's post hoc analyses were performed on manual cell counts to calculate statistically significant differences between group means. IC50 concentrations were calculated by log(inhibitor) versus normalized response analysis using a variable slope calculated from the data.

## **CHAPTER 3 - Extracts prepared from *S. occidentalis* or the cyclic tetrapyrrole, Pheophorbide a, induce vacuolation of the endoplasmic reticulum and the nuclear envelope upon exposure to ambient light**

### **3.1 Introduction**

Historically plants have been used by humans for medicinal purposes in many different ways and over the last century they have been the source of many natural products that are used as therapeutic drugs or molecular tools. In fact, natural products or their derivatives account for about 65 % of all small-molecule approved drugs over the last 34 years (Newman and Cragg, 2016). Despite extensive studies showing that plants are an excellent source of compounds with biological activities, only a small percentage of the estimated 250,000 to 500,000 existing plant species world wide have been investigated (Hostettmann and Marston, 2002; Cragg and Newman, 2013; Ngo et al., 2013). Furthermore, plant species of the northern ecological zones have been largely overlooked, including the ecological zones of Alberta, which host over 1775 known native and established vascular plant species (Moss and Packer, 1983; Uprety et al., 2012; Kernéis et al., 2015). This is surprising as plants in Alberta ecological zones, such as the prairies, have coevolved with numerous abiotic and biotic stressors, such as a short growing period and grazing herbivores, respectively, which are known inducers of natural product formation (Kliebenstein, 2004; Beaubien and Hamann, 2011; Rosenthal and Berenbaum, 2012; Brunetti et al., 2013).

We chose to investigate the plant *Symphoricarpos occidentalis* for compounds with new biological activities against human cells for the following reasons: there are reports indicating that the plant is toxic upon ingestion; it is a medicinal plant used by Indigenous peoples in Canada to treat a variety of maladies; chemical investigations have indicated the presence of compounds of potential biological interest, and extracts prepared from *S.*

*occidentalis* showed toxicity in preliminary assays against human cells in our laboratory. These features suggest that this species contains compounds with interesting biological properties.

One approach to discover natural products with biological activities against human cells is that of phenotypic assays. These are powerful assays to test compounds in relatively complex biological systems without prior knowledge of the identity of a specific drug target or a hypothesis about a compound's role in treating disease (Lee and Berg, 2013). Phenotypic assays frequently use cell-based assays, such as morphology, viability and proliferation, migration or invasion, secretion, or production of a product and have several advantages compared to target based approaches, such as the detection of synergism between compounds or with environmental factors (Cos et al., 2006; Rautio et al., 2008; Zheng et al., 2013). We chose to screen *S. occidentalis* plant extracts initially by detection of morphological changes in human cancer cells and found that co-treatment of cells with plant extract and light induces the appearance of cytoplasmic vacuoles.

Photosensitizers are compounds that can absorb energy from light and subsequently induce a chemical change in other compounds. The cyclic tetrapyrroles make up the largest group of natural photosensitizers investigated for biological activity and include chlorophyll and various intermediates in chlorophyll metabolism, such as pheophorbide, and other derivatives (Nyman and Hynninen, 2004; Brandis et al., 2006). These compounds contain a large conjugated ring system that causes them to absorb light at specific wavelengths, which give rise to a distinct absorption spectrum that includes a Soret band around 400 nm and Q bands between 500-700 nm. Natural cyclic tetrapyrroles also emit fluorescence between 650-700 nm when excited at the absorption bands. These properties allow their detection by

absorption and fluorescence spectroscopy in a mixture with other compounds, and their subcellular localization by fluorescence microscopy (Roeder et al., 1990; Mangos and Berger, 1997; Eichwurzel et al., 2000).

Photosensitizer activity is strongly dependent on several characteristics, such as subcellular localization, association with membranes or specific proteins, or the type of photoreaction that occurs upon irradiation. The main subcellular targets of cyclic tetrapyrroles are either the ER, mitochondria or lysosomes, and the nuclear envelope has also been proposed as an important target. The ER has become an organelle of interest for photodamage as several successful photosensitizers have been shown to target it, and several mitochondria targeting photosensitizers have been shown to distribute more broadly and target the ER also (Granville et al., 2001; Teiten et al., 2003a; Gomes da Silva et al., 2018). It was recently shown that photosensitizers localizing to the ER, including several cyclic tetrapyrroles, induced its dilation and vacuolation and resulted in a type of cell death termed paraptosis (Gomes da Silva et al., 2018; Kessel, 2018). ER vacuolation and paraptosis are thought to occur in response to ER stress that is induced by a feed-forward, self-amplified loop between ER misfolded protein accumulation, ER  $\text{Ca}^{2+}$  efflux and mitochondrial influx, and ROS generation (Lee et al., 2016; Shubin et al., 2016). ER localization by photosensitizers was shown to be a requirement for ER  $\text{Ca}^{2+}$  depletion and ER vacuolation (Granville et al., 2001; Gomes da Silva et al., 2018; Kessel, 2018).

A number of ER localizing cyclic tetrapyrroles, such as hematoporphyrin derivative, have been suggested to localize also to the nuclear envelope and the authors suggested it as an important target for photosensitizers (Tatsuta et al., 1984; Krammer et al., 1993; Saczko et al., 2007). In particular, it was shown that photodamage to the nuclear envelope induced

the separation of the inner and outer nuclear membrane and an expansion of the nuclear envelope. A similar expansion of the nuclear envelope was also observed when cells either expressed various truncations and mutations of the lamin B receptor, an inner nuclear membrane protein that binds to B-type lamins; or when cells were depleted of Sun proteins, which are part of the LINC complex that regulates spacing between the inner and outer nuclear membrane and binds to A-type lamins (Crisp et al., 2006a; Zwerger et al., 2010; Funakoshi et al., 2011; Cain et al., 2014; Giannios et al., 2017). Furthermore, the ER localizing compound protoporphyrin IX, or the ER localizing photosensitizers hypericin and calphostin C were previously shown to induce the aggregation of A- and B-type lamins, which connect to the LINC complex and lamin B receptor, respectively (Lavie et al., 1999; Chiarini et al., 2008; Singla et al., 2013; Maitra et al., 2015)

In this chapter we will investigate the prairie plant, *S. occidentalis* for compounds with biological activities against human cells. We found that extracts of this plant species induce the vacuolation of the ER and the nuclear envelope in human cells upon exposure to light and that vacuolated cells show an increased lamin A/C signal, particularly at the perinuclear vacuole. Furthermore, we found that the cyclic tetrapyrrole Pha, shows a similar absorption spectrum, and has a similar phenotypic effect on human cells.

## **3.2 Results**

### *3.2.1 Extracts from S. occidentalis leaves are cytotoxic to the HT-29 cell line*

We prepared a series of extracts from *S. occidentalis* leaves using different extraction solvents (Figure 3.1) and tested if they were toxic to human HT-29 cells using the MTT cell viability assay. HT-29 cells were treated with either DMSO (solvent only) or with increasing concentrations of CPT for 96 h, a well-characterized genotoxic natural product, as a positive

control (Hsiang et al., 1985). We also treated cells with increasing concentrations of PP-630-A or PP-630-B for 96 h and determined cell viability by the MTT assay (Figure 3.2). DMSO was not toxic and CPT was toxic with an IC<sub>50</sub> of  $20.2 \pm 4.1$  nM, as expected. The IC<sub>50</sub> value for PP-630-A was  $426.0 \pm 81.4$  µg/mL and the value for PP-630-B was  $154.4 \pm 34.4$  µg/mL. Although both *S. occidentalis* leaf extracts were cytotoxic, the extraction prepared using DCM (PP-630-B) showed approximately three-fold higher toxicity over the EtOH extract. These data revealed that extracts prepared from *S. occidentalis* leaves were toxic to human cells.

### 3.2.2 *Characterization of morphological changes induced by treatment with S. occidentalis extracts*

Based on the toxicities reported by preliminary assays in our laboratory, we also sought to determine whether extracts prepared from *S. occidentalis* induced any phenotypic changes in human cells observed by phase contrast microscopy. We treated HT-29 cells either with DMSO or with 200 ng/mL nocodazole, a compound that induces a rounded phenotype in human cells by arresting cells in mitosis (Vasquez et al., 1997). We also treated cells with 50, 150, and 500 µg/mL of PP-630-A, PP-630-B, or PP-630-C and observed them by phase contrast microscopy. We observed that DMSO treated cells appeared normal, whereas nocodazole treated cells showed a round morphology, as expected (Figure 3.3A). PP-630-A treated cells showed a normal morphology at 50 and 150 µg/mL and we observed aberrant morphologies at 500 µg/mL. PP-630-B treated cells appeared normal at 50 µg/mL, whereas treatment at 150 and 500 µg/mL showed aberrant morphologies. PP-630-C treated cells appeared normal at all concentrations tested. When then observed PP-630-B treated cells at 150 µg/mL at higher magnifications using phase contrast microscopy (Figure 3.3B). DMSO treated cells appeared normal (panel A), whereas cells treated with PP-630-B either

contained large vacuoles (panel B, arrow), small vesicles around the nucleus (panel C, arrow), or they appeared rounded (panel D, arrow) or shrivelled (panel D, arrowhead). These results revealed that extracts prepared from *S. occidentalis* leaves induced aberrant morphologies when applied to HT-29 cells. We chose to investigate further the induction of vacuole-like structures, because there was little scientific information published about this type of morphology in human cells and because there were no data describing compounds from *S. occidentalis* or the taxonomical family Caprifoliaceae that might induce this effect.

Dichloromethane extracts prepared from *S. occidentalis* were difficult to handle due to their sticky nature and showed poor solubilization in DMSO. A sequential extraction of leaves with the non-polar solvent hexane is a common method used to remove non-polar material, including lipids and carotenoids (Lichtenthaler, 1987; Dai and Mumper, 2010). Thus, we prepared a series of extracts from *S. occidentalis* leaves that were sequentially extracted with 75% ethanol, hexane, and DCM. We then treated cells either with DMSO or 200 ng/mL nocodazole for 24 h. In parallel, cells were treated with either 15, 50 or 150  $\mu\text{g}/\text{mL}$  of either PP-630-B, PP-630-D, PP-630-E, or PP-630-F for 24 h and observed by phase contrast microscopy at 24 h. We found that DMSO treated cells appeared normal, whereas nocodazole treated cells showed a round phenotype (Figure 3.4). PP-630-B treated cells appeared normal at 15 and 50  $\mu\text{g}/\text{mL}$  and showed aberrant phenotypes at 150  $\mu\text{g}/\text{mL}$ . PP-630-D and PP-630-E treated cells appeared normal at 15, 50 or 150  $\mu\text{g}/\text{mL}$ . PP-630-F treated cells appeared normal at 15  $\mu\text{g}/\text{mL}$ , but we observed aberrant morphologies at 50 and 150  $\mu\text{g}/\text{mL}$ . Because we repeatedly observed aberrant phenotypes, including the vacuole-like structures, in PP-630-F treated cells at 50  $\mu\text{g}/\text{mL}$  we chose to use this extract in subsequent experiments to investigate the vacuolated phenotype.

### 3.2.3 *The vacuolated phenotype occurs in different cell lines*

We sought to determine whether the vacuolated phenotype was a cellular process that occurs across different cell lines. We acquired seven different cell lines representing four cancer tissues and one normal cell type: brain glioblastomas (A172, U-87 MG, M059K), breast adenocarcinoma (MDA-MB-231), lung carcinoma (A549), bone osteosarcoma (U2OS), and normal lung fibroblasts (WI-38). These seven cell lines and HT-29 cells were treated with either DMSO or PP-630-F at 50  $\mu\text{g}/\text{mL}$  for 24 h and observed by phase contrast microscopy. DMSO treated cells appeared normal in all cell lines tested (Figure 3.5). In contrast, we observed that PP-630-F treatment induced a vacuolated phenotype in each of the cancer cell lines and the WI-38 cells at 50  $\mu\text{g}/\text{mL}$ . These results revealed that the vacuolated phenotype was a biological phenomenon that might be induced by a compound(s) present in *S. occidentalis* extracts. We selected the U2OS cell line for further experiments because we were able to observe the vacuole-like structures easier in this cell type. Furthermore, U2OS cells are a widely used cell line, which became beneficial when comparing our results to those from the literature (Niforou et al., 2008; Beck et al., 2011; Hadjadj et al., 2016).

### 3.2.4 *Cells develop a vacuolated phenotype after imaging at room conditions*

During the course of our experiments, we noticed that the induction of the vacuolated phenotype might be linked to the act of observing of the cells in addition to treatment with *S. occidentalis* extracts. This timing in the observation of cells relative to the appearance of vacuoles suggested that a cell culture parameter might influence the appearance of vacuoles in PP-630-F treated cells. Therefore, we sought to identify this parameter by testing the timing of imaging by light microscopy. We treated separate dishes of U2OS cells with 50  $\mu\text{g}/\text{mL}$  of PP-630-F and imaged them either at 6 h, at 24 h or 48 h and then at subsequent

time points until 72 h. DMSO treated cells were observed at each timepoint and a separate culture of cells treated with 50  $\mu\text{g}/\text{mL}$  of PP-630-F were not observed until 72 h. DMSO treated cells appeared normal at each timepoint and PP-630-F treated cells observed at 72 h also appeared normal (Figure 3.6). PP-630-F treated cells initially observed at 6 h showed a vacuolated phenotype at 24, 30 and 42 h and were dead by 48 h and subsequent timepoints. PP-630-F treated cells initially observed at 24 h showed a vacuolated phenotype only at 42, 48, and 54 h and were dead by 66 h and 72 h. PP-630-F treated cells initially observed at 48 h showed a vacuolated phenotype at 66 and 72 h. These results revealed that the act of observing cells, which is performed by removing a plate from the incubator and placement onto an inverted phase contrast microscope at room conditions (ambient environment), induced the vacuolated phenotype in PP-630-F treated cells.

### *3.2.5 U2OS cells acquire vacuoles in a concentration and ambient incubation duration-dependent manner when treated with PP-630-F*

Having confirmed that the vacuolated phenotype in PP-630-F treated cells required a second event in addition to PP-630-F treatment, we then tested the effects of extract concentration or incubation duration at ambient conditions. We estimated that observation and imaging of cells took 20 minutes at ambient room conditions and our previous experiment demonstrated that ambient exposure at 6 h, followed by observation at 16 h, repeatedly showed the vacuolated phenotype. Thus, we treated U2OS cells either with DMSO and incubated them at ambient conditions for 20 min at 6 h, or treated cells with 50  $\mu\text{g}/\text{mL}$  of PP-630-F and incubated them at standard human cell culture conditions for 20 min at 6 h. U2OS cells were also treated with either 15, 25, or 50  $\mu\text{g}/\text{mL}$  of PP-630-F and incubated at ambient conditions for 20 min at 6 h and observed by phase contrast microscopy at 16 h. DMSO treated cells incubated at room conditions appeared normal by 16 h (Figure

3.7). Cells treated with 50  $\mu\text{g}/\text{mL}$  PP-630-F and incubated at standard conditions also appeared normal at 16 h. We found that cells treated with PP-630-F at 15  $\mu\text{g}/\text{mL}$  and incubated at room conditions appeared normal, whereas cells treated at 25  $\mu\text{g}/\text{mL}$  showed a vacuolated phenotype and treated at 50  $\mu\text{g}/\text{mL}$  were dead. These results revealed that the vacuolated phenotype was induced by co-incubation of PP-630-F treated cells at room conditions and in a concentration-dependent manner. We selected 25  $\mu\text{g}/\text{mL}$  PP-630-F treatment for future experiments.

We next sought to test the relationship between the vacuolated phenotype and the duration of incubation at room conditions. We incubated treated cells at ambient room conditions for increasing durations at 6 h and observed them by phase contrast microscopy at 16 h. U2OS cells were treated either with DMSO and incubated at ambient room conditions for 30 min or with 25  $\mu\text{g}/\text{mL}$  PP-630-F and incubated at standard conditions for 30 min. We also treated cells at 25  $\mu\text{g}/\text{mL}$  and incubated them at ambient room conditions for either 10, 20, or 30 min at 6 h and observed cells by phase contrast microscopy at 16 h. We found that DMSO treated cells incubated at room conditions for 30 min appeared normal at 16 h (Figure 3.7). We also observed that 25  $\mu\text{g}/\text{mL}$  PP-630-F treated cells incubated at room conditions for 10 minutes appeared normal, whereas 20 min incubation induced the vacuolated phenotype, and 30 minutes incubation caused cell death. Together these data suggested that the vacuolated phenotype was dependent on both PP-630-F extract concentration and duration of incubation at room conditions. These experiments were used to set up the treatment protocol for subsequent experiments: treatment of U2OS cells for 6 h, followed by incubation at room condition for 20 minutes and observation by phase contrast microscopy at 16 h. We were now working to characterize two agents that were required to induce

vacuoles in human cells: a compound present in *S. occidentalis* leaves, and an environmental event.

### 3.2.6 *The vacuolated phenotype requires co-treatment with light*

We reasoned that transferring cells from an incubator to the ambient laboratory conditions causes changes in temperature, light exposure or pH. Therefore, we tested if temperature, light, or CO<sub>2</sub> concentration were required for the induction of vacuoles in PP-630-F treated cells. U2OS cells were treated for 6 h and then incubated either at room conditions or at room conditions and either maintained at 37°C, shielded from light (dark), dark and maintained at 5% CO<sub>2</sub>, or dark and maintained at 37°C to determine whether one of these factors would change the induction of the vacuolated phenotype. U2OS cells were treated with either DMSO and incubated at ambient room conditions or with 25 µg/mL PP-630-F and incubated at either at standard or ambient room conditions for 20 min. U2OS cells were also treated with 25 µg/mL and incubated at following conditions: room and 37°C; room and dark; room, dark and 5% CO<sub>2</sub>; room, dark and 37°C. We observed that at 16 h DMSO treated cells appeared normal, PP-630-F treated cells incubated at standard conditions appeared normal and PP-630-F treated cells incubated at room conditions showed a vacuolated phenotype (Figure 3.8A). U2OS cells treated with PP-630-F and maintained at 37°C during room incubation showed the vacuolated phenotype at 16 h, whereas PP-630-F treated cells shielded from light appeared normal. PP-630-F treated cells shielded from light and maintained either at 5% CO<sub>2</sub> or 37°C also appeared normal at 16 h. These results revealed that exposure to light, or light irradiation was likely the environmental parameter to induce a vacuolated phenotype in *S. occidentalis* extract treated cells.

In a separate experiment, we sought to determine whether the *S. occidentalis* extractions prepared with either ethanol or hexane, as well as extract prepared from another plant from our library, *Thermopsis rhombifolia*, which is not from the Caprifoliaceae family, was able to induce the vacuolated phenotype when exposed to ambient light conditions. U2OS cells were treated either with DMSO or 25  $\mu\text{g}/\text{mL}$  PP-630-F and incubated at ambient light conditions for 20 min at 6 h. Cells were also treated with 25  $\mu\text{g}/\text{mL}$  of PP-630-D or PP-630-E and incubated ambient light conditions for 20 min at 6 h. We found that DMSO treated cells appeared normal at 16 h, whereas PP-630-F treated cells appeared vacuolated (Figure 3.8B). PP-630-D or PP-630-E did not show the vacuolated phenotype at 16 h. In a separate experiment, U2OS cells were treated either with DMSO or 25  $\mu\text{g}/\text{mL}$  PP-630-F and incubated at ambient light conditions for 20 min at 6 h. Cells were also treated with 25  $\mu\text{g}/\text{mL}$  of PP-120-F (*T. rhombifolia*), a DCM extract prepared in a similar manner to PP-630-F and incubated ambient light conditions for 20 min at 6 h. We found that DMSO treated cells appeared normal at 16 h, whereas PP-630-F treated cells appeared vacuolated (Figure 3.8C). PP-120-F treated cells did not show the vacuolated phenotype at 16 h. These data revealed that although the vacuolated phenotype required a photoinduction, the photoactive compound(s) were not present in all plant extracts or at the concentration that induces the vacuolated phenotype.

### 3.2.7 Characterization of the photoinduction event in PP-630 treated cells

We reasoned that co-treatment with ambient light may activate compound(s) in *S. occidentalis* extracts or induce biological changes in cells that are then affected by *S. occidentalis* extracts. Hence, we sought to determine whether PP-630-F treated media could be pre-activated by incubation at ambient light or whether cells could be pre-activated by

ambient light incubation prior to PP-630-F treatment. To investigate the first question, we treated U2OS cells either with DMSO or 25  $\mu\text{g}/\text{mL}$  PP-630-F for 6 h and incubated cells at ambient light for 20 min (co-treatment). We also treated U2OS media only with 25  $\mu\text{g}/\text{mL}$  of PP-630-F for 6 h, incubated it at ambient light for 20 min, and added it to U2OS cells (pre-treatment). We found that DMSO treated cells appeared normal, whereas cells co-treated with PP-630-F and ambient light showed a vacuolated phenotype at 16 h, as expected (Figure 9A). Cells that were treated with pre-activated media (pre-treatment) did not show the vacuolated phenotype at 16 h. To investigate the second question, we then incubated U2OS cells at ambient light at different timepoints either before or after PP-630-F treatment and observed them by phase contrast microscopy at 16 h. Cells were treated with DMSO and incubated for 20 min at ambient light for 16 h. Cells were also treated with 25  $\mu\text{g}/\text{mL}$  PP-630-F and incubated for 20 min at ambient light either 2, 1 or 0.5 h prior to treatment, immediately after treatment, or 0.25, 0.5, 1, 2, 4, or 8 h after treatment. DMSO treated cells did not show vacuoles at 16 h (Figure 3.9B). We observed that incubation at ambient light 2, 1, or 0.5 h prior to PP-630-F treatment did not induce a vacuolated phenotype. U2OS cells incubated either immediately after PP-630-F treatment or 0.25 h after treatment also did not show a vacuolated phenotype. U2OS cells that were treated with PP-630-F for 0.5, 1, 2, 4, or 8 h prior to incubation at ambient light developed vacuolated phenotype by 16 h.

We then counted the number of vacuolated cells at 16 h after incubation at ambient light. DMSO treated cells did not develop vacuoles (Figure 9C). As described above, cells incubated at ambient light prior to PP-630-F treatment or immediately after treatment did not induce the vacuolate phenotype. We found that treatment with PP-630-F for 0.25 and 0.5 h prior to incubation at ambient light-induced vacuoles in 1 % and 70 % of cells, respectively.

Treatment with PP-630-F for 1, 2, 4, or 8 h prior to incubation at ambient light all induced vacuoles in approximately 90 % of cells. Overall, these results revealed that cells required treatment with PP-630-F prior to incubation at ambient light and specifically for at least 1 h prior to incubation at ambient light to develop the vacuolated phenotype in 90 % of cells. In subsequent experiments we treated with PP-630-F for 1 h prior to incubation at ambient light for 20 min.

### 3.2.8 *Incubation at ambient light increases cytotoxicity of PP-630 against human cells*

Our initial results suggested that the vacuolated phenotype may be related to the toxicity of PP-630-F against human cells. Therefore, we hypothesized that treatment of cells with increasing concentrations of PP-630-F followed by incubation at ambient light conditions will increase the extract's toxicity against human cells when compared to incubation at standard conditions. Either HT-29 or U2OS cells were treated with either DMSO (solvent only) or with increasing concentrations of CPT for 96 h. We also treated cells with increasing concentrations of PP-630-F and either incubated cells at standard or ambient conditions for 20 min at 1 h. We then determined cell viability by the MTT assay at 96 h. DMSO was not toxic and CPT was toxic with an IC<sub>50</sub> of  $12.8 \pm 4.2$  nM and  $223.0 \pm 58.2$  nM against HT-29 and U2OS cells, respectively (Figure 3.10). The IC<sub>50</sub> value for PP-630-F against U2OS cells was  $65.7 \pm 12.4$  and  $7.8 \pm 0.5$   $\mu\text{g/mL}$  for standard and ambient light incubation, respectively. The IC<sub>50</sub> value for PP-630-F against HT-29 cells was  $26.4 \pm 2.9$  and  $8.1 \pm 1.8$   $\mu\text{g/mL}$  for standard and ambient light incubation, respectively. These results revealed that PP-630-F was cytotoxic against both cell lines, with different potencies, and that toxicity increased when cells were treated under vacuole inducing conditions.

### 3.2.9 *Vacuolated cells are alive as determined by propidium iodide impermeability*

Having established a protocol to induce the vacuolated phenotype, we wanted to investigate its biological characteristics. A first step was to determine whether the vacuolated cells were alive or dead. We incubated cells with the DNA binding dye, propidium iodide (PI), which is impermeant to live cells, and imaged them by fluorescence microscopy (Yeh et al., 1981; Sasaki et al., 1987). U2OS cells were treated with either DMSO or 1  $\mu$ M of staurosporine, a known inducer of cell death, for 24 h (Bertrand et al., 1994). Cells were also co-treated with 25  $\mu$ g/mL PP-630-F and 20 min ambient light for 16 h. We observed that DMSO treated cells did not show PI staining, whereas staurosporine treated cells were dead and stained positive with PI (Figure 3.11). Cells co-treated with PP-630-F and ambient light appeared vacuolated and did not stain with PI. Therefore, these results revealed that the vacuolated cells were alive, enabling us to proceed to characterize this phenotype.

### 3.2.10 *PP-630 and ambient light-induced vacuoles are not acidic or lipid droplets*

At this point we established the vacuolated phenotype as a robust response to PP-630-F and ambient light treated cells and sought to identify the origin of the vacuoles. Literature data indicated that increased cellular autophagy may be observed as vacuoles in cells (Lawrence and Brown, 1992). We used the dye acridine orange (AO), a fluorescent compound that identifies acidic vesicles and allows the detection of autophagy (Thomé et al., 2016). AO fluoresces green when in the cytoplasm and when bound to DNA, and it fluoresces red in acidic environments. Nuclei were stained with the DNA binding dye Hoechst 33342. We treated cells with either DMSO or incubated cells in an amino-acid free medium for 6 h, which is known to induce the accumulation of autophagic vesicles (Munafó and Colombo, 2001). Further, U2OS cells were also co-treated with 25  $\mu$ g/mL PP-630-F and 20 min

ambient light for 16 h to induce the vacuolated phenotype. We observed that AO staining of DMSO treated cells resulted in a green fluorescent nucleus and cytoplasm and small red puncta throughout the cytoplasm (Figure 3.12). U2OS cells incubated in amino acid-free medium for 6 h showed a green fluorescent nucleus and cytoplasm with large, dark puncta around the nuclei in the cytoplasm. We also observed large, red puncta around the nuclei that overlapped with the dark puncta from the green filter. U2OS cells co-treated with PP-630-F and ambient light contained green fluorescent nuclei and cytoplasm with one or large, dark vacuoles around the nucleus and dark puncta in the cytoplasm. We also found some red puncta throughout the cytoplasm that did not overlap with either the large vacuole or puncta observed using the green filter. These results showed that the vacuoles induced by PP-630-F and ambient light co-treatment were not autophagic vacuoles.

Literature indicated that the vacuoles in PP-630-F and ambient light treated cells may represent lipid droplet formation or phospholipid accumulation, which are intracellular lipid or phospholipid inclusions that have been shown to accumulate various stressors or treatments, such as oxidative stress or cationic amphiphilic compounds (Gubern et al., 2009; Lee et al., 2015a; Velázquez and Graef, 2016). We used the dye Nile red, a lipophilic compound that accumulates in lipid droplets (Greenspan et al., 1985). We treated U2OS cells with either DMSO or 100  $\mu$ M oleic acid for 24 h, which induces lipid droplet accumulation (Brasaemle et al., 1997). We also co-treated cells with PP-630-F and 20 ambient light for 16 h. DMSO treated cells appeared normal by phase contrast microscopy and little Nile red fluorescence was detected by fluorescence microscopy (Figure 3.13). Oleic acid treated cells appeared normal with white puncta in the cells by phase contrast microscopy and green fluorescence was observed in cells by fluorescence microscopy. We observed that PP-630-F

and ambient light treated cells showed a vacuolated phenotype by phase contrast microscopy and little Nile red fluorescence was detected by fluorescence microscopy, similar to DMSO treated cell. These results revealed that the PP-630-F and ambient light-induced vacuoles were not lipid droplets.

### 3.2.11 Identification of a photosensitizing compound, Pheophorbide a

Knowing that co-treatment with *S. occidentalis* extracts and ambient light induces a vacuolated phenotype we searched the literature for relevant information. We found that certain compounds, termed photosensitizers, can sensitize cells to light in a process termed photosensitization. We identified the cyclic tetrapyrrole compounds of plant photosensitizers, which include chlorophyll and its derivatives, as potential active compounds in *S. occidentalis* extracts because a small number of semisynthetic cyclic tetrapyrroles have previously been shown to induce vacuolation in human cells. We identified the metabolite derivative, Pheophorbide a (Pha), as a potential candidate as it has previously been shown to be toxic to cells upon light exposure (Hajri et al., 2002). The structure of Pha is shown in Figure 3.14.

### 3.2.12 Co-treatment of Pheophorbide a and ambient light induces a vacuolated phenotype similar to *S. occidentalis* extracts

We have identified the cyclic tetrapyrrole compound Pha as a potential compound in *S. occidentalis* extracts that photosensitizes human cells to light. However, Pha has not been reported to induce cytoplasmic vacuolation. Therefore, we sought to determine whether Pha was able to induce the vacuolated phenotype when co-treated with ambient light. U2OS cells were treated with either DMSO or 25  $\mu\text{g}/\text{mL}$  PP-630-F and either co-treated with 20 min ambient light or not. Cells were also treated with 0.15, 0.5 or 1.5  $\mu\text{g}/\text{mL}$  of Pha and either

co-treated with 20 min ambient light or not. We observed that cells treated with DMSO appeared normal by phase contrast microscopy when co-treated with ambient light or not (Figure 3.15). PP-630-F treated cells did not induce the vacuolated phenotype at 16 h, whereas cells co-treated with PP-630-F and ambient light showed the vacuolated phenotype, as expected. Cells treated with either 0.15, 0.5 or 1.5  $\mu\text{g}/\text{mL}$  did not show a vacuolated phenotype at 16 h, whereas cells co-treated with light appeared normal at 0.15  $\mu\text{g}/\text{mL}$ , showed a vacuolated phenotype at 0.5  $\mu\text{g}/\text{mL}$  and were dead at 1.5  $\mu\text{g}/\text{mL}$ . These results revealed that Pha and ambient light co-treatment induced a vacuolated phenotype in human cells, similar to PP-630-F treated cells, which was not previously been reported.

### 3.2.13 Absorption and fluorescence spectral scans of *S. occidentalis* leaf extracts show similar spectra to Pheophorbide a.

Chlorin cyclic tetrapyrroles, such as Pha, absorb light strongly around 410 and 660 nm. Hence, we sought to determine whether the active *S. occidentalis* extract absorbs light at these wavelengths. We performed absorption spectral scans on *S. occidentalis* extracts previously tested in phenotypic assays or on Pha by reading the absorbance of dissolved extracts or compounds between 200-1000 nm at 5 nm intervals. We dissolved AO at 1  $\mu\text{g}/\text{mL}$  in water, a common compound with a known absorption maximum of 490 nm in water, as a control (Lyles and Cameron, 2002). We also dissolved Pha at 10  $\mu\text{g}/\text{mL}$  in DMSO and the *S. occidentalis* leaf extracts PP-630-A (EtOH), PP-630-B (DCM), PP-630-C (H<sub>2</sub>O), PP-630-D (seq. EtOH), PP-630-E (seq. HEX), PP-630-F (seq. DCM), and of PP120-C (*T. rhombifolia*, seq. DCM) at 500  $\mu\text{g}/\text{mL}$  in DMSO. The absorption spectra of DMSO (extract and Pha solvent) and water (AO solvent) were read to zero the readings. We found that 1  $\mu\text{g}/\text{mL}$  AO showed a large absorption peak at 490 nm, as expected (Figure 3.16A). Pha showed two large absorption peaks at 415 and 665 nm (Figure 13.6B). We found that PP-630-A showed a peak

at 335 nm, whereas PP-630-B showed peaks at 415 and 665 nm and PP-630-C showed a peak at 335 nm (Figure 3.16C). PP-630-D showed a similar peak to PP-630-A at 340 nm, whereas PP-630-E showed peaks at 415 and 665 nm and PP-630-F showed peaks at 335, 415 and 665 nm (Figure 3.16D). PP-120-C showed peaks at 335, 415 and 665 nm. These results revealed that Pha absorption peaks, identified at 415 and 665 nm, were found in the DCM and hexane extracts but not in the 75% EtOH or water extracts, indicating that Pha or Pha-like structures may be present in these extracts. Based on these results and the vacuole inducing activity of Pha, we continued to investigate the vacuolated phenotype using both PP-630-F and Pha.

#### *3.2.14 Perinuclear origin of vacuolation*

Having shown that a vacuolated phenotype is observed at 16 h, we then sought to determine the origin of the vacuoles. We used time-lapse microscopy and observed cells at 30-minute intervals in the dark after incubation of treated cells at ambient light for 20 min. Cells were treated with either DMSO, 25  $\mu\text{g/mL}$  PP-630-F or 0.5  $\mu\text{g/mL}$  Pha and ambient light co-treatment for 20 min. We found that cells treated with DMSO appeared normal at 0 and 16 h after incubation at ambient light (Figure 3.17). Cells treated with PP-630-F appeared normal at 0 h and showed a vacuolated phenotype at 16 h. We found that cells developed a vacuole at the perinuclear area at 1 h after ambient light incubation, which developed into the large perinuclear vacuole observed at 16 h. Similarly, Pha treated cells appeared normal at 0 h and showed a vacuolated phenotype at 16 h. We found that Pha treated cells also developed a vacuole at the perinuclear area at 1 h after ambient light incubation, which developed into the large perinuclear vacuole observed at 16 h. These results indicated that vacuolation originates at the perinuclear area, which subsequently develops into the large perinuclear vacuole in the vacuolated phenotype.

### 3.2.15 *Pheophorbide a and PP-630 emit fluorescence and localize to the perinuclear area*

We reasoned that if the location of biological activity for PP-630-F or Pha was related to the localization of PP-630-F or Pha, then PP-630-F or Pha should localize to the perinuclear area and colocalize with the vacuoles. Cyclic tetrapyrroles, such as Pha, typically emit fluorescence around 670 nm when excited around 400 or 660 nm (Gerola et al., 2011). Hence, we sought to confirm whether PP-630-F or Pha emitted fluorescence to determine whether PP-630-F or Pha could be visualized by fluorescence microscopy. We performed fluorescence spectral scans on PP-630-F and Pha upon excitation at specific wavelengths detected in the absorption spectra. We dissolved AO to 1  $\mu\text{g}/\text{mL}$  in water, a common dye with a known fluorescence peak at 530 nm when excited at of 492 nm (Lyles and Cameron, 2002). We also dissolved PP-630-F to 500  $\mu\text{g}/\text{mL}$  and Pha to 10  $\mu\text{g}/\text{mL}$  in DMSO and performed fluorescence spectral scans between 350-700, 434-699 and 679-699 nm upon excitation at 335, 415, or 660 nm, respectively. We found that AO showed a fluorescence peak at 529 nm when excited at 490 nm, as expected (Figure 3.18A). Fluorescence spectral scans of PP-630-F showed a fluorescence peak at 674 nm upon excitation at either 335 or 415 nm and no distinct peak when excited at 660 nm (Figure 3.18B-D). Fluorescence spectral scans on Pha showed no peak upon excitation at 335 nm, a fluorescence peak at 610 and 674 nm upon excitation at 415 nm, and no distinct peak when excited at 660 nm (Figure 3.18B-D). These data showed that Pha emits fluorescence at 674 nm when excited at 415 and 660 nm and that PP-630-F shows a similar fluorescent emission at 674 when excited at either 330 or 415 nm but not when excited at at 610 nm.

The emission of fluorescence by PP-630-F or Pha when excited with specific wavelengths provided a rationale to localize the fluorescence of PP630-F or Pha by

fluorescence microscopy. We imaged cells by phase contrast or fluorescence microscopy using a Texas Red filter set (Ex:586/15, Em:647/57), either just prior to incubation at ambient light conditions at 1 h, or 3 h after incubation at ambient light conditions (Figure 3.19). Cells were treated with either DMSO, 25  $\mu\text{g}/\text{mL}$  PP-630-F or 0.5  $\mu\text{g}/\text{mL}$  Pha for 1 h and observed, or treated for 1 h, co-treated with 20 min ambient light and observed at 3 h. We found that DMSO treated cells appeared normal by phase contrast microscopy and did not show any fluorescence by fluorescence microscopy at 3 h. We observed that prior to ambient light incubation, PP-630-F treated cells appeared normal by phase contrast microscopy and fluorescence was observed to be concentrated at the perinuclear area by fluorescence microscopy. At 3 h after ambient light incubation, fluorescence was also located at the perinuclear area and vacuoles developed from the perinuclear area. Similarly, we observed that Pha treated cells appeared normal at 1 h after treatment, and fluorescence was observed at the perinuclear area. At 3 h after incubation at ambient light, fluorescence was also located at the perinuclear area and vacuoles developed from the perinuclear area. These results revealed that the fluorescence of PP-630-F or Pha concentrates at the perinuclear area by the timepoint cells are incubated at ambient light conditions and is also present at the perinuclear area when perinuclear vacuolation originates.

We noted that the vacuoles developing at the perinuclear area in PP-630-F or Pha treated cells at 3 h either originated from the fluorescent area (arrows) or outside of the fluorescent area (arrowheads). We counted the number of vacuoles developing outside of the fluorescent area for DMSO, PP-630-F or Pha treated cells at 3 h after incubation at ambient light and determined the percent of vacuoles that originate outside of the extract or Pha fluorescence (Figure 3.20). We found that DMSO treated cells did not develop any vacuoles.

Vacuoles originated outside of the fluorescent area in either PP-630-F or Pha and ambient light treated cells  $63 \pm 3 \%$  or  $62 \pm 3 \%$ , respectively. These results revealed that vacuolation did not originate from the main fluorescent area in most of the cells.

### *3.2.16 Perinuclear vacuolation is different from a known vacuole-inducing compound, cyclosporine A*

During a literature search, we found that the natural product, cyclosporine A (CsA), had previously been reported to induce a vacuolated phenotype by inducing persistent ER stress and leading to its vacuolation (Zupanska et al., 2005; Ram and Ramakrishna, 2014). Therefore, we sought to compare CsA induced vacuolation to PP-630-F or Pha and ambient light-induced vacuolation by phase contrast microscopy. We imaged cells at 3, 16, and 48 h, when PP-630-F and Pha vacuolation onset was observed, when the PP-630-F or Pha vacuolated phenotype was observed, and when the vacuolated phenotype for CsA treated cells was reported, respectively (Zupanska et al., 2005; Ram and Ramakrishna, 2014). U2OS cells were treated either with DMSO or 20  $\mu$ M CsA for 48 h. Cells were also co-treated with 25  $\mu$ g/mL PP-630-F or 0.5  $\mu$ g/mL Pha and 20 min ambient light at 1 h for 48 h. We found that DMSO treated cells appeared normal at 3, 16, and 48 h (Figure 3.21). We observed that CsA treated cells appeared normal at 3 and 16 h, but showed a vacuolated phenotype at 48 h. PP-630-F and ambient light treated cells showed the onset of vacuolation at 3 h, a vacuolated phenotype at 16 h and dead cells at 48 h. Similarly, Pha and ambient light treated cells showed the onset of vacuolation at 3 h, a vacuolated phenotype at 16 h and dead cells at 48 h. Furthermore, CsA treated cells showed similar smaller vacuoles throughout the cytoplasm but did not show a distinct vacuole located at the perinuclear area, when compared to either PP-630-F or Pha and ambient light treated cells. These results revealed that the

development of a vacuolated phenotype for PP-630-F or Pha and ambient light treated cells was different from CsA induced vacuolation.

### *3.2.17 The vacuolated phenotype shows a dispersed, vacuolated endoplasmic reticulum*

We observed that vacuoles throughout the cytoplasm in PP-630-F or Pha and ambient light treated cells appeared similar to CsA induced vacuoles by phase contrast microscopy (Section 3.2.16). Since CsA induces vacuolation of the ER by inducing persistent stress on the ER, we sought to determine whether vacuolation in PP-630-F or Pha and ambient light treated cells also involved disturbance of the ER (Zupanska et al., 2005; Ram and Ramakrishna, 2014). We used a dye specific to the ER, ER Cytopainter, and observed treated cells by phase contrast and fluorescence microscopy. We treated U2OS cells either with DMSO or 20  $\mu$ M CsA for 48 h. We also treated cells with 25  $\mu$ g/mL PP-630-F or 0.5  $\mu$ g/mL Pha and 20 min ambient light at 1 h for 16 h. We found that DMSO treated cells appeared normal by phase contrast microscopy and fluorescence of the ER dye was located at the perinuclear area by fluorescence microscopy (Figure 3.22). CsA treated cells showed a vacuolated phenotype by phase contrast microscopy and a widely dispersed fluorescence of the ER dye. Furthermore, vacuoles observed by phase contrast microscopy were delineated by the ER dye (Figure 3.22, arrow). Cells co-treated with PP-630-F and ambient light showed a vacuolated phenotype with a large perinuclear vacuole and vacuoles throughout the cytoplasm by phase contrast microscopy. The ER dye appeared dispersed throughout the cytoplasm and delineated the vacuoles, similar to CsA (Figure 3.22, arrows). Similarly, Pha and ambient light treated cells showed a vacuolated phenotype with a large perinuclear vacuole and vacuoles throughout the cytoplasm by phase contrast microscopy. The ER dye also appeared dispersed throughout the cytoplasm and delineated the smaller vacuoles

(Figure 3.22, arrows). We also noted that in PP-630-F or Pha and ambient light treated cells, the large perinuclear vacuoles observed by phase contrast microscopy were not well delineated by the ER-specific dye (Figure 3.22, arrowheads). These results showed that PP-630-F and Pha treated cells showed a dispersed ER similar to CsA treated cells, that the cytoplasmic vacuoles observed by phase contrast microscopy were delineated by the ER dye, and that the large perinuclear vacuoles were not well delineated by the ER dye.

### *3.2.18 The vacuolated phenotype is not inhibited by translation inhibition*

CsA induces vacuolation by persistent stress on the endoplasmic reticulum (ER) and the protein translation inhibitor, cycloheximide (CHX), has previously been shown to significantly reduce the formation of the vacuolated phenotype in CsA treated cells (Zupanska et al., 2005; Ram and Ramakrishna, 2014). Therefore, we sought to determine whether vacuolation induced by co-treatment with either PP-630-F or Pha and light was also reduced when cells were co-treated with CHX. U2OS cells were either co-treated with 10  $\mu\text{g}/\text{mL}$  of CHX or not and then treated either with DMSO or 20  $\mu\text{M}$  CsA for 48 h, or with 200  $\text{ng}/\text{mL}$  nocodazole for 24 h, which is a compound known to arrest cells in mitosis (Vasquez et al., 1997). We also treated cells with 25  $\mu\text{g}/\text{mL}$  PP-630-F or 0.5  $\mu\text{g}/\text{mL}$  Pha and 20 min ambient light for 16 h with or without CHX co-treatment. We observed that DMSO treated cells either co-treated with CHX or not appeared normal at 48 h (Figure 3.23A). Nocodazole treated cells appeared rounded at 24 h and appeared similar to DMSO treated cells when co-treated with CHX. CsA treated cells showed a vacuolated phenotype at 48 h and appeared similar to DMSO treated cells when co-treated with CHX. PP-630-F and ambient light treated cells showed a vacuolated phenotype at 16 h and also co-treated with CHX. Similarly, Pha and ambient light treated cells showed a vacuolated phenotype at 16 h

and also when co-treated with CHX. We then counted the number of vacuolated cells in either DMSO, 20  $\mu$ M CsA, 25  $\mu$ g/mL PP-630-F or 0.5  $\mu$ g/mL Pha and ambient light treated cells either co-treated with CHX or not and calculated the percent vacuolated cells (Figure 3.23B). We found that DMSO treated cells did not induce any vacuoles when co-treated with CHX or not. CsA-treated cells induced vacuoles in  $55 \pm 4$  % of cells, which was significantly different from DMSO treated cells. When co-treated with CHX, we observed significantly reduced vacuolation at  $1 \pm 1$  %, which was not significantly different from DMSO treated cells. PP-630-F and ambient light induced a vacuolated phenotype in  $92 \pm 1$  % of cells and did not significantly change to  $94 \pm 2$  % when co-treated with CHX. PP-630-F treated cells showed a significantly higher percentage of vacuolated cells, both co-treated with CHX or not, when compared to DMSO or CsA treated cells either co-treated with CHX or not. Similarly, Pha and ambient light induced a vacuolated phenotype in  $93 \pm 1$  % of cells, which did not significantly change to  $93 \pm 1$  % when cells were co-treated with CHX. Pha also had a significantly higher percentage of vacuolated cells, both co-treated with CHX or not, when compared to DMSO or CsA treated cells either co-treated with CHX or not. These results revealed that PP-630-F or Pha induced vacuolation occurs in a greater percentage of cells than when cells are treated with CsA. Furthermore, vacuolation was not significantly reduced when PP-630-F or Pha and light treated cells were co-treated with CHX, unlike the CsA treatment.

### *3.2.19 The vacuolated phenotype originates mainly outside of the endoplasmic reticulum*

We previously observed that vacuolation induced in human cells by PP-630-F or Pha and ambient light disperses the ER, yet the large perinuclear vacuoles, which originate at 1 h after ambient light incubation and are not present in CsA treated cells, were not delineated

by the fluorescent ER dye. To investigate this further, we sought to determine whether the perinuclear vacuole develops from the ER by staining treated cells with the ER dye at 3 h after incubation at ambient light and imaging of cells by phase contrast and fluorescence microscopy. We treated U2OS cells either with DMSO, 25  $\mu\text{g}/\text{mL}$  PP-630-F or 0.5  $\mu\text{g}/\text{mL}$  Pha and incubated cells at ambient light for 20 min at 1 h. We found that DMSO treated cells appeared normal by phase contrast microscopy and showed a perinuclear fluorescence of the ER dye at 3 h after incubation at ambient light (Figure 3.24A). At 3 h, PP-630-F treated cells showed the development of a large perinuclear vacuole by phase contrast microscopy and a perinuclear fluorescence of the ER dye. A closer observation showed that vacuoles developed either within the fluorescent area (arrow) or outside the fluorescent area (arrowhead). Similarly, we found that Pha treated cells showed the development of a large perinuclear vacuole by phase contrast microscopy and a perinuclear fluorescence of the ER dye. Vacuoles also developed either within the fluorescent area (arrow) or outside the fluorescent area (arrowhead). We then counted the number of vacuoles developing outside of the fluorescent area in DMSO, PP-630-F or Pha treated cells at 3 h after incubation at ambient light (Figure 3.24B). We found that DMSO treated cells did not develop any vacuoles. Vacuoles developed outside of the ER fluorescent area in either PP-630-F or Pha and ambient light treated cells in  $66 \pm 5 \%$  or  $67 \pm 3 \%$  of cells, respectively. Together, these results revealed that vacuolation originates mostly from outside the ER fluorescent area.

### 3.2.20 *Perinuclear vacuolation induces an increase in lamin A/C signal at the nuclear lamina*

Previous evidence has shown that specific mutations of the lamin B receptor induced a perinuclear vacuolation in U2OS cells that originated from the nuclear envelope and appeared similar to our vacuolated phenotype (Zwerger et al., 2010). Furthermore, hepatic

accumulation of Pha-related compound protoporphyrin-IX in erythropoietic protoporphyria has been shown to induce the aggregation of lamins under ambient light conditions (Maitra et al., 2015). Therefore, we sought to determine whether a connection exists between nuclear lamin aggregation and perinuclear vacuolation. We determined whether nuclear lamina was disrupted in cells treated with PP-630-F or Pha and ambient light using antibodies specific to lamin A/C. U2OS cells were treated either with DMSO, 25  $\mu\text{g}/\text{mL}$  PP-630-F or 0.5  $\mu\text{g}/\text{mL}$  Pha and incubated at ambient light conditions for 20 min at 1 h. We found that DMSO treated cells appeared normal by phase contrast microscopy and showed a homogenous lamin A/C staining by fluorescence microscopy at 16 h (Figure 3.25). In contrast, PP-630-F and ambient light treated cells showed a vacuolated phenotype by phase contrast microscopy and both the nuclear lamina and the nucleus appeared flattened at the location of the perinuclear vacuole. Similarly, we observed that Pha and ambient light treated cells showed a vacuolated phenotype by phase contrast microscopy and the nuclear lamina and nucleus appeared flattened at the location of the perinuclear vacuole.

We then measured the lamin A/C intensity across nuclei of either DMSO, PP-630-F or Pha treated cells and found that a subpopulation of cells treated with PP-630-F (left) or Pha (right) showed more intense lamin A/C staining (Figure 3.26A, green traces). Furthermore, for both PP-630-F or Pha we noted a peak of intense staining, corresponded to intense lamin staining at the location of the perinuclear vacuole (Figure 3.26A, arrows). Another subpopulation did not show intense lamin A/C staining or a peak (red traces) and appeared similar to DMSO treated cells (black traces). We then counted the number of cells with intense lamin staining and reported the percent vacuolated cells with intense staining (Figure 3.26B). We found the DMSO treated cells did not induce any vacuolation or intense

lamin staining, whereas PP-630-F and Pha induced the vacuolated phenotype. We found that PP-630-F or Pha and ambient light-induced intense lamin A/C staining and a peak intensity at the perinuclear vacuole in  $59 \pm 10$  % and  $64 \pm 2$ % of cells, respectively. These results indicated that PP-630-F or Pha and ambient light-induced vacuolation was often associated with intense lamin staining, especially at the nuclear location of the perinuclear vacuoles.

### 3.3 Discussion

In this section we report that extracts from the prairie plant *Symphoricarpos occidentalis* are toxic to human cells and induce cytoplasmic vacuolation of the ER and the nuclear envelope when exposed to ambient light conditions. We also observed an increased lamin A/C signal, particularly at the location of the perinuclear vacuole. Furthermore, we found that the known plant photosensitizer, Pha, induces a similar, photoinduced vacuolation and that extracts of *S. occidentalis* show an absorption and fluorescence spectrum that is typical to cyclic tetrapyrroles.

We investigated the native prairie plant, *S. occidentalis*, for compounds with novel biological activities because it is reported as a medicinal plant by Indigenous peoples in Canada, reported to be toxic upon ingestion, was shown to contain number of compounds of potential biological interest, and contained a biological activity against human cells in initial screening assays in our laboratory (Amyot, 1885; Chavant et al., 1975; Lewis, 1979; Bunjes, 2004). In fact, *S. occidentalis* is listed as a toxic plant in the Canadian Poisonous Plants Information System (Munro, 2000). We tested extractions with three commonly used solvents, water, 75% EtOH and DCM because they extract a wide range of compounds (Eloff, 1998; Dai and Mumper, 2010; Sasidharan et al., 2011). We found that *S. occidentalis* DCM leaf extracts were most toxic to human cells and induced morphological changes in HT-29

cells. Among these morphologies, we observed an unusual morphology in which cells contained large vacuoles. A sequential extraction of leaves with 75% EtOH, hexane and DCM indicated that the bioactive compound was non-polar and retained in the DCM extract. Furthermore, the sequential extraction of *S. occidentalis* leaves with 75% EtOH and hexane also provided a DCM extract with better solubility in our solvent vehicle, DMSO. Thus, we chose this extract for further experiments.

Cytoplasmic vacuolation in human cells is generally reported to occur as an adaptive response to limit damage by toxic insults or viral infections (Henics and Wheatley, 1999; Shubin et al., 2016). Accordingly, we found that *S. occidentalis* extract-induced vacuolation occurred in all cancer cell lines and one normal cell line that we tested, which indicated that the observed cytoplasmic vacuolation could be a common biological phenomenon. This also suggested that *S. occidentalis* extracts likely interact with important cellular pathways. Among the cell lines tested, we found that the vacuolated phenotype was particularly striking in U2OS cells, which is a larger, non-polarized cell line that allowed for easier observation of the phenotype. Furthermore, the U2OS cell line is commonly used, highly characterized and favoured for their fast growth (Niforou et al., 2008; Beck et al., 2011; Hadjadj et al., 2016). Thus, to enable easier characterization of the vacuolated phenotype, we selected this cell line for further experiments.

Using the phenotypic approach, we noted that the extracts worked with our imaging conditions and found that they were critical to the observation of the vacuolated phenotype. Since various environmental conditions, including light, temperature and CO<sub>2</sub> can have effects on human cell culture, we reasoned that removal of cells from the incubator during imaging may induce additional toxic effects on the cells (Zigler et al., 1985; Gregory and

Milner, 1994; Kim et al., 2004). By a process of elimination, we determined that solely the presence of light was responsible for the induction of the vacuolated phenotype. We then eliminated the possibility that light-induced the creation of toxic substances in extract-treated media or that light pre-sensitized cells to the extract. We also showed that a minimum treatment duration was required prior to induction of the activity with light, which indicated that the bioactive compound(s) in the *S. occidentalis* extract required cellular uptake and distribution prior to light activation of the biological activity. Combined, this information guided us to the topic of photosensitization.

Photosensitizers are compounds that induce toxic stress mainly by entering cells by diffusion or endocytosis and subsequently damage macromolecules upon photoactivation with light. These compounds induce chemical changes in other compounds by direct interaction with substrates and by induction of singlet oxygen species, which can result in a variety of cellular effects, such as cell death or autophagy (Agostinis et al., 2011). Furthermore, a photosensitizer's toxicity and the cellular response to the toxic insult are in part dependent on the concentration of photosensitizer or the radiant exposure and oxygen concentration that cells are treated with or exposed to, respectively. Accordingly, our results showed that the *S. occidentalis* extract was toxic both at high extract concentrations or at longer ambient light incubation durations and that light co-treatment increased extract toxicity 10-fold. This provided a strong indication that a phototoxic compound is present in *S. occidentalis*. Notably, another plant in the family Caprifoliaceae, *Lonicera japonica* (Japanese honeysuckle), has previously been reported to contain phototoxicity (Leung et al., 2008). However, the authors did not isolate the photoactive compound or observe a vacuolated phenotype.

A number of phototoxic compounds have previously been identified from plants, including the cyclic tetrapyrrole Pha that is produced during chlorophyll catabolism. Since Pha and several natural Pha derivatives involved in chlorophyll metabolism are known to be phototoxic against human cells, we performed a morphological screen on Pha in our assays (Hörtensteiner and Kräutler, 2011; Xodo et al., 2012). We tested Pha at different concentrations under ambient light co-treatment and found that it induced a vacuolated phenotype similar to *S. occidentalis* extracts and was toxic at a higher concentration. Thus, our results agree with other findings that have previously shown that Pha induces light-dependent cell death (Tang et al., 2006; Radestock et al., 2007; Busch et al., 2009; Rapozzi et al., 2009; Tang et al., 2010; Adzhar Kamarulzaman et al., 2011; Hoi et al., 2012; Xodo et al., 2012; Cheung et al., 2013). Although Pha has not previously been reported to induce a vacuolated phenotype, we found this as a robust response in either *S. occidentalis* extract or Pha treated cells as > 90% of cells showed the vacuolated phenotype when co-treated with light.

Because Pha induced the formation of vacuoles, we then sought to determine whether Pha or other cyclic tetrapyrroles may be present in the *S. occidentalis* extract. We screened *S. occidentalis* extracts for the characteristic absorption bands of cyclic tetrapyrroles at around 400 nm (Soret) and in the green and red spectrum (Q bands) (Gouterman, 1959, 1961; Roeder et al., 1990). Cyclic tetrapyrroles are ubiquitously present in plants as intermediates of chlorophyll metabolism and chlorophyll itself, many of which can be extracted readily with non-polar solvents, such as DCM (Heaton and Marangoni, 1996; Fiedor et al., 2003; Hörtensteiner and Kräutler, 2011). Thus, this correlates with the detection of cyclic tetrapyrrole specific absorption bands in the DCM, sequential DCM and sequential hexane

extracts of *S. occidentalis*, to a lesser extent in the 75% EtOH extract and not in the water extract. This is also supported by the detection of peaks characteristic to cyclic tetrapyrroles in the DCM extract of a species of a different taxonomical family (*T. rhombifolia*) in our results. Furthermore, different cyclic tetrapyrrole photosensitizers, such as Pha and Pha derivatives, have previously been isolated from plant material using either non-polar solvents, such as chloroform, or with repeated 100% EtOH extractions followed by chromatographic isolation (Stermitz et al., 2000; Wongsinkongman et al., 2002; Chan et al., 2006; Ong et al., 2009; Adzhar Kamarulzaman et al., 2011; Tan et al., 2011).

Interestingly, the *S. occidentalis* DCM extract induced the vacuolated phenotype, whereas neither the hexane extract nor the *T. rhombifolia* DCM extract induced the vacuolated phenotype, despite the presence of cyclic tetrapyrrole peaks. Notably, certain plants or extracts have previously been reported to contain cyclic tetrapyrroles with high phototoxicity (Glinski et al., 1995; Shioi et al., 1996; Stermitz et al., 2000; Wongsinkongman et al., 2002; Chan et al., 2006; Ong et al., 2009; Adzhar Kamarulzaman et al., 2011; Tan et al., 2011; Jong et al., 2013). For example, Ong et al. investigated 155 extracts from 93 terrestrial species for photo-toxic activity against human cells and found that only 30 extracts were photoactive, and they stated that the reason for this observation was not clear (Ong et al., 2009). Considering that cyclic tetrapyrroles of different polarity and photoactivity are present in plants and considering the cyclic tetrapyrrole peaks in the absorption spectra of *S. occidentalis* extracts, we reason that the activity of the *S. occidentalis* extract is likely derived from a phototoxic cyclic tetrapyrrole derivative (Wongsinkongman et al., 2002; Brandis et al., 2006). However, it is unlikely that chlorophyll is the phototoxic agent in the *S. occidentalis* extract responsible for cytoplasmic vacuolation due to its high tendency to

aggregate in water and its poor cellular uptake (Semeraro et al., 2018). Hence, we reason that the DCM extraction of *S. occidentalis* may contain either higher concentrations of Pha or Pha related compounds, or higher concentrations of cyclic tetrapyrroles with high phototoxicities when compared to the hexane or 75% ethanol *S. occidentalis* extract or the *T. rhombifolia* DCM extract. In support of this, Villacorta et al. suggested that the abundance of photosensitizing molecules may be a distinctive property of certain plants (Villacorta et al., 2017). However, because extracts are complex mixtures of compounds we cannot make conclusions about the photoactive compound at this point. We have initiated bioassay-guided fractionation of *S. occidentalis* in collaboration with Dr. Raymond Andersen (University of British Columbia) to determine the photoactive compound(s) in *S. occidentalis*.

Having determined that Pha also induces the vacuolated phenotype we then sought to characterize further the vacuolated phenotype. Upregulated autophagic degradation of damaged cellular material or necrotic cell death are two processes that can manifest as vacuolation by light microscopy and both were previously reported in Pha treated cells (Kroemer et al., 2009; Choi et al., 2014; Yoon et al., 2014a). Furthermore, upregulated autophagic degradation was suggested to occur at photosensitizer concentrations and radiant exposures that do not induce immediate cell death, whereas necrosis was suggested to occur at high concentrations and/or radiant exposures that prevent execution of programmed cell death (Piette et al., 2003; Piette, 2015). Oxidative stress has been shown to induce lipid droplet formation, which suggested that the vacuoles may be lipid droplets induced by singlet oxygen species and reactive oxygen species (Gubern et al., 2009; Lee et al., 2015a; Velázquez and Graef, 2016). However, *S. occidentalis* extract or Pha induced vacuoles did

not represent acidic vesicles, lipid droplets, and vacuolated cells did not have a ruptured, necrotic plasma membrane, which indicated a different origin of the vacuoles.

Several ER targeting cyclic tetrapyrrole derivatives and non-cyclic tetrapyrrole photosensitizers have recently been reported to induce vacuolation of the ER and to undergo paraptotic cell death. Paraptosis is a type of cell death that had previously been described for a number of ER stress-inducing compounds, such as cyclosporine A (CsA) (Ciechomska et al., 2013; Ram and Ramakrishna, 2014). We confirmed that CsA induced vacuoles and that vacuoles were derived from the ER. Furthermore, we found that of the *S. occidentalis* or Pha and light-induced vacuoles were also derived from the ER, except the large perinuclear vacuole which did not appear well delineated by the ER dye and suggested a different origin. Since it is commonly regarded that photosensitizer photodamage is correlated to subcellular localization and since others have shown that ER localization is a requirement for ER vacuolation, our results indicate that the ER is an important site of *S. occidentalis* extract or Pha localization and photodamage (Berg and Moan, 1994; Henderson et al., 1997; MacDonald et al., 1999). In support of this, our fluorescence localization studies show that *S. occidentalis* extract or Pha localize to the perinuclear area before light exposure, as well as to the ER-derived membranes after light exposure. Therefore, our results extend previous findings that indicated Pha localizes to the mitochondria and are in accordance with the authors noting a non-mitochondrial, perinuclear localization of Pha (Radestock et al., 2007; Tang et al., 2009a; Bui-Xuan et al., 2010; Hoi et al., 2012). Furthermore, others have shown that Pha was able to induce ER stress and increase intracellular  $\text{Ca}^{2+}$  concentrations in treated human cancer cells (Inanami et al., 1999; Bui-Xuan et al., 2010). These events are typically reported for ER localizing photosensitizers, such as hypericin or redaporfin, which further

supports our suggestion of ER localization by Pha (Teiten et al., 2003b; Buytaert et al., 2006a; Buytaert et al., 2007; Gomes da Silva et al., 2018; Kessel, 2018).

Surprisingly, we found that most of the perinuclear vacuole(s) that developed initially did not originate from the ER dye fluorescence or the fluorescence area of *S. occidentalis* or Pha, and the large perinuclear vacuoles were not delineated by the ER dye. Thus, our results suggested that membranes at the perinuclear area, such as the nuclear envelope, were likely a primary site of *S. occidentalis* extract or Pha photodamage. This suggestion is supported by other localization studies with different oligomeric mixtures of the Pha-related compound hematoporphyrin derivative, which were found to localize to the nuclear envelope, induce the separation of the nuclear envelope membranes, and form of a large vacuole upon irradiation (Tatsuta et al., 1984; Krammer et al., 1993). Furthermore, by a morphology literature search, we identified that U2OS cells expressing specific truncations of the lamin B receptor, an inner nuclear membrane protein, induced a similar vacuolated phenotype in U2OS cells (Zwerger et al., 2010). Specifically, the perinuclear vacuole represented an expansion of the nuclear envelope. Thus, our results and the literature indicated that the perinuclear vacuole originated from the nuclear envelope and that lamins and lamin-associated proteins may be involved in the generation of this vacuole.

It has previously been observed that the ER localizing cyclic tetrapyrrole, protoporphyrin IX, or the ER localizing photosensitizers hypericin and calphostin C induce crosslinking and aggregation of lamin A/C and lamin B1 (Lavie et al., 1999; Chiarini et al., 2008; Singla et al., 2013; Maitra et al., 2015). Considering that specific lamin B receptor mutations induced perinuclear vacuolation and a similar vacuolated phenotype as *S. occidentalis* or Pha, we examined lamin A/C protein by fluorescence microscopy and found

lamin A/C accumulation in the nucleus. Additionally, we showed that lamin accumulation occurred particularly at the site of the perinuclear vacuole, which had not previously been reported and suggests a link between lamin accumulation and expansion of the nuclear envelope.

When we characterized the onset or cause of the vacuolated phenotype by comparison to CsA treated cells, we found that vacuolation occurred earlier and was not inhibited by protein translation inhibition. CsA disrupts protein folding and inhibits ER-associated degradation, leading to the accumulation of ER protein aggregates and deregulation of  $\text{Ca}^{2+}$  homeostasis, which is suggested to induce an osmotic influx of water into the ER and induce vacuolation (Ram and Ramakrishna, 2014). We reason that the difference in vacuolation onset and inhibition by a protein translation inhibitor may be based on a number of differences in the treatments. First, since vacuolation of the nuclear envelope was observed prior to ER vacuolation and since the nuclear envelope and the ER are connected, then ER vacuolation may result from disruption and vacuolation of the nuclear envelope. Lamin A/C accumulation at the location of the perinuclear vacuole may play an important factor in nuclear envelope vacuolation. Second, photodamage by *S. occidentalis* or Pha may induce sufficient ER stress by causing immediate protein misfolding and inhibition of ER-associated degradation over the short duration of light irradiation, likely by singlet oxygen production and direct macromolecule photodamage. In contrast, CsA inhibits cyclophilins, which are important in protein folding, and therefore likely relies on continuous protein synthesis to build up protein aggregation and ER stress (Ram and Ramakrishna, 2014). Accordingly, our results showed the onset of vacuolation between 24-48 h for CsA treated cells, compared to 1 h for *S. occidentalis* or Pha. Third, vacuolation may occur by mechanisms independent of

continuous protein synthesis, which has been shown for a number of compounds, although the authors did not provide any explanations for this (Chen et al., 2008; Jeong et al., 2015; Venkatesan et al., 2016). However, since ER Ca<sup>2+</sup> depletion was suggested by others to play a critical role in ER vacuolation and occur prior to protein accumulation, and since Pha or other ER localizing cyclic tetrapyrroles have previously been shown to induce a rapid cytosolic Ca<sup>2+</sup> increase, it is possible that vacuolation may occur in the absence of protein synthesis for ER localizing photosensitizers by inducing an osmotic imbalance (Yoon et al., 2014c; Jeong et al., 2015; Yumnam et al., 2016). Accordingly, the Ca<sup>2+</sup> chelator BAPTA-AM reduced redaporfin induced vacuolation (Ram and Ramakrishna, 2014; Gomes da Silva et al., 2018). Lastly, recent evidence shows that protein translation inhibition accelerates paraptosis, which demonstrates the complexity of the connection between protein synthesis, protein misfolding, ER vacuolation and paraptosis, and indicates the requirement for further investigations (Wang et al., 2017).

In summary, we conclude that *S. occidentalis* extracts or Pha and exposure to ambient light induce a phototoxic stress on human cells, which results in the vacuolation of the ER and the nuclear envelope, and the accumulation of lamin A/C. Our observations show that this cytoplasmic vacuolation occurs in a number of cancer tissues and normal human cells, which suggests a common biological response to this toxic insult. We have characterized the induction of this phenotype and show that it is dependent on co-treatment with ambient light, treatment concentration and ambient light incubation duration. Co-treatment with ambient light also increases extract toxicity and suggests that vacuolation is followed by cell death, a phenomenon that has previously been proposed for paraptotic cell death. By spectroscopic and phenotypic analyses, we conclude that cyclic tetrapyrroles are likely present in the

photoactive extracts of *S. occidentalis* and *T. rhombifolia* and that specific cyclic tetrapyrroles are likely responsible for cytoplasmic vacuolation induced by the photoactive *S. occidentalis* extract. We propose that the ER and the nuclear envelope are important targets of *S. occidentalis* extract or Pha and that photodamage to these locations induces their vacuolation independent of continuous protein synthesis. Furthermore, we suggest that *S. occidentalis* extract or Pha induce photodamage to structural proteins associated with the nuclear envelope membranes, such as lamins or lamin-associated proteins, which induces the separation of the nuclear envelope membranes and an expansion of the nuclear envelope.

Several important questions remain to be answered based on our results. What is the photoactive compound in *S. occidentalis*? What is the subcellular localization and target of this compound or Pha and how is this target related to cytoplasmic vacuolation? What are the precise events that lead to the vacuolation of either the nuclear envelope or the ER? On the spectrum of cellular responses to increasing photodamage, where is vacuolation located? Which wavelengths of light induce cytoplasmic vacuolation? We have shown that cells are either viable, vacuolated or dead at short, medium and long ambient light incubation durations, respectively. Hence, it is essential to determine the exact wavelengths and radiant energy requirements that induce vacuolation to compare further the *S. occidentalis* extract to Pha and to unravel further the mechanism of photoinduced vacuolation. We address this in the next chapter.

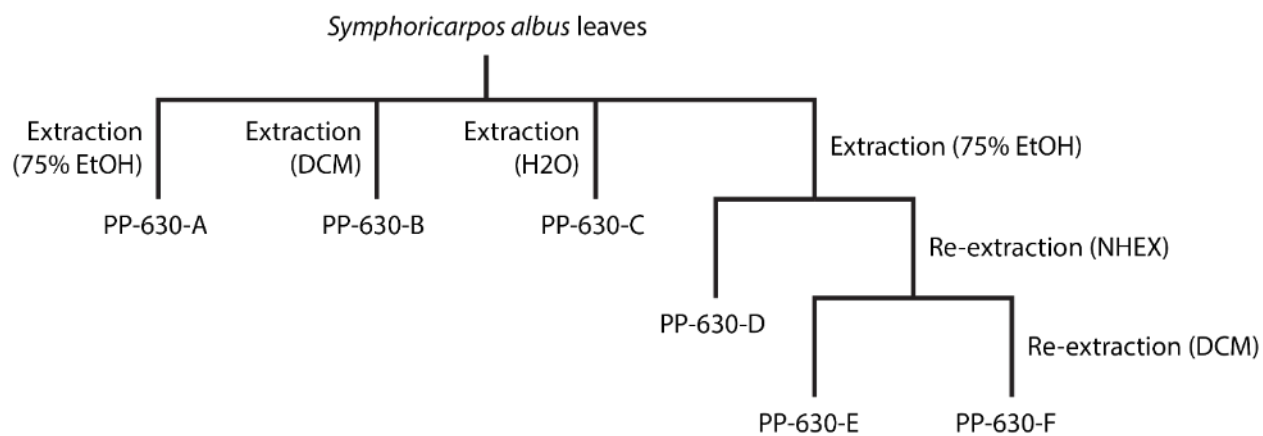


Figure 3.1. Scheme for the extraction of *S. occidentalis* leaves with different solvents and the PP abbreviations used throughout this thesis.

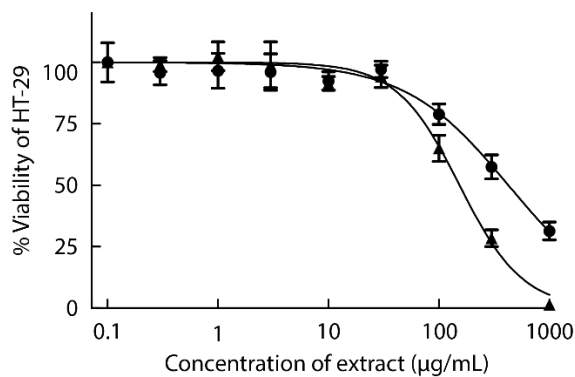


Figure 3.2. Extracts prepared from *S. occidentalis* leaves are toxic to HT-29 cells. HT-29 cells were treated with increasing concentrations of either PP-630-A (75% EtOH; circles) or PP-630-B (DCM; triangles) for 96 h and the cell viability was measured by the MTT assay. Mean percentages of viability were calculated from three experiments and standard errors of the means are shown. The mean IC<sub>50</sub> concentrations of the 75% ethanol extract was  $426.0 \pm 81.4$  µg/mL and of the DCM extract was  $154.4 \pm 34.4$  µg/mL.

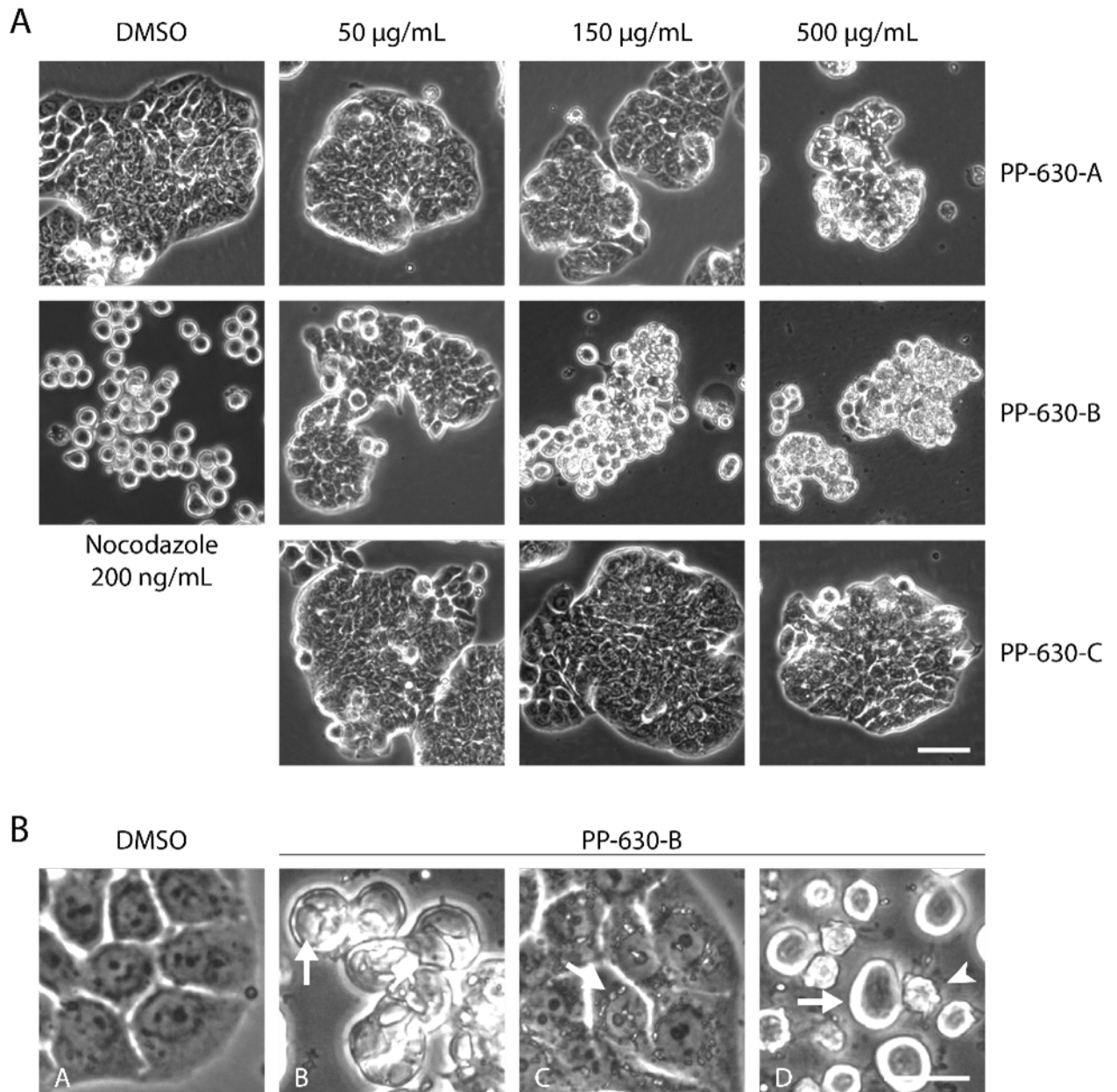


Figure 3.3. *S. occidentalis* leaf extracts induce phenotypic changes in human cells. (A) HT-29 cells were treated with extracts prepared from *S. occidentalis* leaves using 75% ethanol (PP-630-A), dichloromethane (PP-630-B) or water (PP-630-C) and HT-29 cells were treated with 50, 150, or 500  $\mu\text{g/mL}$  (weight of extract per mL of media) of dried extract for 24 h. Cells were treated with DMSO as a negative control and 200 ng/mL nocodazole as a positive control for a morphological change. Scale bar = 50  $\mu\text{m}$ . (B) HT29 cells were treated with either DMSO or 150  $\mu\text{g/mL}$  PP-630-B for 24 h and observed by higher magnifications of phase contrast microscopy. DMSO treated cells appeared normal, whereas PP-630-B treated cells contained either large vacuoles (panel B, arrow), small vesicles around the nucleus (panel B, arrow), or appeared rounded (panel D, arrow) or shrivelled (panel D, arrowhead). Scale bar = 25  $\mu\text{m}$ .

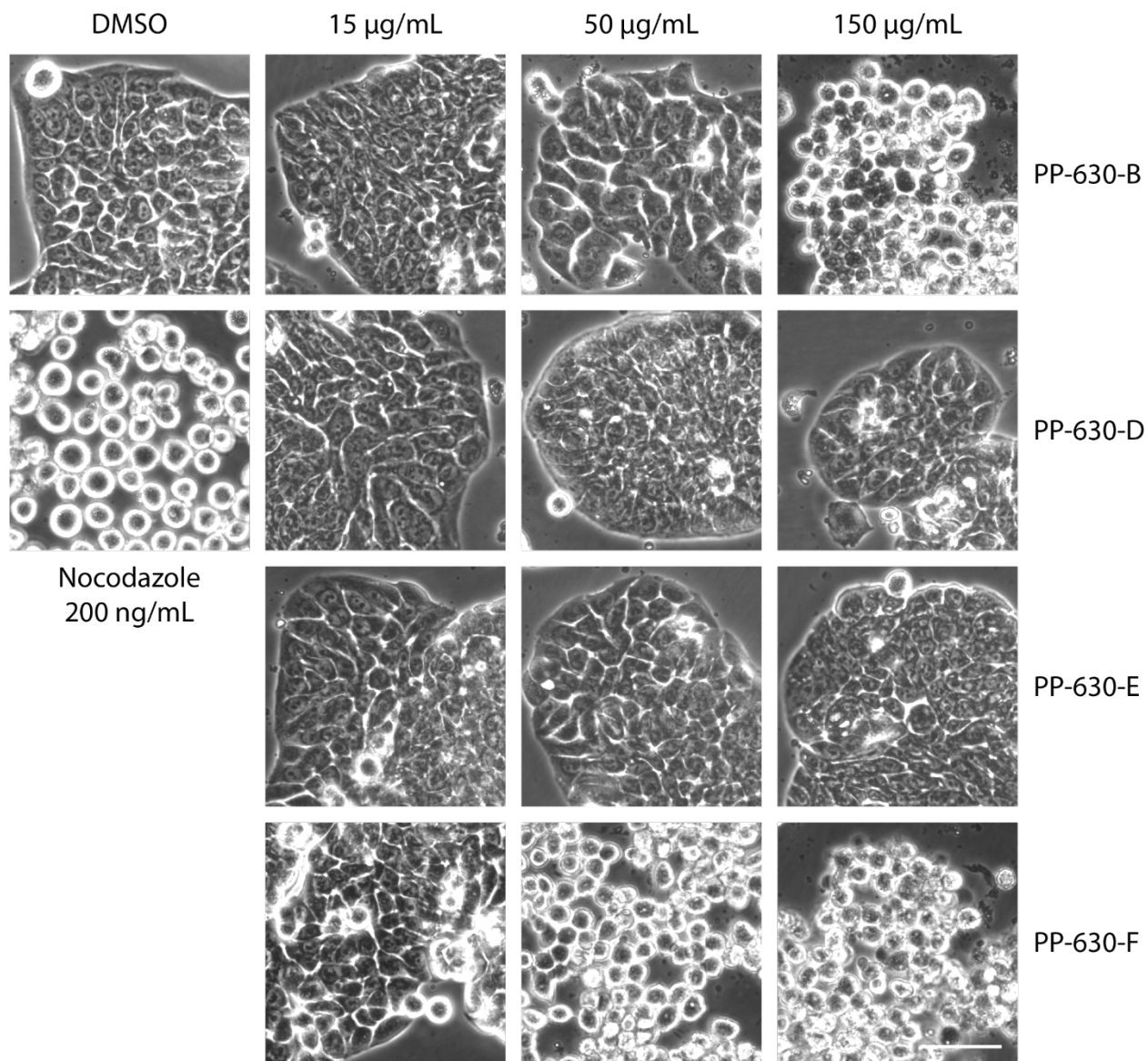


Figure 3.4. Induction of an aberrant morphologies in HT-29 cells is retained in the DCM extract in a sequential extraction of *S. occidentalis* leaves with 75% EtOH, HEX and DCM.

HT-29 cells were treated with either DMSO, 200 ng/ml nocodazole, or 15, 50 or 150  $\mu\text{g/mL}$  of either PP-630-B (DCM), PP-630-D (seq. 75% EtOH), PP-630-E (seq. HEX) or PP-630-F (seq. DCM) for 24 h and observed by phase-contrast light microscopy. Scale bar = 50  $\mu\text{m}$ .

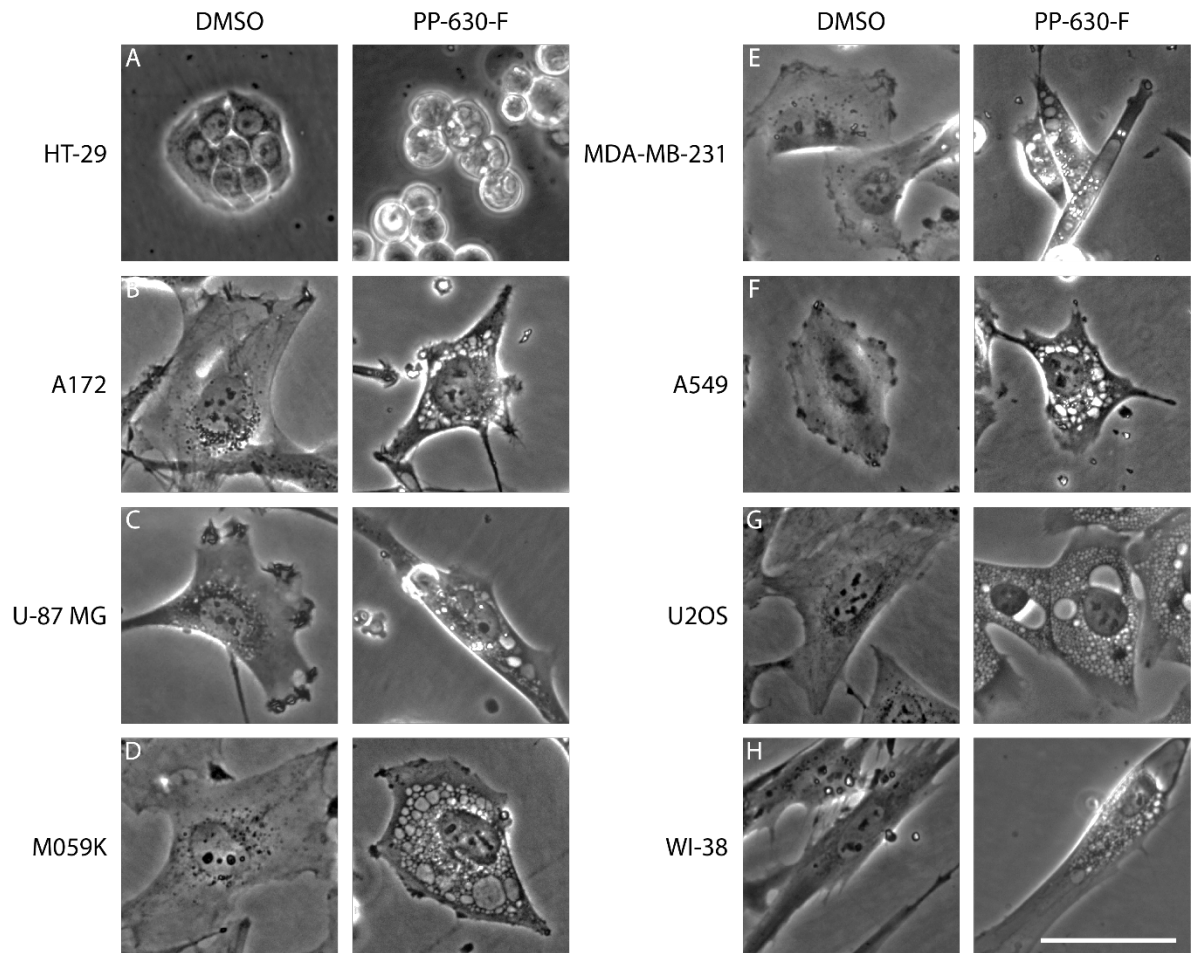


Figure 3.5 *S. occidentalis* leaf extract induces a vacuolated phenotype in different cell lines. (A) HT-29 (colorectal adenocarcinoma), (B) A172 (brain glioblastoma), (C) U-87 MG (brain glioblastoma), (D) M059K (brain glioblastoma), (E) MDA-MB-231 (breast adenocarcinoma), (F) A549 (lung carcinoma), (G) U2OS (bone osteosarcoma) and (H) WI-38 (normal lung fibroblasts). Cells were treated with either DMSO (left) or 50  $\mu\text{g}/\text{mL}$  of PP-630-F (right) and imaged at 24 h by phase contrast microscopy. Scale bar = 50  $\mu\text{m}$ .

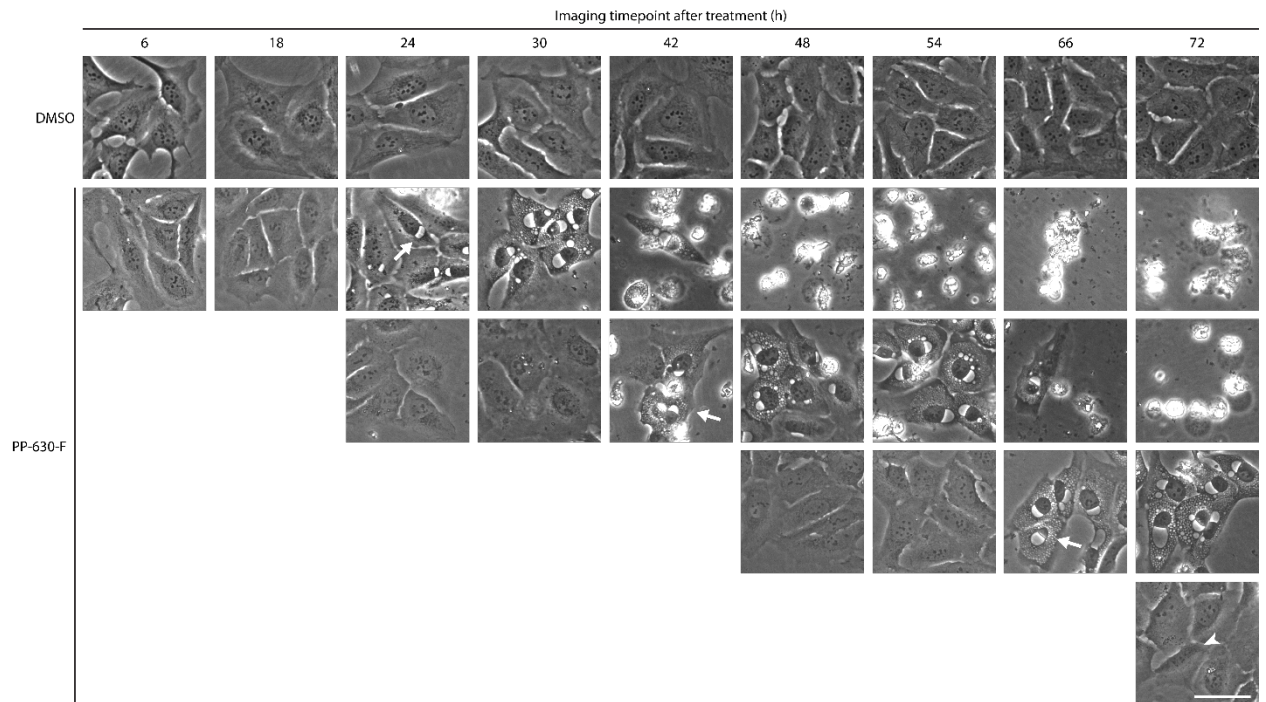


Figure 3.6. Vacuolation is induced in *S. occidentalis* leaf extract treated cells after cells have been imaged by phase contrast microscopy. U2OS cells were treated with either DMSO or 50  $\mu\text{g}/\text{mL}$  PP-630-F and imaged by phase contrast microscopy starting either at 6, 24, 48 or 72 h after treatment. Cells were imaged at indicated time points after the initial imaging. Arrows indicate the onset of the vacuolated phenotype in PP-630-F-treated cells previously imaged. Arrowhead indicates PP-630-F-treated cells at 72 h that did not develop the vacuolated phenotype when not previously imaged. Scale bar = 50  $\mu\text{m}$ .

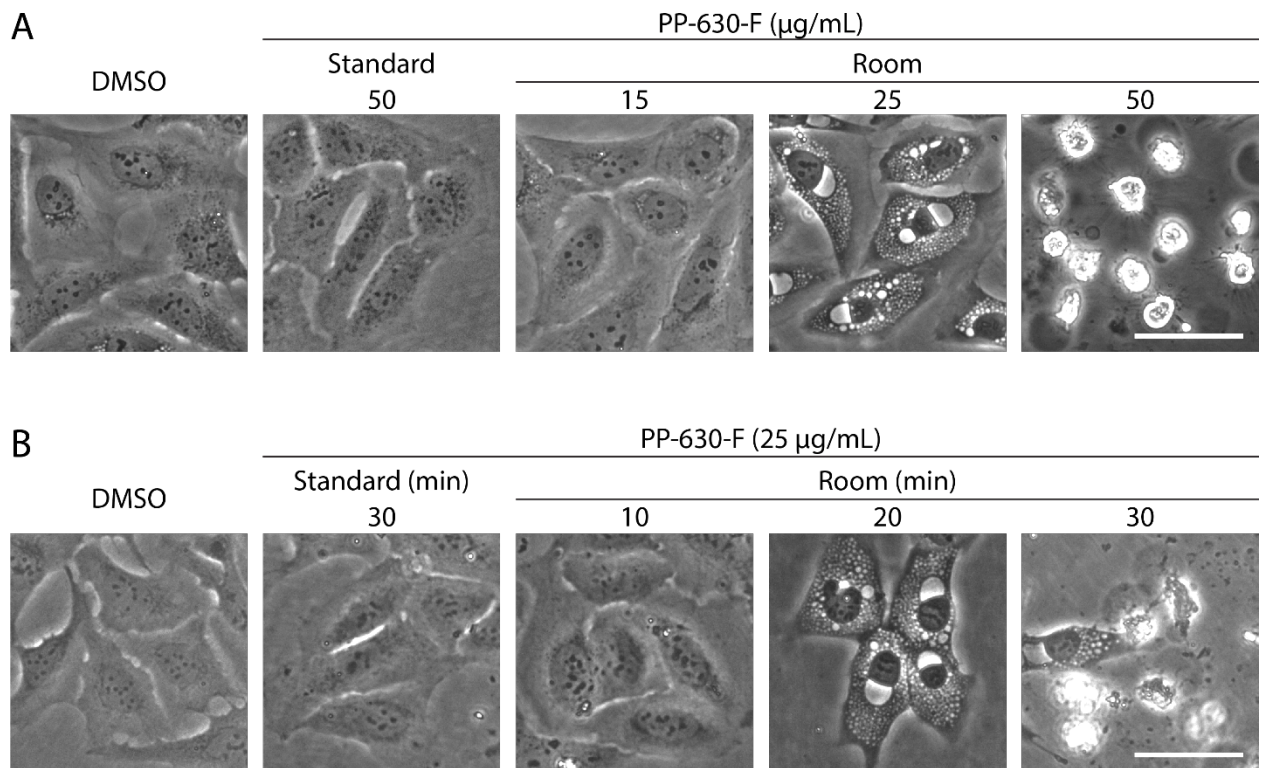


Figure 3.7. Vacuolation of cells is dependent on the concentration of *S. occidentalis* leaf extract and duration of incubation at room conditions. (A) U2OS cells were treated with either DMSO or either 15, 25 or 50  $\mu\text{g/mL}$  of PP-630-F and exposed to room conditions (22°C, atmospheric CO<sub>2</sub>, ambient light) at 6 h for 20 min. U2OS cells treated with 50  $\mu\text{g/mL}$  of PP-630-F were incubated at standard conditions (37°C, 5% CO<sub>2</sub>, dark) at 6 h for 20 min as a negative control. Cells were imaged at 16 h by phase contrast microscopy. Scale bar = 50  $\mu\text{m}$ . (B) U2OS cells were treated with 25  $\mu\text{g/mL}$  of PP-630-F and incubated at room conditions (22°C, atmospheric CO<sub>2</sub>, ambient light) at 6 h for either 10, 20 or 30 min. As a control, U2OS cells treated with DMSO or PP-630-F were incubated at room or standard conditions (37°C, 5% CO<sub>2</sub>, dark) for 30 min, respectively. Cells were imaged at 16 h by phase contrast microscopy. Scale bar = 50  $\mu\text{m}$ .

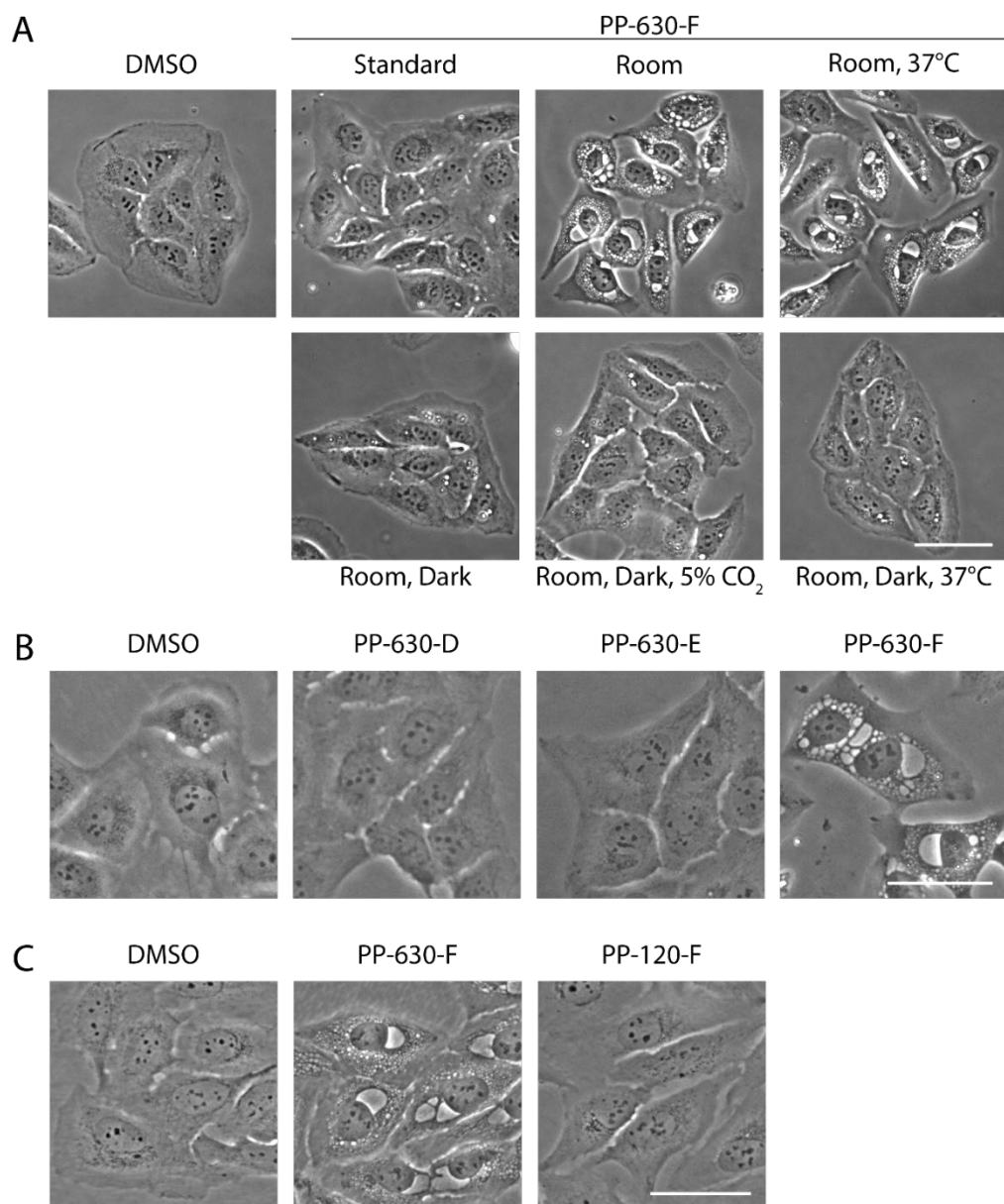


Figure 3.8. Cells acquire vacuoles by co-treatment with PP-630-F and ambient light. (A) U2OS cells were treated with 25  $\mu\text{g}/\text{mL}$  of PP-630-F and incubated at following conditions for 20 min at 6 h: standard (37°C, 5% CO<sub>2</sub>, dark); room (22°C, atmospheric CO<sub>2</sub>, ambient light); room and 37°C; room and dark; room, 5% CO<sub>2</sub> and dark; room, dark and 37°C. DMSO treated cells were exposed to room conditions for 20 min at 6 h as a control. Cells were imaged at 16 h by phase contrast microscopy. Scale bar = 50  $\mu\text{m}$ . (B) U2OS cells were treated with either DMSO or 25  $\mu\text{g}/\text{mL}$  of PP-630-D (75% EtOH), PP-630-E (hexane), or PP-630-F (DCM). Treated cells were exposed to ambient light for 20 min at 6 h and imaged at 16 h by phase contrast microscopy. Scale bar = 50  $\mu\text{m}$ . (C) U2OS cells were treated with either DMSO or 25  $\mu\text{g}/\text{mL}$  of PP-630-F (DCM) or PP-120-F (*T. rhombifolia*; DCM). Treated cells were exposed to ambient light for 20 min at 6 h and imaged at 16 h by phase contrast microscopy. Scale bar = 50  $\mu\text{m}$ .

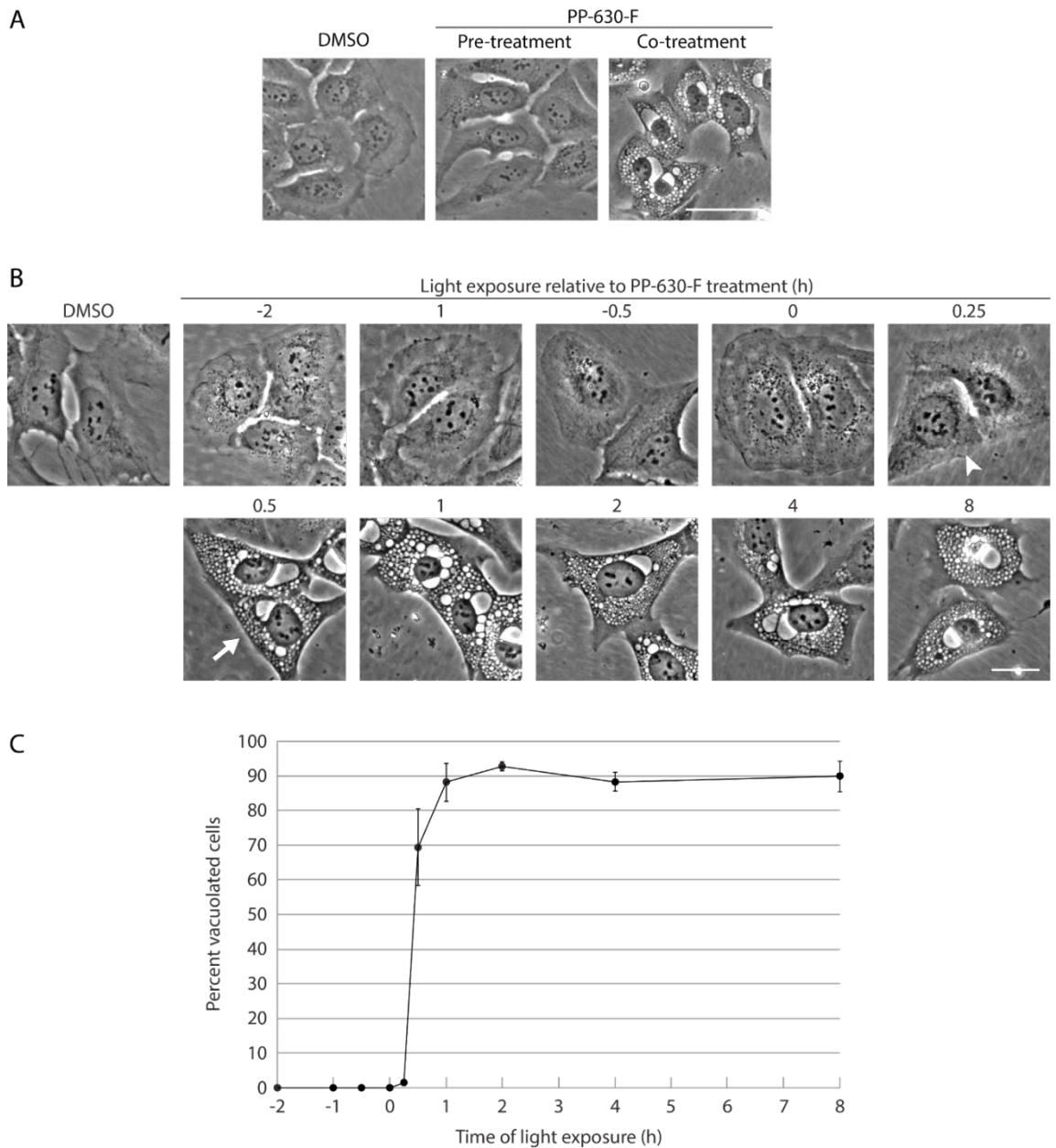


Figure 3.9. Vacuolation requires *S. occidentalis* leaf extract treatment prior to ambient light exposure. (A) U2OS cells were treated with either DMSO or 25  $\mu\text{g}/\text{mL}$  PP-630-F and 20 min ambient light at 6 h, or media that was treated separately with 25  $\mu\text{g}/\text{mL}$  PP-630-F and 20 min ambient light at 6 h and added to cells. Cells were imaged at 16 h by phase contrast microscopy. Scale bar = 50  $\mu\text{m}$ . (B) U2OS cells were either treated with DMSO and 20 min ambient light, or PP-630-F at 25  $\mu\text{g}/\text{mL}$  and incubated at ambient light for 20 min at indicated time points before or after extract treatment. Cells were imaged a 16 h by phase contrast microscopy. Scale bar = 50  $\mu\text{m}$ . (C) Cells in (A) were counted manually as vacuolated (arrow) and non-vacuolated (arrowhead) using Image J software. The mean percent vacuolated cells were calculated from three experiments and standard errors of the means are shown. DMSO treatment did induce any vacuolated cells.

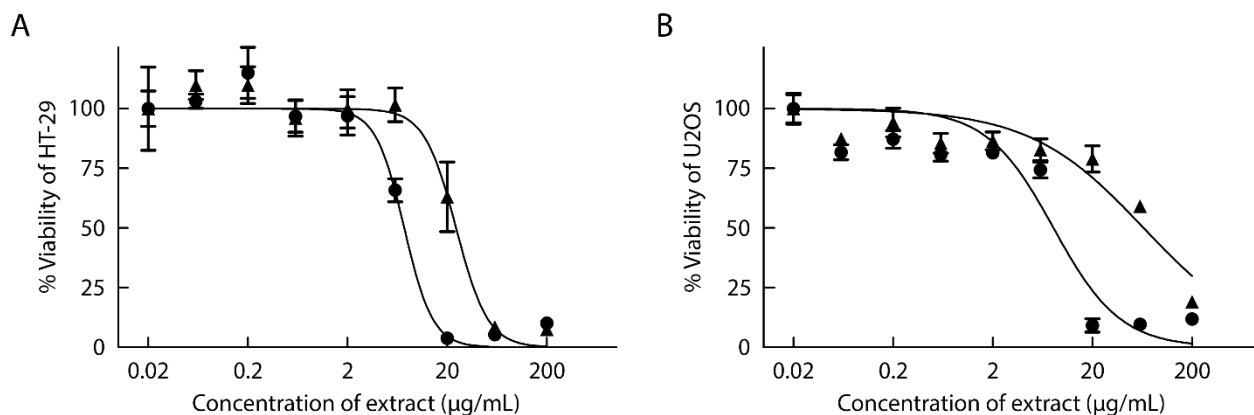


Figure 3.10. Co-treatment with *S. occidentalis* leaf extracts and light increases extract toxicity. (A) U2OS or (B) HT-29 cells were treated with increasing concentrations of PP-630-F for 96 h and either exposed to 20 min of ambient light at 1 h (triangle) or kept in the dark (circle). The MTT assay was used to measure cell viability. Each treatment was run in triplicate and the results from each treatment condition were normalized to treatment with 0.1% (v/v) DMSO. Mean percentages of viability were calculated from three experiments and standard errors of the means are shown. The mean IC<sub>50</sub> concentrations of PP-630-F against U2OS cells was  $8.1 \pm 1.8 \mu\text{g/mL}$  and  $26.4 \pm 2.9 \mu\text{g/mL}$  with and without light, respectively. The mean IC<sub>50</sub> concentrations of PP-630-F against HT-29 cells was  $7.8 \pm 0.5 \mu\text{g/mL}$  and  $65.7 \pm 12.4 \mu\text{g/mL}$  with and without light, respectively.

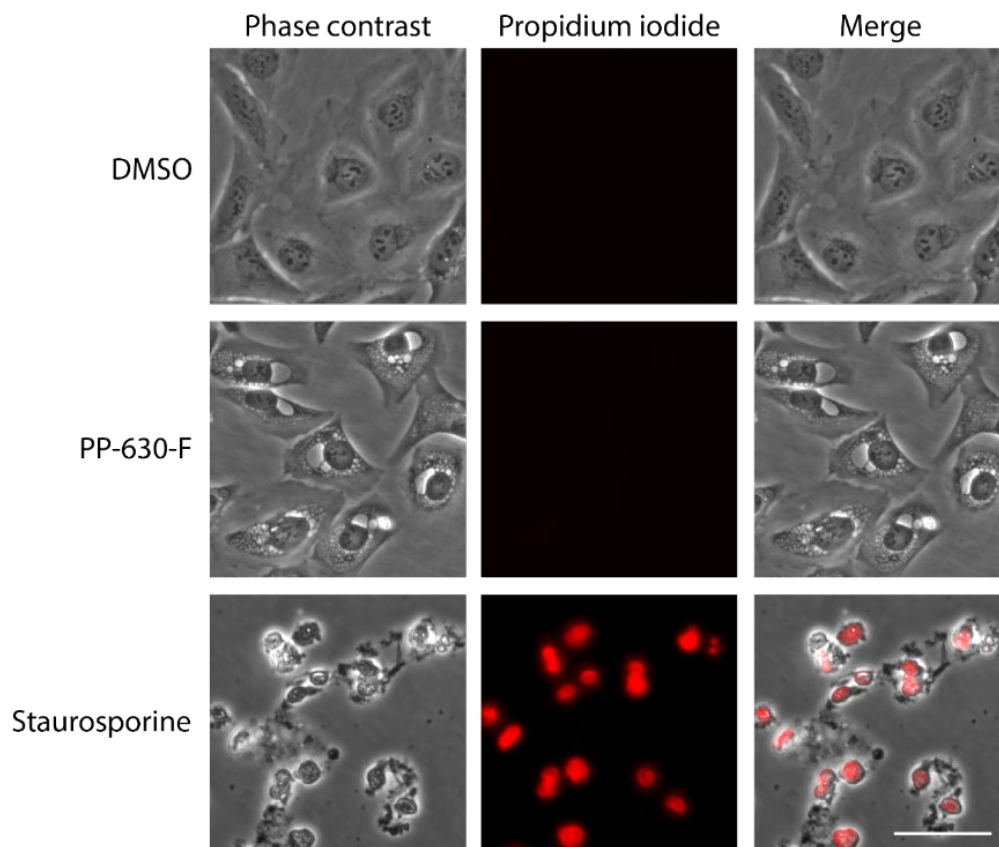


Figure 3.11. Vacuolated cells are alive as determined by staining with the membrane-impermeable dye propidium iodide. U2OS cells were treated with either DMSO, 25  $\mu\text{g/mL}$  PP-630-F and 20 min of ambient light at 1 h or 1  $\mu\text{M}$  staurosporine. Cells were incubated with 1  $\mu\text{g/mL}$  PI for 15 min at 16 h or 24 h for PP-630-F or DMSO and staurosporine, respectively. Cells were imaged by phase contrast and fluorescence microscopy and exposure settings were kept constant throughout. Scale bar = 50  $\mu\text{m}$ .

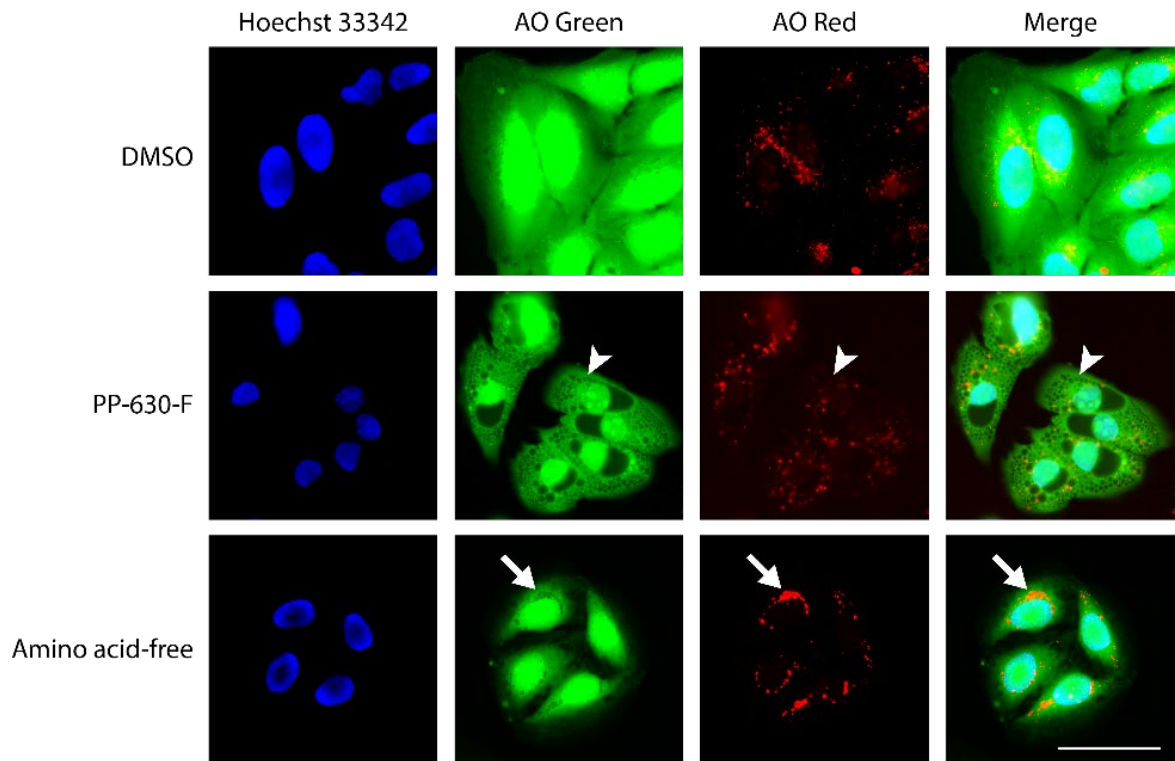


Figure 3.12. *S. occidentalis* leaf extract and light-induced vacuoles are not acidic vesicles as determined by AO staining. U2OS cells were treated with either DMSO or 25  $\mu\text{g}/\text{mL}$  PP-630-F and 20 min of ambient light at 1 h or incubated for 6 h in an amino acid-free solution. Cells were incubated with 1  $\mu\text{g}/\text{mL}$  of AO and Hoechst 33342 for 15 min at 16 h for PP-630-F and DMSO, and at 6 h for the amino acid-free incubation. Cells were imaged by fluorescent microscopy and exposure settings were kept constant throughout. Arrows show fluorescence devoid vacuoles observed with a green filter set filled by fluorescence observed with a red filter set in amino-acid free cultivated cells. Arrowheads show fluorescence devoid vacuoles observed with a green filter set that are not filled by fluorescence observed with a red filter set in PP-630-F treated cells. Scale bar = 50  $\mu\text{m}$ .

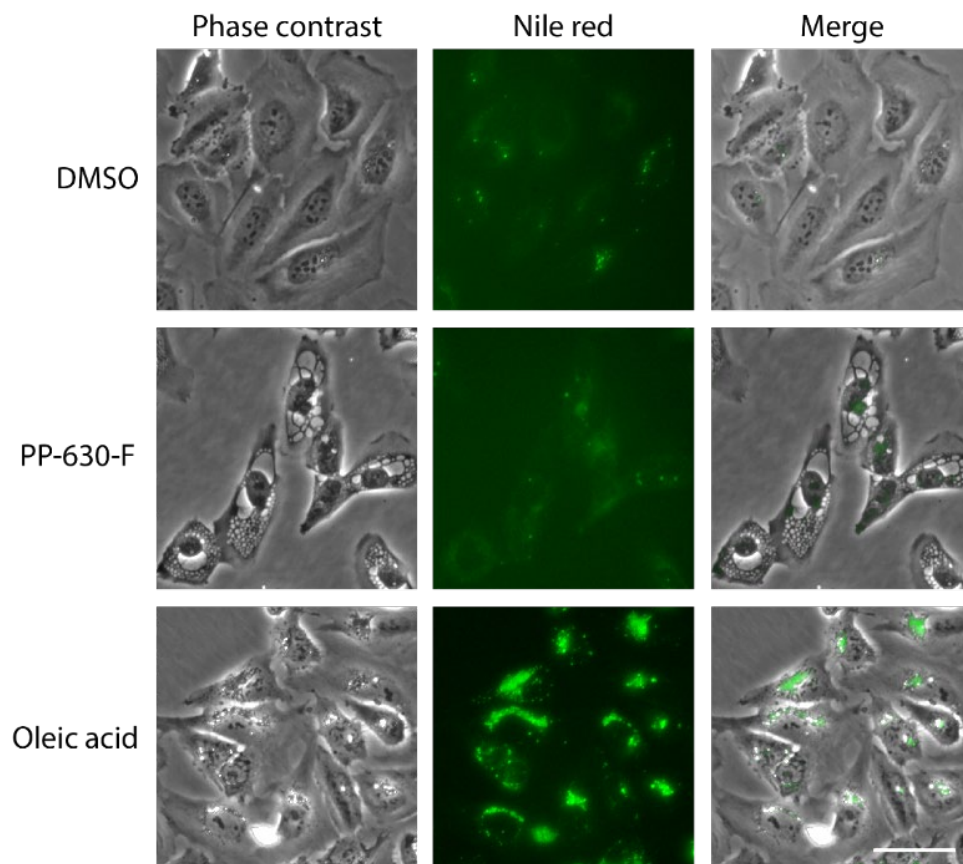


Figure 3.13. *S. occidentalis* leaf extract and light-induced vacuoles are not lipid droplets as determined by Nile red staining. U2OS cells were treated either with 25  $\mu\text{g}/\text{mL}$  PP-630-F and 20 min of ambient light at 1 h for 16 h or with DMSO or 100  $\mu\text{M}$  oleic acid for 24 h.

Cells were incubated with 1  $\mu\text{g}/\text{mL}$  Nile red for 15 min at 16 or 24 h for PP-630-F or DMSO and oleic acid, respectively. Cells were imaged by phase contrast and fluorescent microscopy and exposure settings were kept constant throughout. Scale bar = 50  $\mu\text{m}$ .

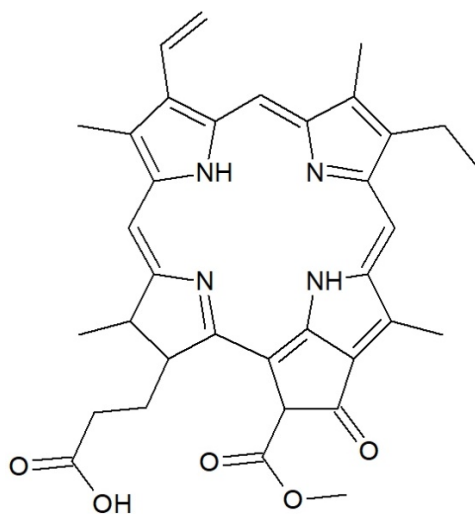


Figure 3.14. The structure of Pheophorbide a. Adapted from Wongsinkongman et al. (2002).

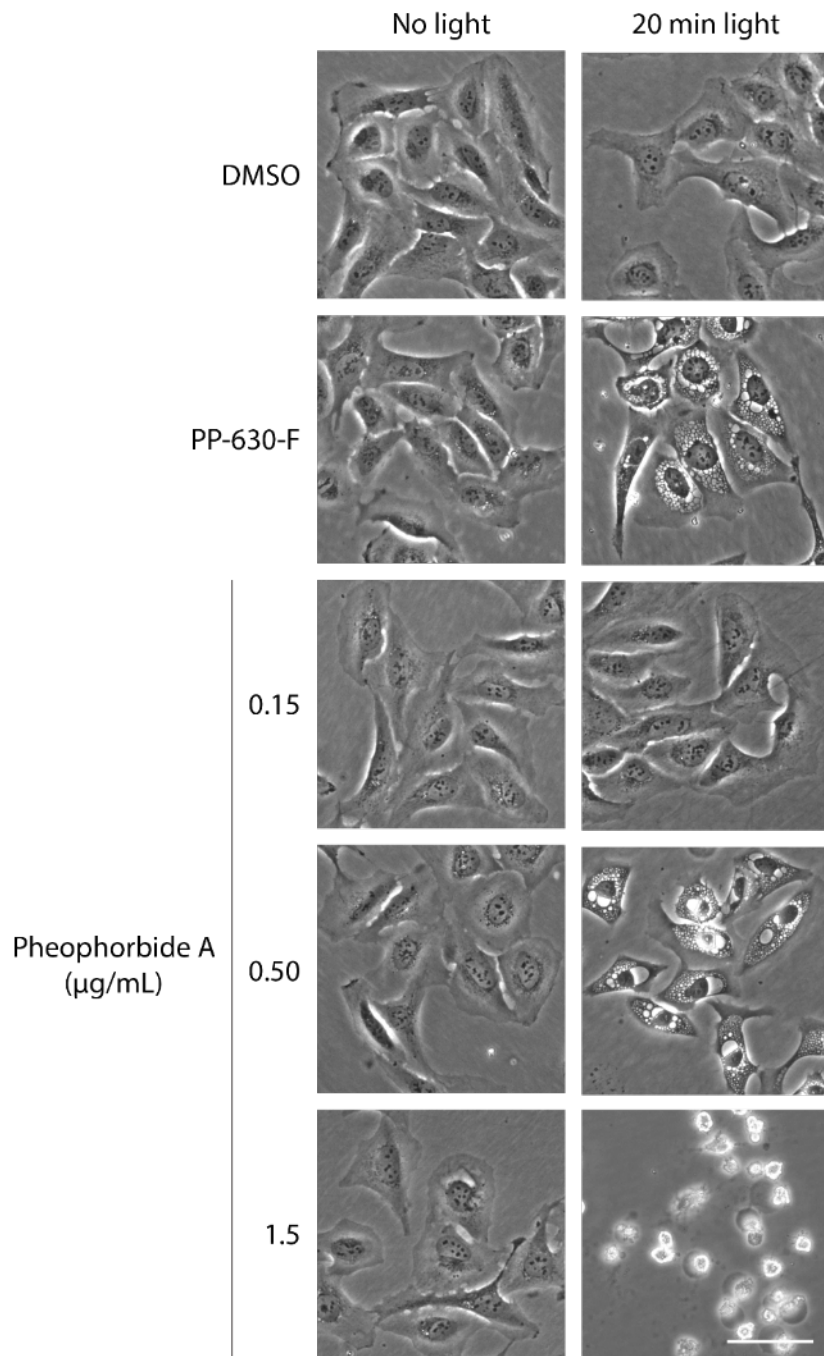


Figure 3.15. Treatment with Pheophorbide a induces a vacuolated phenotype similar to *S. occidentalis* leaf extracts. U2OS cells were treated with either DMSO, 25  $\mu\text{g/mL}$  PP-630-F or either 0.15, 0.5, or 1.5  $\mu\text{g/mL}$  of Pheophorbide a and either exposed to 20 min of ambient light conditions or maintained at standard conditions at 1 h. Cells were imaged at 16 h by phase contrast microscopy. Scale bar = 50  $\mu\text{m}$ .

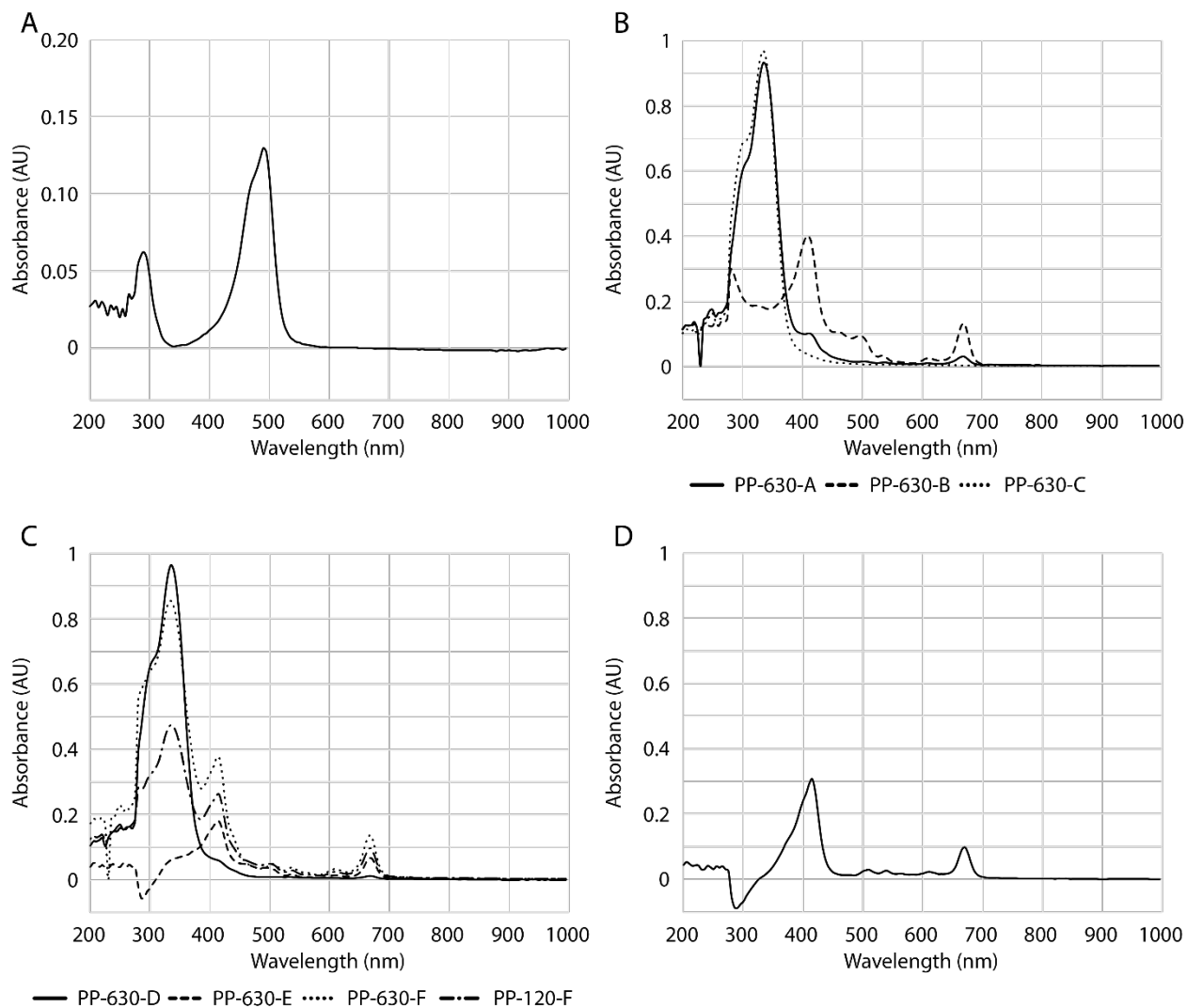


Figure 3.16. *S. occidentalis* leaf extracts show a similar absorption spectrum to Pheophorbide a. Plant extracts or Pha were dissolved in DMSO at 500 or 10  $\mu\text{g}/\text{mL}$ , respectively. AO was dissolved in water at 1  $\mu\text{g}/\text{mL}$ . Absorbance was measured at 5 nm intervals between 200-1000 nm. (A) Major absorption peaks were identified for AO (—) at 290 and 490 nm. (B) Major absorption peaks were identified for PP-630-A (—) at 335 nm; PP-630-B (---) at 415 and 665 nm; PP-630-C (•••) at 335 nm. (C) Major absorption peaks were identified for PP-630-D (—) at 335 nm; PP-630-E (---) at 415 and 665 nm; PP-630-F (•••) at 335, 415 and 665 nm; PP-120-F (-•-) at 335, 415 and 665 nm. (D) Major absorption peaks were identified for Pha (—) at 415 and 665 nm. Extracts and Pha or AO were normalized to the absorbance spectrum of DMSO or water, respectively.

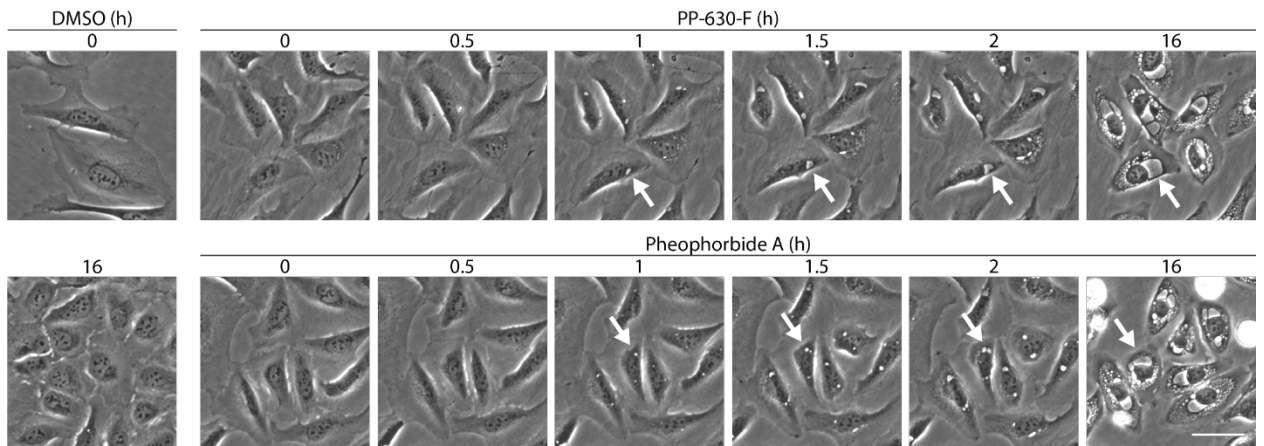


Figure 3.17. Onset of vacuolation in *S. occidentalis* leaf extract or Pha and light occurs at the perinuclear area. U2OS cells were treated with either 25  $\mu\text{g}/\text{mL}$  PP-630-F or 0.5  $\mu\text{g}/\text{mL}$  Pha for 1 h, followed by exposure to 20 min of ambient light, and monitored by time-lapse phase contrast microscopy for 16 h at 30 min intervals. Arrows indicate onset of vacuolation at the perinuclear area in either treatment. Scale bar = 50  $\mu\text{m}$ .

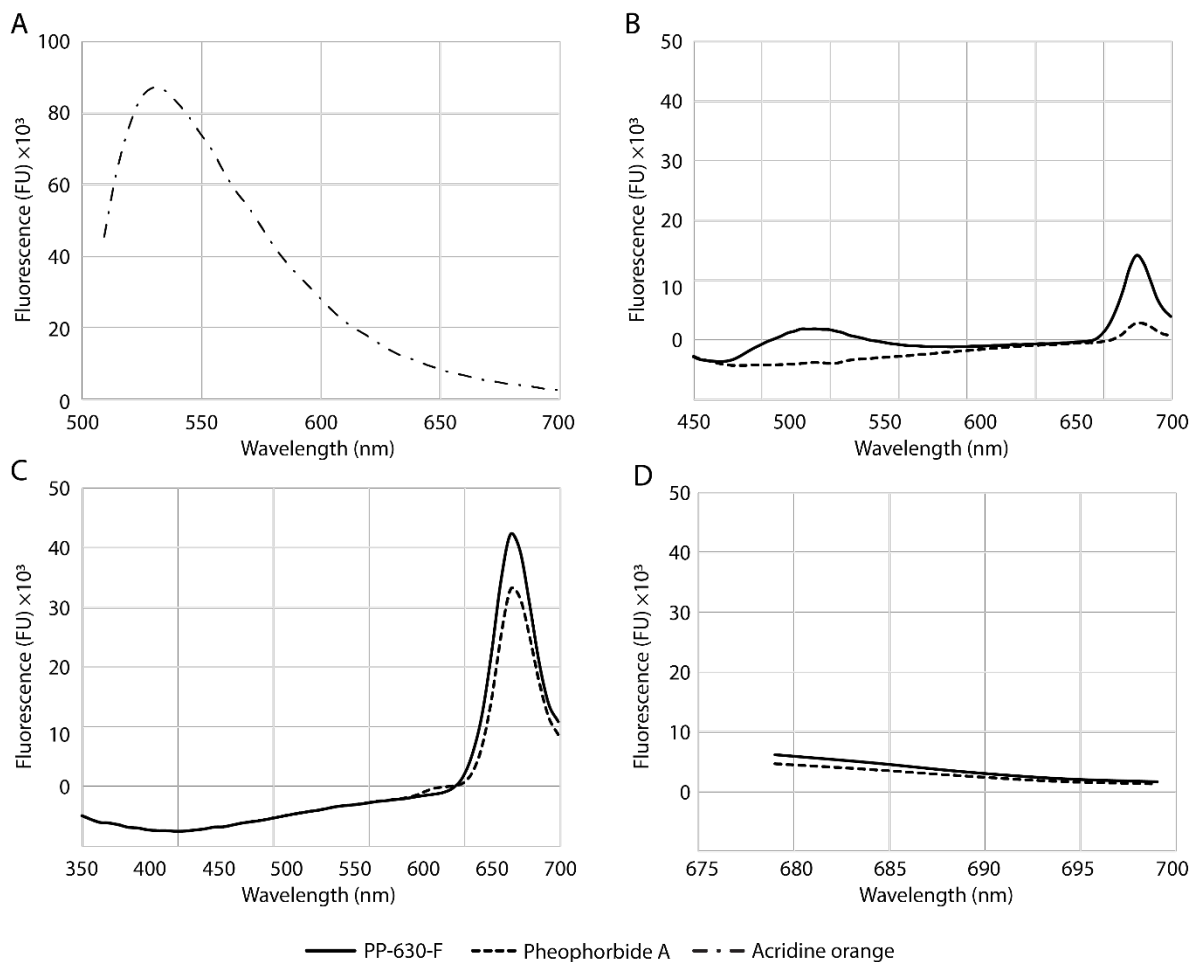


Figure 3.18. Fluorescence spectra of PP-630-F and Pheophorbide a. Plant extracts and Pheophorbide a were dissolved in DMSO at 500 and 10  $\mu\text{g}/\text{mL}$ , respectively and AO was dissolved in water at 1  $\mu\text{g}/\text{mL}$ . (A) Fluorescence peak for AO identified at 529 nm upon excitation at 490 nm. (B) Fluorescence peaks were identified for PP-630-F (—) at 674 nm and Pha (---) at 674 nm. (C) Fluorescence peaks were identified for PP-630-F (—) at 674 nm and Pha (---) at 610 and 610 nm. (D) Fluorescence peaks could not be identified for PP-630-F (—) or Pha (---). Fluorescence emission was measured at 5 nm intervals of (A) AO between 509-699 upon excitation at 490, and of either PP-630-F or Pha between (B) 350-700, (C) 434-699 and (D) 679-699 nm upon excitation at 335, 415 and 660 nm, respectively. Fluorescence measurements of extracts and Pha or AO were normalized to DMSO or water, respectively.

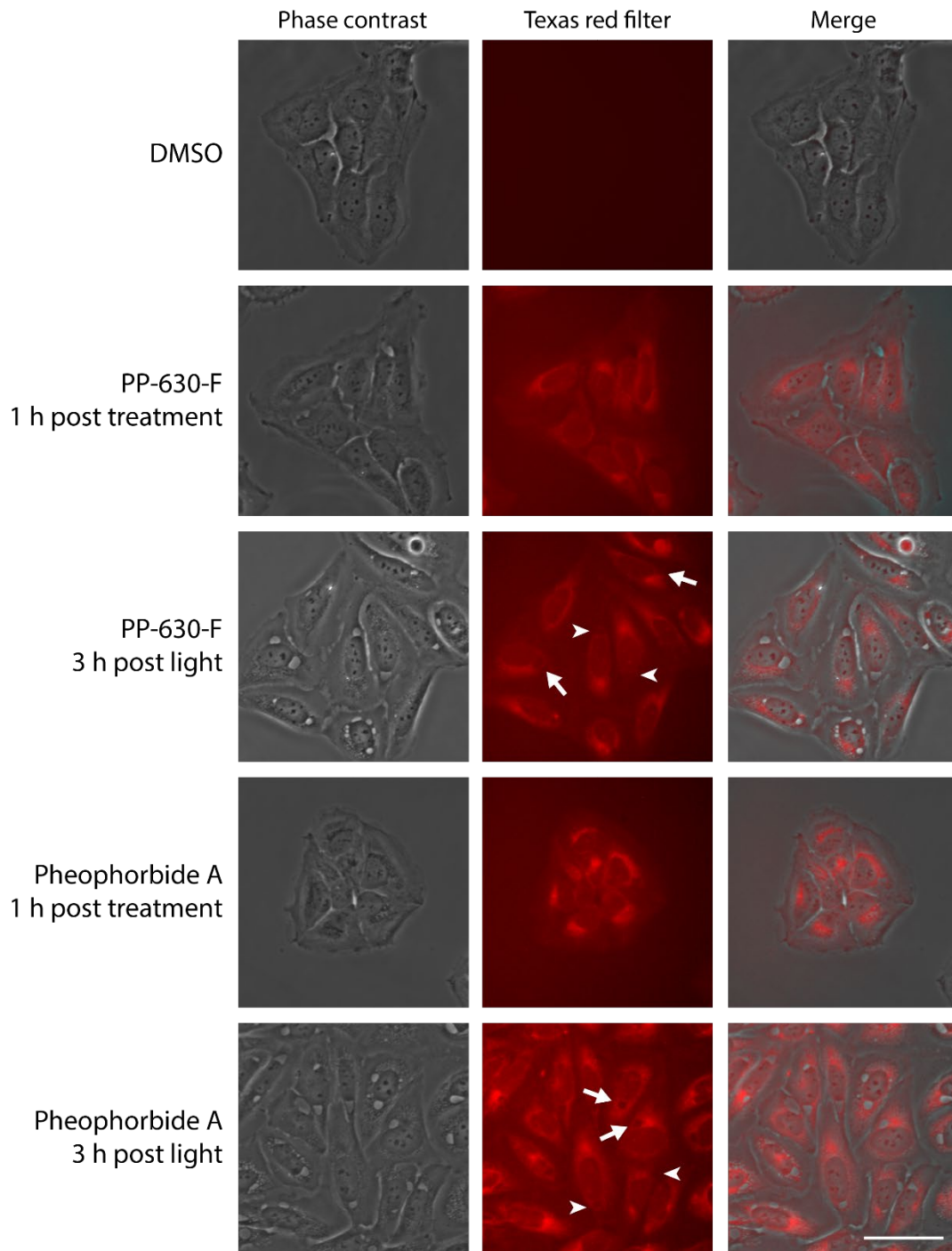


Figure 3.19. *S. occidentalis* leaf extract and Pha fluorescence accumulates at the perinuclear location and vacuolation originates mainly from outside the fluorescence. U2OS cells were treated with either DMSO, 25  $\mu\text{g}/\text{mL}$  PP-630-F or 0.5  $\mu\text{g}/\text{mL}$  Pheophorbide a and exposed to ambient light for 20 min at 1 h after treatment. Cells were imaged by phase contrast or by fluorescence microscopy using a Texas Red filter set (Ex:586/Em:647) at 1 hour after treatment (prior to ambient light) and at 3 h after ambient light exposure. Arrows indicate vacuole formation within the Texas red filter fluorescence and arrowheads indicate vacuole formation outside of the Texas red filter fluorescence. Scale bar = 50  $\mu\text{m}$ .

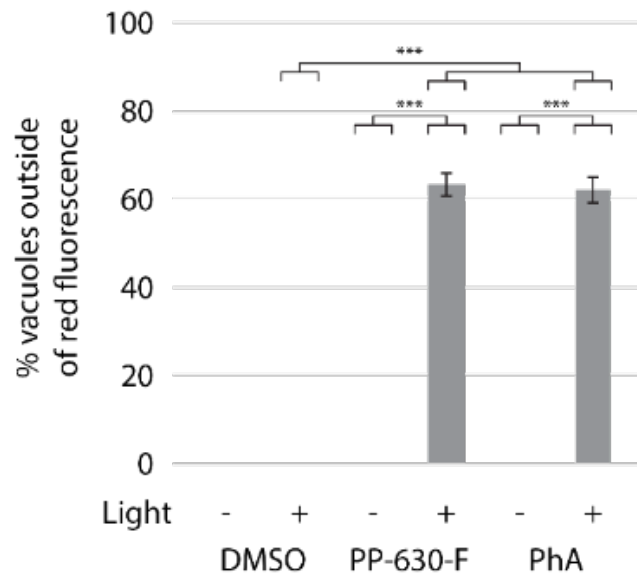


Figure 3.20. *S. occidentalis* leaf extract and Pha vacuolation originates mainly from outside the fluorescence. Vacuoles developing inside and outside of the red fluorescence in Figure 3.21 were counted manually using Image J software and shown are the mean percent vacuoles developing outside the Texas red filter fluorescence and standard errors of the means from three experiments. (\*\*\*)  $p < 0.001$ .

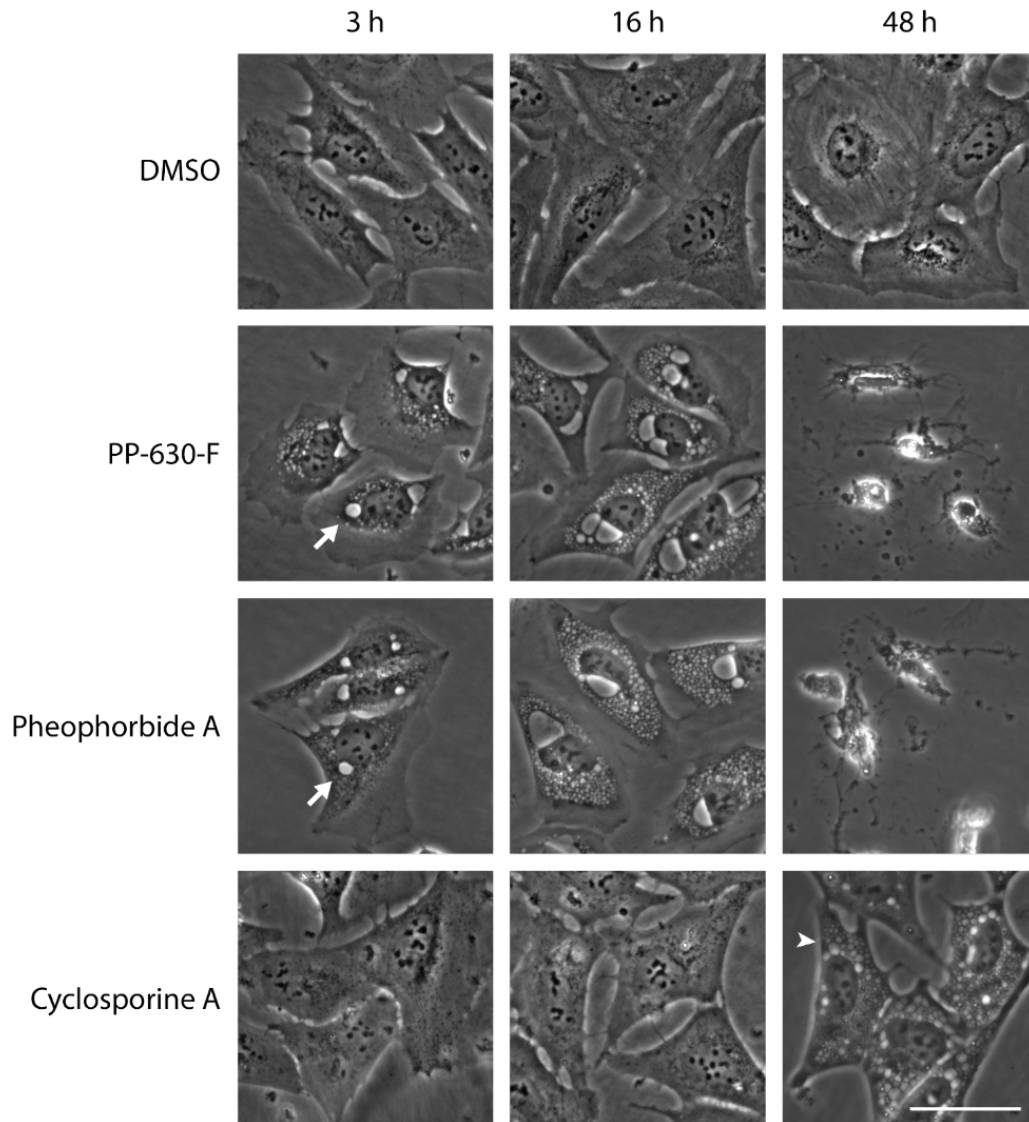


Figure 3.21. Onset of vacuolation in cells treated with either *S. occidentalis* leaf extract or Pheophorbide a and light is different from cyclosporine A. U2OS cells were treated with either DMSO, 20  $\mu$ M cyclosporine A or either 25  $\mu$ g/mL PP-630-F or 0.5  $\mu$ g/mL Pheophorbide a and 20 min of ambient light at 1 h. Cells were imaged at either 3, 16 or 48 h after treatment. Arrows indicate the onset of vacuolation in either PP-630-F or Pheophorbide a and light treated cells at 2 h. Arrowhead indicates a vacuolated cell in cyclosporine A-treated cells at 48 h. Scale bar = 25  $\mu$ m.

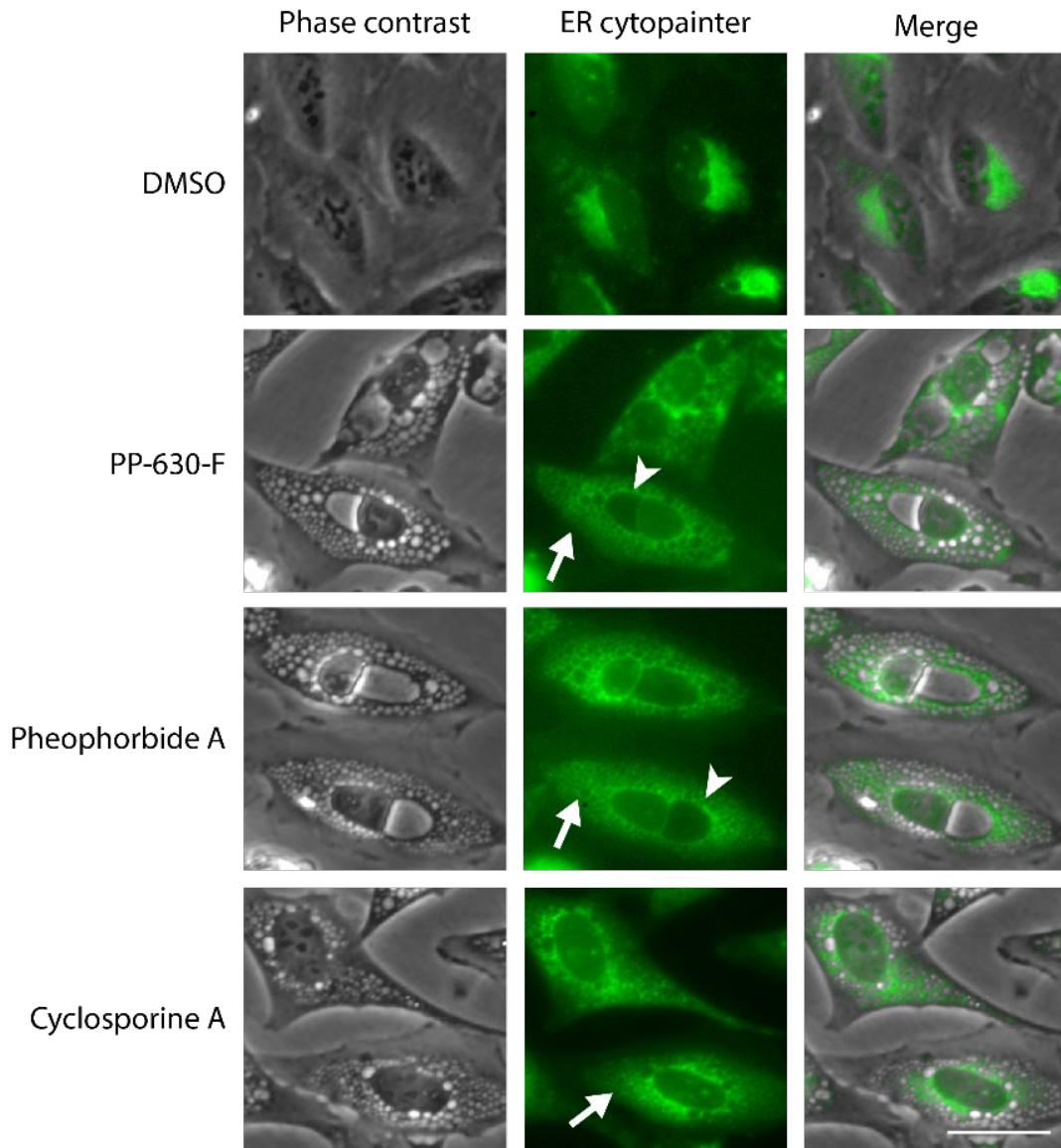


Figure 3.22. *S. occidentalis* leaf extract and light-induced vacuolated cells show a dispersed endoplasmic reticulum. U2OS cells were treated with either DMSO, 20  $\mu$ M cyclosporine A or either 25  $\mu$ g/mL PP-630-F or 0.5  $\mu$ g/mL Pheophorbide a and 20 min of ambient light at 1 h. Cells were incubated with 1X of ER Cytopainter (ab139481) for 15 min at 16 h for PP-630-F and Pheophorbide a, and at 48 h for cyclosporine A and DMSO. Cells were imaged by phase contrast and fluorescent microscopy and exposure settings were kept constant throughout. Arrows indicate dispersed endoplasmic reticulum in PP-630-F, Pheophorbide a or cyclosporine A treated cells and arrowhead indicates large perinuclear vacuole in PP-630-F or Pheophorbide a treated cells. Scale bar = 25  $\mu$ m.

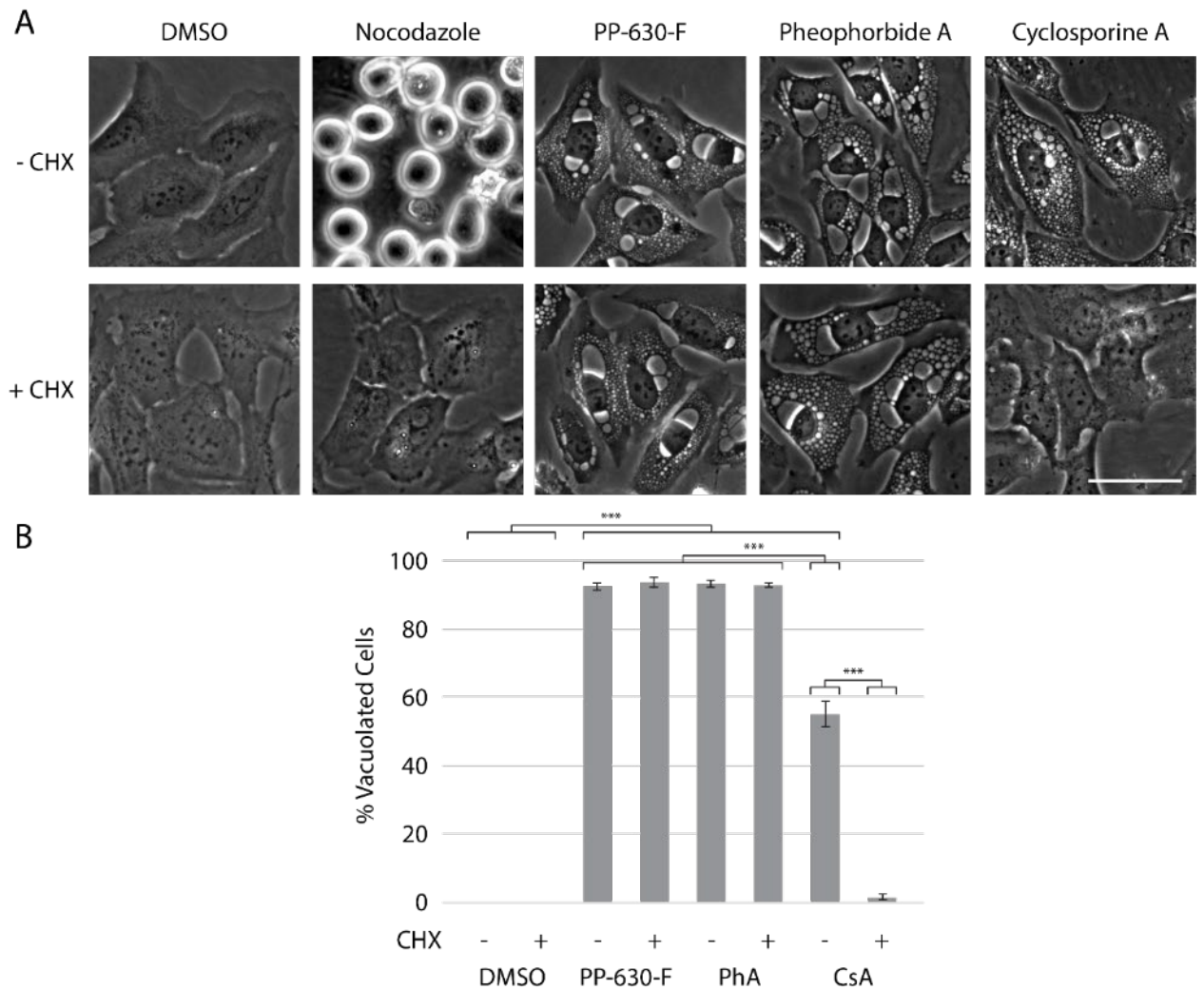


Figure 3.23. Inhibition of protein synthesis does not prevent vacuole formation in cells treated with *S. occidentalis* leaf extract or Pha and light. (A) U2OS cells were either pre-treated with 10  $\mu\text{g}/\text{mL}$  cycloheximide (CHX) for 2 h or not and then treated with either DMSO, 200 ng/mL nocodazole for 24 h, 25  $\mu\text{g}/\text{mL}$  PP-630-F, 0.5  $\mu\text{g}/\text{mL}$  Pheophorbide a for 16 h or 20  $\mu\text{M}$  Cyclosporine A (CsA) for 48 h. PP-630-F and Pheophorbide a treated cells were exposed to ambient light at 1 h. Cells were imaged by phase contrast microscopy. Scale bar = 50  $\mu\text{m}$ . (B) Vacuolated cells from (A) were counted manually using Image J software. The mean percent vacuolated cells were calculated from three experiments and standard errors of the means are shown. (\*\*\*)  $p < 0.001$ .

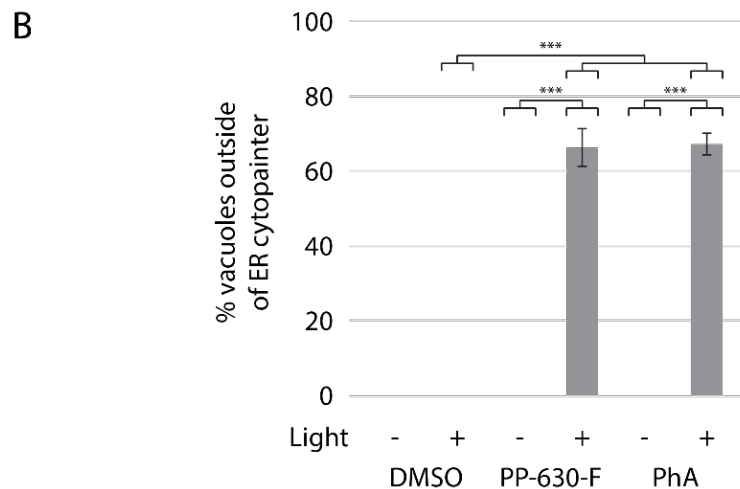
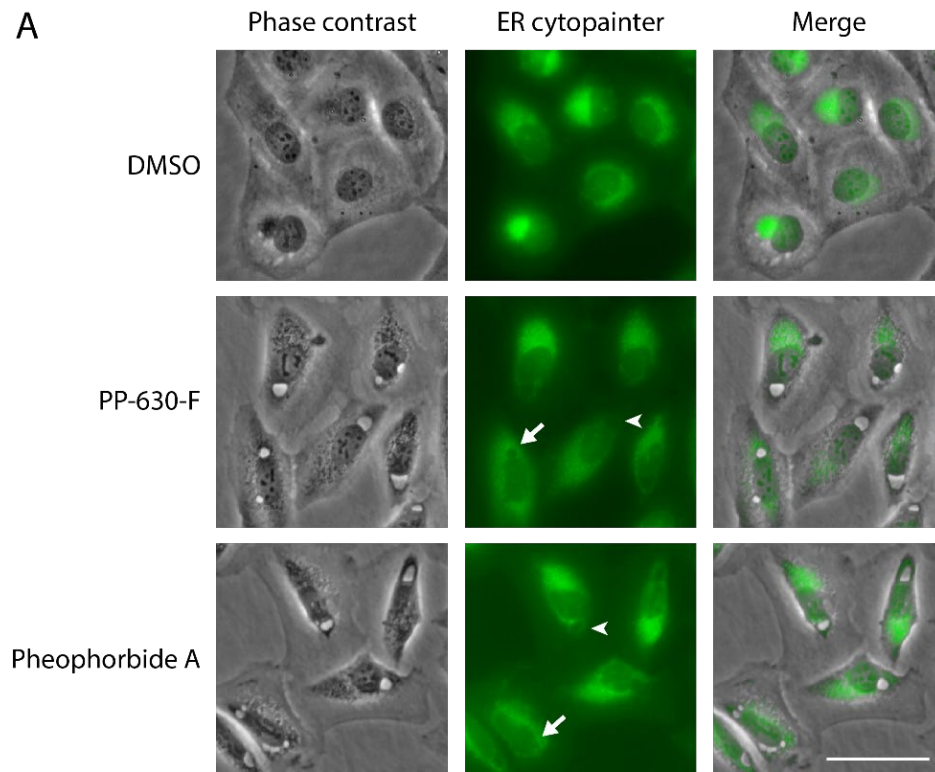


Figure 3.24. Perinuclear vacuoles originate mainly from outside the endoplasmic reticulum. U2OS cells were treated with either DMSO or either 25  $\mu\text{g}/\text{mL}$  PP-630-F or 0.5  $\mu\text{g}/\text{mL}$  Pheophorbide a and 20 min of ambient light at 1 h. Cells were incubated with 1X of ER Cytopainter for 15 min at 3 h after light exposure and imaged by phase contrast and fluorescent microscopy. Arrows indicate vacuole formation within the ER Cytopainter fluorescence and arrowheads indicate vacuole formation outside of the ER Cytopainter fluorescence. Scale bar = 50  $\mu\text{m}$ . (B) Vacuoles developing inside and outside of the ER Cytopainter fluorescence were counted manually using Image J software. The mean percent vacuoles developing outside were calculated from three experiments and standard errors of the means are shown. (\*\*\*)  $p < 0.001$ .

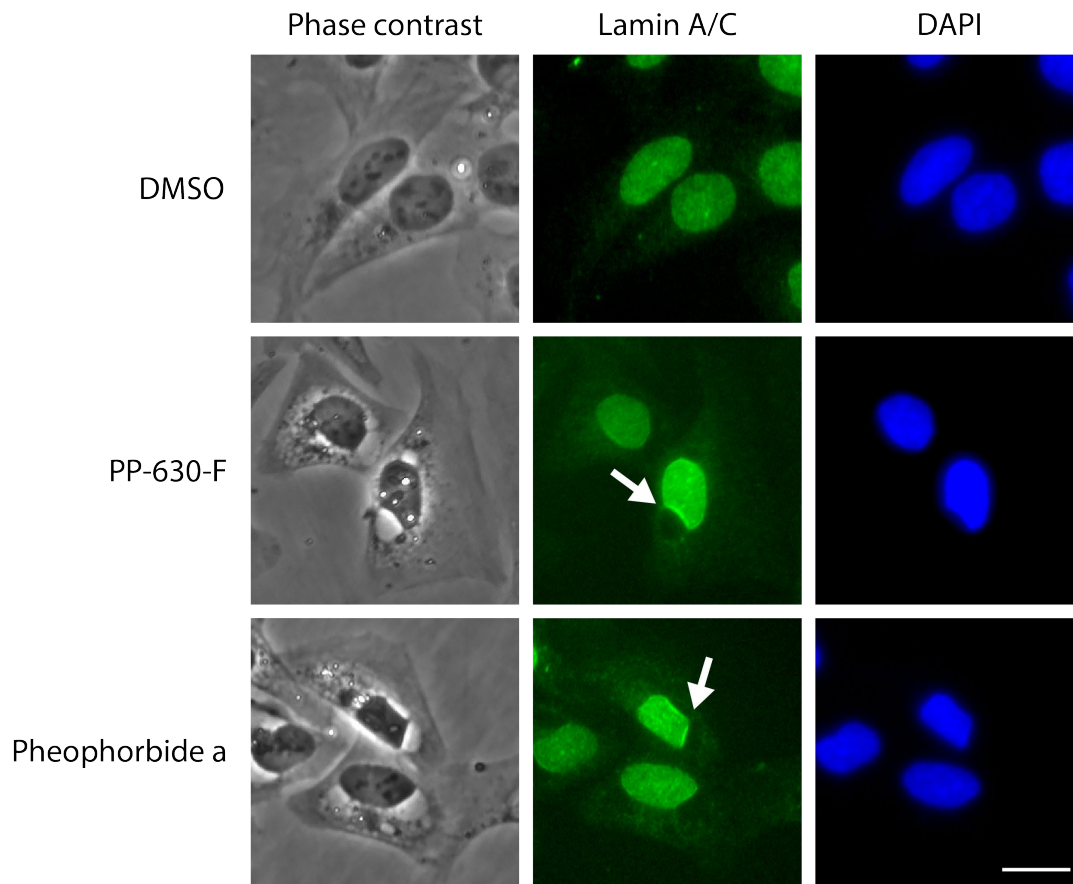


Figure 3.25. Intense lamin A/C staining occurs at the location of the perinuclear vacuoles. U2OS cells were treated with either DMSO, 25  $\mu\text{g}/\text{mL}$  PP-630-F or 0.5  $\mu\text{g}/\text{mL}$  Pheophorbide a and exposed to ambient light for 20 min at 1 h. (A) Cells were imaged at 16 h by phase contrast and fluorescent microscopy using either the nuclear stain, DAPI, or antibodies specific to lamin A/C. Arrows indicate intense lamin staining at the location of the perinuclear vacuoles. Scale bar = 20  $\mu\text{m}$ .

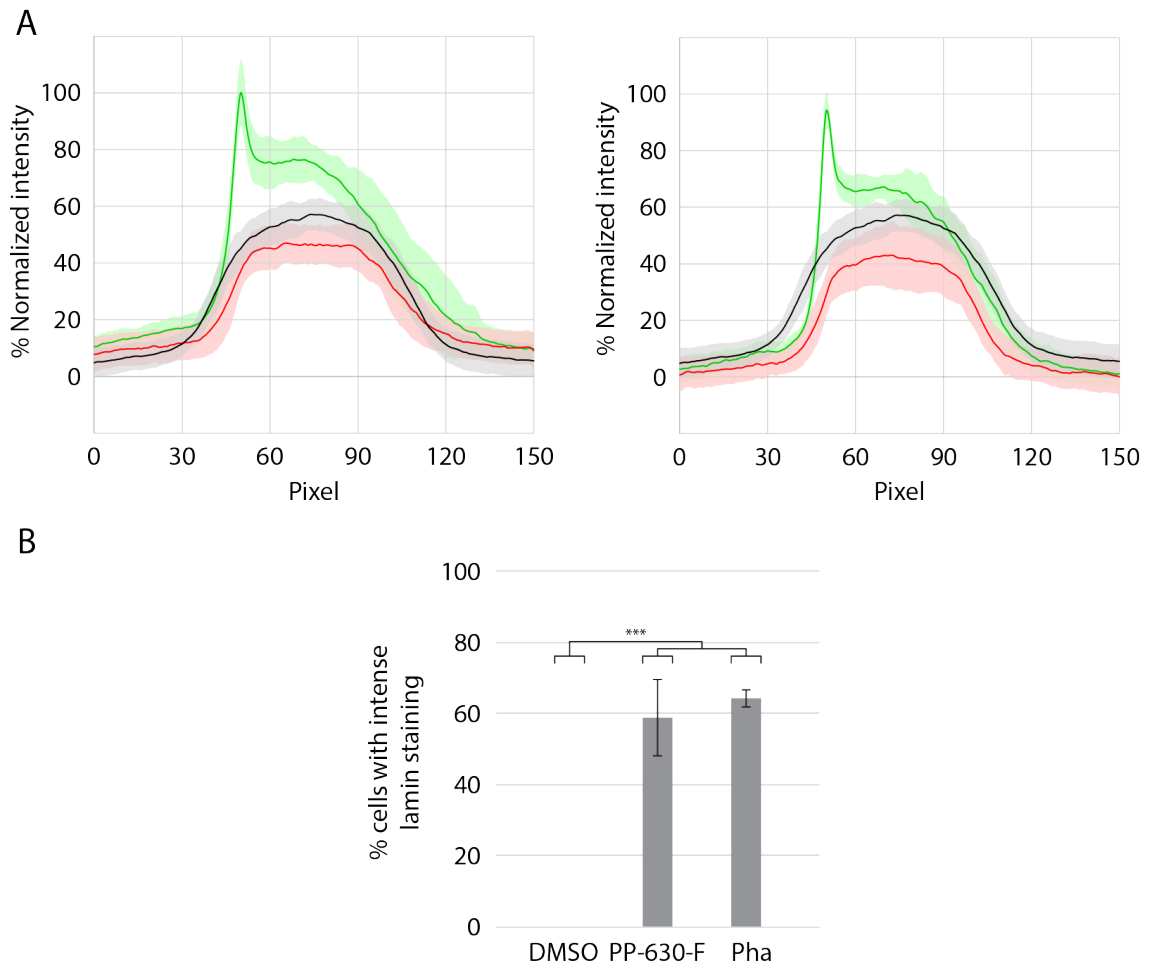


Figure 3.26. Intense lamin A/C staining occurs at the location of the perinuclear vacuoles. U2OS cells were treated with either DMSO, 25  $\mu\text{g}/\text{mL}$  PP-630-F or 0.5  $\mu\text{g}/\text{mL}$  Pheophorbide a and exposed to ambient light for 20 min at 1 h. (B) Fluorescence intensity of lamin A/C in Figure 3.35 was measured across nuclei in either DMSO (black traces), PP-630-F (left) or Pha (right) treated cells. Extract or Pha treated cell nuclei either showed intense (green traces) or not intense (red traces) staining with lamin A/C. Each treatment was run in triplicate and shown are the mean and standard deviation of 45 nuclei. Measurements were normalized to cytoplasmic intensity and the highest intensity across all treatments. (C) Cells with intense lamin staining at the perinuclear vacuole from (B) were counted using Image J software and shown are the mean percent cells with intense lamin staining and standard errors of the means from three experiments. (\*\*\*)  $p < 0.001$ .

## CHAPTER 4 – Comparison of the wavelengths and radiant exposures required to induce vacuolation in *S. occidentalis* extract or Pheophorbide a treated cells

### 4.1 Introduction

In our previous chapter we identified that extracts from *S. occidentalis* induce the vacuolation of the ER and nuclear envelope and are toxic to human cells when treated cells are exposed to ambient light. Based on literature information and spectral analysis, we identified the cyclic tetrapyrrole Pha and found that it had a similar effect against human cells when exposed to ambient light conditions. Hence, in this chapter we seek to compare Pha to the extract further by examining the sections of the light spectrum and the radiant exposures that elicit the vacuolation response.

Photosensitizers absorb light energy at specific wavelengths and induce chemical changes in other compounds. The specific wavelengths that are absorbed correspond to the energy difference between the ground state ( $S_0$ ) of the photosensitizers and one of its excited states ( $S_1, S_2, \dots$ ), and this energy can subsequently be used to induce changes in surrounding compounds. Plants produce a number of natural photosensitizers, including hypericin, sanguinarine, riboflavin, curcumin or psoralens, that absorb light at 570, 470, 440, 420, or 320-400 nm, respectively (Pathak, 1984; Arnason et al., 1992; Abrahamse and Hamblin, 2016). Furthermore, plants also naturally contain a group of photosensitizers termed cyclic tetrapyrroles, which includes chlorophyll, intermediates in chlorophyll metabolism and their derivatives.

Due to the intrinsic nature of chlorophyll to harvest energy from a broad spectrum of ultraviolet and visible light and transfer it to an acceptor molecule, chlorophyll and chlorophyll derivatives are natural photosensitizers. Cyclic tetrapyrroles make up the largest group of natural photosensitizers investigated for biological activity (Nyman and Hynninen,

2004; Brandis et al., 2006). These molecules contain a lengthened  $\pi$ -system that results in greater delocalization of electrons and lowers the energy required for the corresponding  $\pi$ - $\pi^*$  transition to an excited state ( $S_0$  to  $S_1$ ). As a result, cyclic tetrapyrrole photoactivity can be induced with light in the red section of the visible spectrum (red-most Q band; 600-700 nm), unlike other natural plant photosensitizers that do not absorb light above 600 nm wavelengths (Roeder et al., 1990; Eichwurzel et al., 2000). Furthermore, cyclic tetrapyrroles also contain a large absorption band termed the Soret band around 400 nm, which represents  $S_0$  to  $S_2$  transitions (Giovannetti, 2012). Excitation of a photosensitizer at either the Soret or Q bands, induces excited states from which photosensitizers may undergo transition to a triplet state and subsequently return to  $S_0$  either by electron transfer/hydrogen abstraction from a substrate or by direct transfer of energy to molecular oxygen to produce highly reactive singlet oxygen.

Broad spectrum lamps covering most absorption bands of natural photosensitizers are generally used when plant extracts are examined for photobiological activity against human cells (Ong et al., 2009; Tan et al., 2011). In contrast, irradiation of photosensitizer treated cells is subsequently optimized to wavelengths that cover the respective absorption bands of the photosensitizer using optical filters, lasers or light-emitting diodes (LEDs) (Castano et al., 2005).

The objective of this chapter is to compare *S. occidentalis* extract or Pha further by examining the sections of the ambient light spectrum that induce cytoplasmic vacuolation, as well as to determine the radiant exposures required to induce cytoplasmic vacuolation at wavelengths that correspond to the two largest absorption bands of cyclic tetrapyrroles.

## 4.2 Results

### 4.2.1 Identification of vacuole-inducing sections of the ambient electromagnetic spectrum in cells treated with PP-630 or Pha

In our previous chapter we identified that *S. occidentalis* leaf extracts or Pha can induce a vacuolated phenotype in human cells when co-treated with ambient light. In this chapter we sought to compare further the effect of *S. occidentalis* extract and Pha on human cells by identifying specific wavelengths that induce vacuolation. We used optical glass filters to screen the ambient light spectrum for sections that can induce the vacuolated phenotype and then calculated the percent vacuolated cells at 16 h. We treated cells either with DMSO, 25  $\mu\text{g}/\text{mL}$  PP-630-F or 0.5  $\mu\text{g}/\text{mL}$  Pha and incubated cells either at ambient light conditions or at standard conditions for 20 min. We also treated cells with either 25  $\mu\text{g}/\text{mL}$  PP-630-F or 0.5  $\mu\text{g}/\text{mL}$  Pha and incubated cells at ambient light conditions covered with filters shown in Figure 4.1. We found that DMSO treated cells did not induce vacuolation in cells incubated either at ambient light conditions or standard conditions (Figure 4.2). PP-630-F or Pha treated cells showed the vacuolated phenotype when cells were incubated at ambient light conditions and did not show the vacuolated phenotype when incubated at standard conditions, as expected. We noted that vacuolated phenotype in PP-630-F or Pha treated cells occurred in either  $> 90\%$  or in  $< 1\%$  of the cells, with ranges of 93 - 96 % and 0 %, and of 91 - 96 % and 0 - 1 % for PP-630-F and Pha, respectively. We also found that the vacuolation response was not significantly different between PP-630-F and Pha treated cells in any treatment ( $p < 0.05$ ). Thus, both Pha and PP-630-F treatments are grouped together in our description of the results.

We observed  $< 1\%$  vacuolation when treated cells were incubated at standard conditions and  $> 90\%$  vacuolation when cells were incubated at ambient conditions, as

expected (Figure 4.2). Similarly, > 90 % vacuolation occurred when cells were exposed to the visible section (300-700 nm; Figure 4.1A) of the ambient light spectrum, whereas the non-visible section (200-400 nm, >700 nm; Figure 4.1B) induced < 1% vacuolation. Further sectioning the visible spectrum with optical filters, we found that cells exposed to light above 580 nm (Figure 4.1C) or between 600-700 nm (Figure 4.1D) induced > 90% vacuolation, whereas exposure to light above 700 nm (Figure 4.1E) induced < 1% vacuolation, indicating that wavelengths between 600-700 nm can induce vacuolation. Furthermore, we found that cells exposed to light between 300-500 nm (Figure 4.1F) induced > 90% vacuolation, whereas light between 300-400 nm (Figure 4.1G) resulted in < 1% vacuolation, indicating that wavelengths between 400-500 nm can induce vacuolation. These results showed that ambient light between 400-500 nm and between 580-700 nm can induce vacuolation in human cells.

#### 4.2.2 *Light specific to 408 nm or 660 nm induces vacuoles in cells treated with either S. occidentalis leaf extract or Pheophorbide a*

We compared our filter results to the absorption spectra for PP-630-F and Pha and noted that the vacuole inducing sections of the electromagnetic spectrum overlapped with peaks detected at 413 and 660 nm. Therefore, we sought to determine whether irradiation of PP-630-F or Pha treated cells with wavelengths specific to 413 or 660 nm can induce the vacuolated phenotype. Using LEDs we irradiated cells with increasing radiant exposures ( $\text{J}/\text{cm}^2$ ) at these wavelengths and calculated the percent vacuolated cells at 16 h. U2OS cells were treated either with DMSO, 25  $\mu\text{g}/\text{mL}$  of PP-630-F or 0.5  $\mu\text{g}/\text{mL}$  of Pha and incubated at ambient light for 20 min. Cells were also treated with 25  $\mu\text{g}/\text{mL}$  of PP-630-F or 0.5  $\mu\text{g}/\text{mL}$  of Pha and irradiated at increasing radiant exposures ( $\text{J}/\text{cm}^2$ ) with LEDs specific to either 408 nm or 660 nm.

We found that DMSO treated cells incubated at ambient light did not develop the vacuolated phenotype, whereas PP-630-F and Pha induced the vacuolated phenotype in  $95 \pm 6\%$  and  $98 \pm 1\%$  of cells, respectively, as expected (Figure 4.3). We observed that PP-630-F induced  $> 90\%$  vacuolation in response to 1.25, 1.50 or 1.75 J/cm<sup>2</sup> at 408 nm, whereas  $< 30\%$  of cells showed a vacuolated phenotype at 0.75, 1 or 2 J/cm<sup>2</sup>, and no vacuolated cells were observed at 0.25, 0.5, 2.25 or 2.5 J/cm<sup>2</sup> (Figure 4.3A). In response to 660 nm irradiation, PP-630-F treated cells showed  $> 90\%$  vacuolation at 1 or 1.25 J/cm<sup>2</sup>, whereas  $< 30\%$  showed a vacuolated phenotype at 0.75 or 1.5 J/cm<sup>2</sup>, and no vacuolated cells were observed at 0.25, 0.5, 1.75, 2, 2.25 or 2.5 J/cm<sup>2</sup>. We observed that Pha-treated cells showed  $> 90\%$  vacuolation in response to 1.25 J/cm<sup>2</sup> at 408 nm, whereas  $< 60\%$  showed a vacuolated phenotype at 0.75, 1, 1.5 or 1.75 J/cm<sup>2</sup>, and no vacuolated cells were observed at 0.25, 0.5, 2, 2.25 or 2.5 J/cm<sup>2</sup> (Figure 4.3B). In response to 660 nm irradiation, Pha treated cells also showed  $> 90\%$  vacuolation at 1.25 J/cm<sup>2</sup>, whereas  $< 60\%$  showed a vacuolated phenotype at 1, 1.5 or 1.75 J/cm<sup>2</sup>, and no vacuolated cells were observed at 0.25, 0.5, 0.75, 2, 2.25 or 2.5 J/cm<sup>2</sup>. Comparing PP-630-F to Pha, we noted that PP-630-F treated cells to have a plateau of  $> 90\%$  vacuolation for either 408 or 660 nm radiant exposures, whereas Pha treated cells responded with  $> 90\%$  vacuolation at 1.25 J/cm<sup>2</sup>. These results revealed that vacuolation can be induced in either PP-630-F or Pha treated cells with radiation specific to either 408 or 660 nm at radiant exposures between 1-1.75 J/cm<sup>2</sup>.

### 4.3 Discussion

In this chapter we identified that specific wavelengths and radiant exposures can induce the vacuolated phenotype in either *S. occidentalis* extract or Pha treated cells. We employed optical filters to screen the light spectrum and found that sections between 400-

500 nm or 600-700 nm can induce vacuolation, which cover major absorption peaks of the *S. occidentalis* extract or Pha around 415 and 660 nm. We then found that irradiation of treated cells with LEDs specific to these wavelengths can induce vacuolation and determined that an exposure to 1.0-1.5 J/cm<sup>2</sup> induced cytoplasmic vacuolation, whereas higher radiant exposures were toxic, and lower radiant exposures did not induce vacuolation at 16 h post radiant exposure.

Our findings showing that light between 400-500 nm or 600-700 nm, and specifically at 408 nm or 660 nm can induce vacuolation in either *S. occidentalis* extract or Pha treated cells correlates well with the distinct absorption peaks of the Soret band and red-most Q-band of cyclic tetrapyrroles, such as Pha, around 413 and 660 nm, as determined in the previous chapter and by others (Roeder et al., 1990). Similarly, others have shown that Pha photodamage can be elicited by similar means, such as commercial lamps and 610 nm long pass filters, or LEDs specific to 660 nm (Tang et al., 2006; Li et al., 2007; Tang et al., 2009a). Our results further support the suggestion that the photoactive agent(s) in the *S. occidentalis* extract is likely a cyclic tetrapyrrole, since naturally occurring photosensitizers that do not belong to the group of cyclic tetrapyrroles, including hypericin (590 nm), sanguinarine (470 nm), riboflavin (440 nm), curcumin (420 nm) or psoralens (320-400 nm), absorb light maximally below 600 nm and not specifically at 660 nm (Pathak, 1984; Arnason et al., 1992; Abrahamse and Hamblin, 2016).

Comparing LED induced vacuolation and toxicity of *S. occidentalis* to Pha, we found that similar radiant exposures induced > 90% vacuolation or were toxic to either *S. occidentalis* extract or Pha treated cells at both 408 and 660 nm. Our data for Pha induced toxicity (0.8 μM; > 2.00 J/cm<sup>2</sup> at 660 nm) agrees well with others that have reported Pha

toxicity against human cells at concentrations of 0.1-2  $\mu\text{M}$  Pha and radiant exposures of 1-100  $\text{J}/\text{cm}^2$  at around 660 nm, respectively (Hajri et al., 1999; Hajri et al., 2002; Lee et al., 2004; Tang et al., 2006; Li et al., 2007; Busch et al., 2009; Rapozzi et al., 2009; Tang et al., 2009a; Tang et al., 2009b; Bui-Xuan et al., 2010; Tang et al., 2010; Ahn et al., 2013; Cheung et al., 2013; Yoon et al., 2014a; Kim et al., 2016). However, we noted an absence of literature reporting Pha toxicity upon irradiation between 400-500 nm or specifically at 408 nm and we reason that this is likely a therapy approach as 408 nm light lies outside the “optical window” (600-1300 nm) that is preferred during photodynamic therapy, as it permits deeper tissue penetration (Castano et al., 2004).

We noted that > 90% vacuolation occurred at a single radiant exposure of either 408 or 660 nm radiation in Pha treated cells, whereas in *S. occidentalis* extract treated cells, > 90% vacuolation occurred at multiple radiant exposures at either wavelength. We reason that this difference may be due to the complex mixture of compounds in the *S. occidentalis* extract, including different cyclic tetrapyrroles, which have been shown to be present in different plant extractions (Cheng et al., 2001; Adzhar Kamarulzaman et al., 2011; Tan et al., 2011). These compounds could potentially affect light absorption, photoactivity of the active compound(s) and toxicity of the extract, which then may result in a broader range of radiant exposures that induce vacuolation. Additionally, different cyclic tetrapyrroles may contribute to the vacuolating effect at different radiant exposures or the active compound may induce the vacuolating effect over a broader range of radiant exposure compared to Pha. This may also explain the lower radiant exposure of 660 nm radiation required to induce vacuolation in *S. occidentalis* treated cells compared to 408 nm, whereas in Pha treated cells the same radiant exposure was required.

Comparing our results to the literature, we note that it is possible that Pha may also induce vacuolation over a range of radiant exposures at 408 nm or 660 nm radiation and at a lower radiant exposure of specific wavelengths, but we did not detect it at the radiant exposure increments tested (250 mJ/cm<sup>2</sup>). For example, others have shown that viability of Pha treated cells can decrease significantly over 25 mJ/cm<sup>2</sup> increments, which indicates that a range of biological mechanisms and signalling pathways can be affected by radiant exposure differences 10-fold smaller than our increments (250 mJ/cm<sup>2</sup>) (Wyld et al., 2001; Chan et al., 2009; Reiners et al., 2010). We remain to perform bioassay-guided fractionation of *S. occidentalis* and identify the active compound in future experiments to address further these observations and to determine whether the different vacuolation responses to 408 nm and 660 nm irradiation observed between the *S. occidentalis* extract and Pha are due to the influence of other compounds or because the active compound in *S. occidentalis* induces vacuolation at different radiant exposures than Pha.

We also noted that the vacuolated phenotype occurred as we increased the radiant exposure, whereas lower radiant exposures did not induce vacuoles whereas higher radiant exposures were toxic to cells by 16 h. Others have proposed that ‘high dose photodynamic therapy’ conditions (high photosensitizer and light dose) promote either apoptosis or necrosis, whereas suboptimal, ‘low dose photodynamic therapy’ conditions result in cell survival (Piette et al., 2003; Piette, 2015). Thus, our results indicate that vacuolation may occur on this spectrum of cellular responses to increasing radiant exposure and damage to the ER and nuclear envelope. Similarly, ER vacuolation and paraptotic cell death were previously shown to be dependent on the concentration of ER stress-inducing compounds (Yoon et al., 2014b). Hence, this indicates a potential threshold for vacuolation or toxicity

within the cell, which can be elicited in our experiments by increasing the radiant exposure. This dependency on radiant exposure or photosensitizer concentration has not specifically been addressed by authors that observed vacuolation in response to ER photodamage previously, and further experiments using *S. occidentalis* or Pha and light as a molecular tool may provide information on the relationship between radiant exposure, molecular signalling and cellular vacuolation response (Kaul and Maltese, 2009; Gomes da Silva et al., 2018; Kessel, 2018).

In summary, our findings show that cytoplasmic vacuolation can be elicited in either *S. occidentalis* extract or Pha treated cells with wavelengths between 400-500 nm or 600-700 nm and specifically at 408 nm or 660 nm, which cover characteristic absorption bands of natural cyclic tetrapyrroles. This further supports the presence of photoactive cyclic tetrapyrroles in *S. occidentalis* extracts. We also found that > 90% vacuolation occurred only for a single radiant exposure in Pha treated cells, whereas *S. occidentalis* treated cells showed > 90% vacuolation in response to a range of radiant exposures and a lower radiant exposure at 660 nm. We reason that these differences are likely due to the presence of other compounds in the plant extract, including cyclic tetrapyrroles with different photoactivities, that affect light absorption and extract photoactivity and toxicity. Lastly, we identified that vacuolation occurred at radiant exposures that were not immediately toxic to cells, and we suggest that vacuolation is likely part of a cellular response to increasing photodamage to the ER and the nuclear envelope by increasing the radiant exposure.

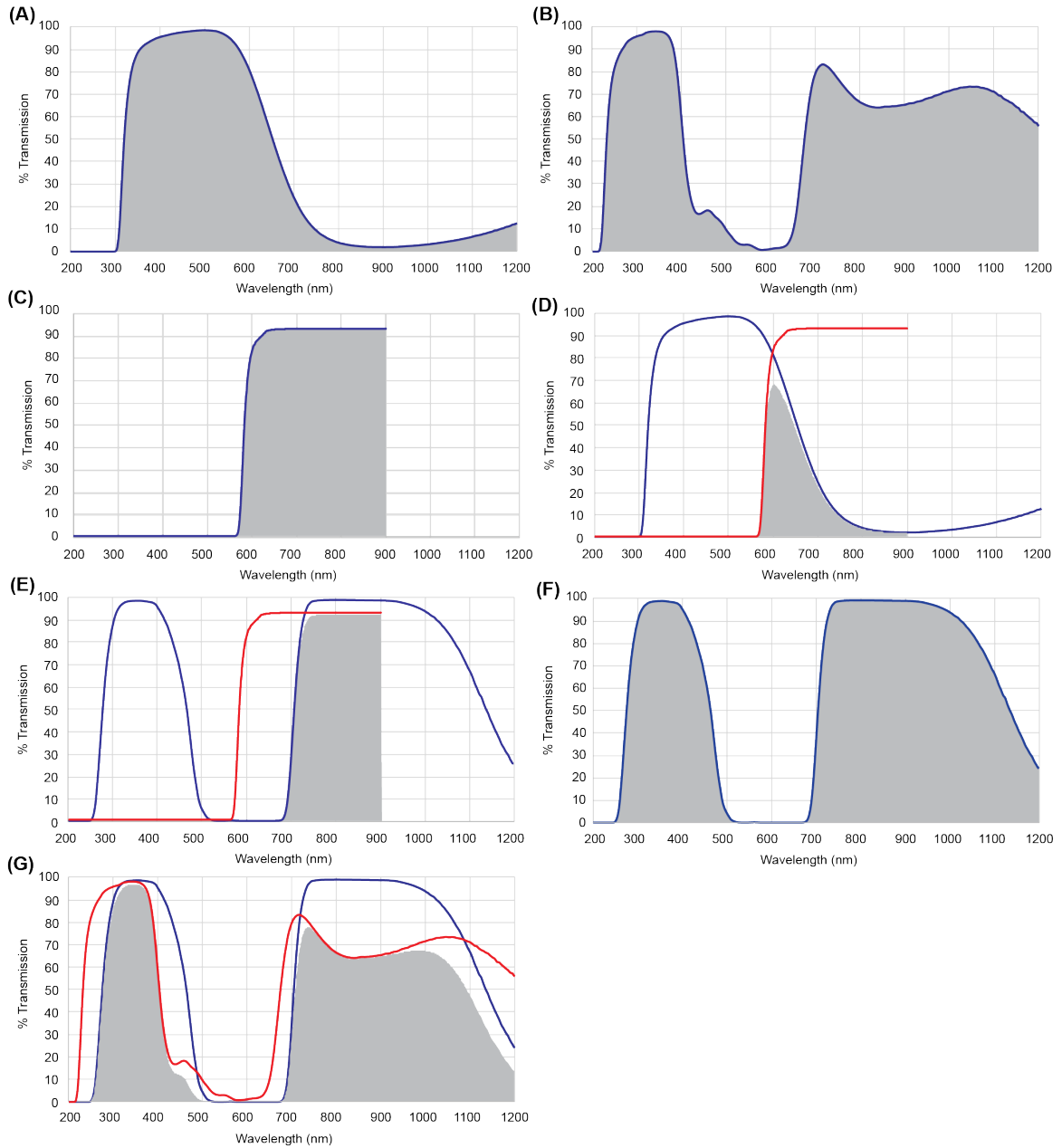


Figure 4.1. Transmission spectra of various filters used in the identification of vacuole-inducing sections of the ambient light spectrum. Ambient light was divided into different section: (A) visible (300-700 nm); (B) non-visible, UV and far red (200-400 nm, >700 nm); (C) >580 nm, (D) 600-700 nm, (E) >700 nm, (F) 300-400 nm and (G) 300-500 nm. Grey areas represent transmission of light through the respective filters.

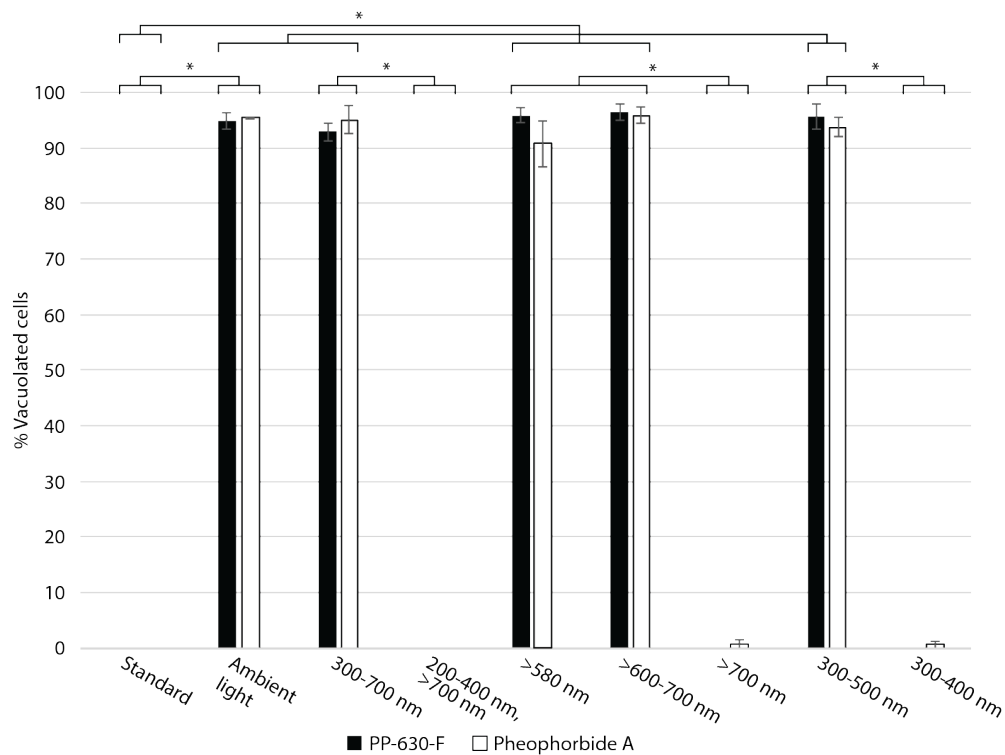


Figure 4.2. Identification of vacuole-inducing sections of the ambient light spectrum in cells treated with either *S. occidentalis* leaf extract or Pha. U2OS cells were treated with either DMSO, 25  $\mu\text{g}/\text{mL}$  PP-630-F or 0.5  $\mu\text{g}/\text{mL}$  Pha and either incubated at standard or ambient conditions for 20 min at 1 h. Cells were also treated with 25  $\mu\text{g}/\text{mL}$  PP-630-F or 0.5  $\mu\text{g}/\text{mL}$  Pha and exposed to ambient light filtered through a combination of optical glass filters that are shown in Figure 4.1 A-G for 20 min. The number of vacuolated cells were counted manually at 16 h using Image J software and the mean percentage of vacuolated cells were calculated from three experiments and standard errors of the means are shown. DMSO treatment did not induce vacuolation. A two-way ANOVA with a Bonferroni post-hoc test was used to compare treatments. No significant differences were found between PP-630-F or Pha treatments ( $p > 0.05$ ) and significant differences are indicated ( $* = p < 0.05$ ).

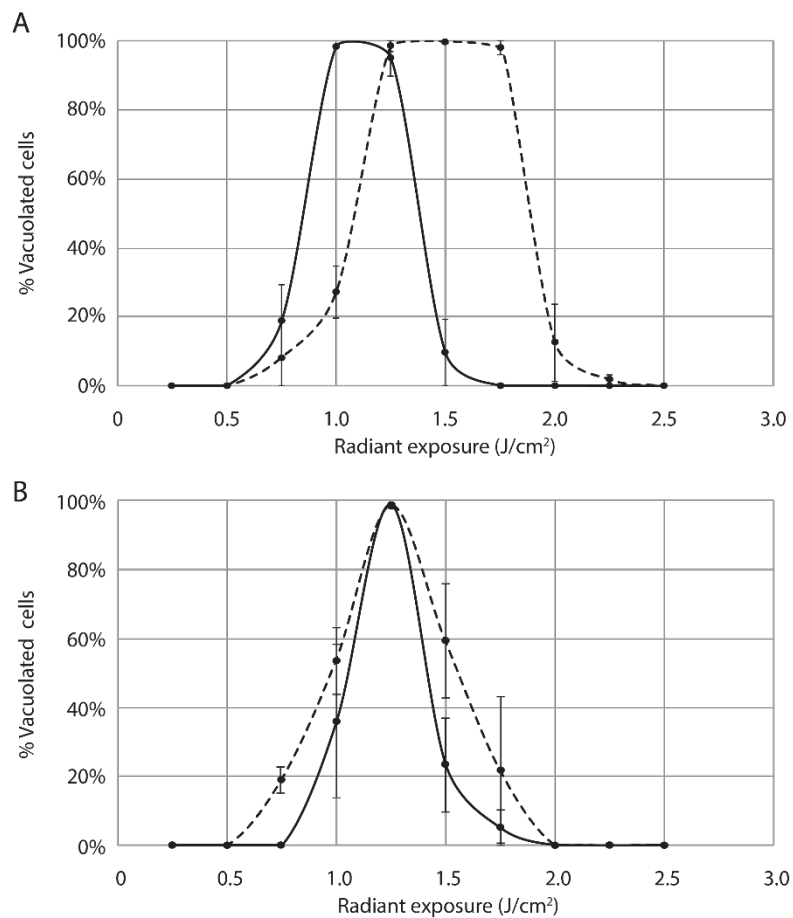


Figure 4.3. Light specific to 408 nm or 660 nm induces vacuoles in cells treated with either *S. occidentalis* leaf extract or Pheophorbide a. U2OS cells were treated with either (A) 25 µg/mL PP-630-F or (B) 0.5 µg/mL Pheophorbide a for 1 h and irradiated at increasing radiant exposures of either blue light (- - -; 408 nm) or red light (—; 660 nm). The number of vacuolated and total cells were counted manually at 16 h using Image J software. The mean percent vacuolated cells of total cells were calculated from three experiments and standard errors of the means are shown. Cells treated with either DMSO, 25 µg/mL PP-630-F or 0.5 µg/mL Pha were incubated at ambient light for 20 min and showed no vacuolation, or vacuolation in  $95 \pm 6\%$  or  $98 \pm 1\%$  of cells, respectively.

## CHAPTER 5 - General discussion

In this thesis we investigated the prairie plant species *Symphoricarpos occidentalis* for natural products with bioactivities against human cells by phenotypic assays. We described the activity of *S. occidentalis* extracts on different human cell lines and found that incubation of *S. occidentalis* DCM extract treated cells at ambient conditions induced an unusual vacuolated phenotype in all cancer cell lines and one normal cell line tested. We then characterized the induction of this vacuolated phenotype in a model cell line, U2OS, and found that it only occurred when *S. occidentalis* extract pre-treated cells were exposed to ambient light. This effect was dependent on extract concentration or duration of ambient light incubation, and co-treatment with ambient light also increased extract toxicity.

We then characterized the vacuolated phenotype and determined that vacuolated cells were alive, and that the cytoplasmic vacuoles originated from the ER, whereas the large, perinuclear vacuole(s) originated from the nuclear envelope. Furthermore, in comparison to the known vacuole-inducing compound, Cyclosporine A, cytoplasmic vacuolation appeared earlier and was not inhibited by protein translation inhibition. We then investigated the nuclear lamina and found an increased nuclear lamin A/C protein signal, particularly at the nuclear location of the perinuclear vacuole. By spectral analysis we identified the cyclic tetrapyrrole, Pheophorbide a, and found that it induces a vacuolated phenotype similar to *S. occidentalis* extracts. We then screened the ambient light spectrum for sections that induce cytoplasmic vacuolation and used LEDs specific to major cyclic tetrapyrrole absorption peaks, and we found that wavelengths between 400-500 nm and 600-700 nm, and specifically at 408 and 660 nm induced vacuolation.

Based on the phenotypic and spectral analyses comparing the *S. occidentalis* extracts and Pha, we propose that *S. occidentalis* contains cyclic tetrapyrroles that induce the vacuolation of human cells and are toxic to human cells upon exposure to light. Furthermore, we propose that *S. occidentalis* extract or Pha localize to the ER and the nuclear envelope and induce their vacuolation upon exposure to light. We also suggest that nuclear envelope vacuolation is due to a phototoxic effect of *S. occidentalis* or Pha on structural proteins associated with the nuclear membrane or nuclear lamina.

### **5.1 The presence of phototoxic cyclic tetrapyrroles in *S. occidentalis* extracts**

In this thesis, we performed a number of experiments that lead us to propose that phototoxic cyclic tetrapyrroles are present in the *S. occidentalis* extract. In Chapter 1, we introduced that a number of natural photosensitizers may exist in plants, including hypericin, riboflavin, curcumin, or the cyclic tetrapyrroles. In Chapter 3, we found that *S. occidentalis* extracts were phototoxic against human cells and showed absorption and fluorescence spectra characteristic of cyclic tetrapyrroles, which was a strong initial indicator for the presence of these photosensitizers in the photoactive *S. occidentalis* extract. In subsequent assays, Pha showed similar phenotypic results to those of the *S. occidentalis* extract, which further supports their presence in the extract. Furthermore, our results in Chapter 4 showed that irradiation of *S. occidentalis* or Pha treated cells at 660 nm induced the vacuolated phenotype, which eliminated many naturally occurring plant photosensitizers as the source of the extract's bioactivity, as they absorb light maximally below 600 nm wavelengths (Pathak, 1984; Abrahamse and Hamblin, 2016). In particular, this also excluded hypericin, which was previously shown to induce ER vacuolation (Kessel, 2018).

Notably, a number of natural cyclic tetrapyrrole derivatives similar to Pha exist and have previously been isolated from different plants, such as Pheophytin, Pheophorbide b, or different Pha esters (Nakamura et al., 1996; Wongsinkongman et al., 2002; Brandis et al., 2006; Adzhar Kamarulzaman et al., 2011). We reason that Pha and these compounds are possibly present in the *S. occidentalis* extract, contribute to the vacuolating activity of the extract and the observed range of radiant exposures, when compared to Pha treated cells. Many cyclic tetrapyrroles localize to multiple subcellular membranes, such as the related pheophorbide-derivatives MPPa, HPPH and DH-II-24. These compounds have been reported to localize to both the mitochondria and the ER, and therefore likely have the potential to induce ER vacuolation, according to Kessel's suggestion that ER localizing photosensitizers induce ER vacuolation (Sun and Leung, 2002; Teiten et al., 2003a; Yoo et al., 2009; Kessel, 2018).

Hence, we suggest that the photoactive molecule(s) in *S. occidentalis* is likely a cyclic tetrapyrrole, but we cannot conclude whether Pha a, a related compound, or multiple cyclic tetrapyrrole photosensitizers together are responsible for the photoactivity of the *S. occidentalis* extract. We have initiated a bioassay-guided fractionation of *S. occidentalis* with Dr. Raymond Andersen (University of British Columbia) to identify the phototoxic compound in *S. occidentalis*.

## **5.2 The ER and nuclear envelope are subcellular targets of *S. occidentalis* and Pheophorbide a**

A novelty of our research is the discovery that *S. occidentalis* extracts or Pha and light co-treatment induced the vacuolation of the ER and the nuclear envelope. We suggest that the photoactive compound(s) in the *S. occidentalis* extract or Pha likely localize to the

membranes of the ER and nuclear envelope and induce photodamage to neighbouring macromolecules, which subsequently leads to the vacuolation of the ER and the nuclear envelope.

To date, Pha has been suggested to localize to the mitochondria (Radestock et al., 2007; Tang et al., 2009a; Bui-Xuan et al., 2010; Hoi et al., 2012). These authors also indicated a non-mitochondrial, perinuclear localization of Pha. Accordingly, we suggest that Pha also localizes to the ER and the nuclear envelope as our data shows *S. occidentalis* or Pha fluorescence at the perinuclear area prior to irradiation and that fluorescence later delineates the vacuoles in vacuolated cells. In accordance with the idea that the primary site of photodamage of a photosensitizer is closely restricted to its localization, previous reports showed that ER localization and photodamage was required for ER vacuolation, as demonstrated by Gomes da Silva et al. or Kessel, whereas nuclear envelope localization and photodamage corresponded with nuclear envelope vacuolation, as demonstrated by Tatsuta et al. Krammer et al. with hematoporphyrin derivatives. This further supports our suggestion of ER and nuclear envelope localization and vacuolation, which also had not previously been reported for plant cyclic tetrapyrroles to our knowledge.

Furthermore, others have shown that Pha induces ER stress, increases intracellular  $\text{Ca}^{2+}$  concentrations, generates ROS, and induces perinuclear lipid peroxidation (Inanami et al., 1999; Rapozzi et al., 2009; Bui-Xuan et al., 2010). These observations are typically reported for ER localizing photosensitizers, such as hypericin or redaporfin (Gomes da Silva et al., 2018; Kessel, 2018). Hence, Pha likely distributes more broadly than previously suggested and likely similar to the distribution of structurally related cyclic tetrapyrroles, such as hematoporphyrin derivative or benzoporphyrin derivative, mTHPC, HPPH, MPPa,

or DH-II-24 (Sun and Leung, 2002; Teiten et al., 2003a; Begum et al., 2009; Yoo et al., 2009; Zheng et al., 2009).

### **5.3 Photodamage to structural proteins of the nuclear envelope and mechanic stress induces vacuolation of the nuclear envelope**

By comparison of the vacuolated U2OS phenotype induced by *S. occidentalis* or Pha to literature data, we found a similar U2OS phenotype, which reportedly occurs when cells are overexpressing specific truncations of the lamin B receptor that are found in the human laminopathies Pelger-Huët anomaly or Greenberg dysplasia (Zwerger et al., 2010). Furthermore, different mixtures of hematoporphyrin derivative were previously shown to localize preferentially to the nuclear membrane in human gastric adenocarcinoma cells and to induce a separation and vacuolation of the nuclear envelope upon irradiation (Tatsuta et al., 1984; Krammer et al., 1993). Although the mechanisms by which nuclear envelope photodamage or specific truncations of the lamin B receptor cause vacuolation of the nuclear envelope is not clear, our findings of an intense lamin A/C signal at the perinuclear vacuole provide some insight.

We propose that *S. occidentalis* extracts or Pha localize, in part, to the membranes of the nuclear envelope and subsequently induce damage to the lipid bilayer and structural proteins associated with these membranes, such as the Sun proteins in the linker of nucleoskeleton and cytoskeleton (LINC) complex or lamins of the nuclear lamina. In support of this, Zwerger et al. and others previously showed that the introduced mutations change the diffusional mobility of the lamin B receptor and lead to the aggregation at distinct microdomains on the nuclear envelope (Zwerger et al., 2010; Tsai et al., 2016; Giannios et al., 2017). The authors suggested that this likely leads to a localized pressure increase inside

the lumen, which indirectly affects structural proteins in the nuclear envelope. Accordingly, others have reported that combined knockdown of the LINC proteins Sun1 and Sun2, which are structural proteins in the nuclear envelope, in *C. elegans* body wall muscle cells or HeLa cells also leads to a separation of the inner and outer nuclear membrane and an expansion of the nuclear envelope (Crisp et al., 2006a; Cain et al., 2014). Specifically, these authors suggested that the mechanistic forces acting on the rather rigid nucleus in *C. elegans* muscle cells or HeLa cells adhered to a tissue-culture dish were mainly responsible for the expansion of the nuclear envelope by pulling the two bilayers apart.

The intense staining of lamin A/C, particularly at the nuclear location of the perinuclear vacuole, observed in our results likely represents an aggregation of lamin A/C. Since lamins of the nuclear lamina interact directly with Sun proteins of the LINC complex, their aggregation may then represent the loss of this interaction upon photodamage, and subsequent mechanical stress may separate the membranes (Yang et al., 2013). In support of this idea, others have previously shown that the ER localizing photosensitizers protoporphyrin IX, hypericin or calphostin C specifically induce the aggregation of lamins, although the authors did not specifically describe observing nuclear envelope vacuolation (Lavie et al., 1999; Ricchelli et al., 1999; Chiarini et al., 2008; Singla et al., 2013; Maitra et al., 2015). Since the ER and outer nuclear membrane are connected, these photosensitizers possibly distribute to the nuclear as well and subsequently photodamage the nuclear envelope membranes and associated structural proteins, such as lamins. In addition, Pha or *S. occidentalis* may localize more preferentially to the nuclear envelope or to specific nuclear envelope locations, which results in vacuolation of the nuclear envelope.

In summary, we propose that nuclear envelope vacuolation and lamin A/C accumulation are connected: *S. occidentalis* extract or Pha photodamage to lamins and/or structural proteins maintaining the perinuclear space of the nuclear envelope, such as Sun proteins, leads to loss of attachment, aggregation of lamins, and separation of the inner and outer nuclear membrane by mechanistic forces from tissue culture attachment and migration. Furthermore, lipid peroxidation previously described in Pha treated cells, may also occur at the membranes of the nuclear envelope, which possibly increases their permeability and contributes to vacuolation by osmotic deregulation of the perinuclear space.

#### **5.4 Photosensitizers as a molecular tool to study cytoplasmic vacuolation, Pelger-Huët anomaly and Greenberg skeletal dysplasia, or cell death**

Another novelty of our research is the future application of *S. occidentalis* and Pha as a molecular tool to characterize and possibly differentiate vacuolation of the ER and the nuclear envelope, determine the relationship between cytoplasmic vacuolation and Pelger-Huët anomaly or Greenberg skeletal dysplasia, and to study photoinduced cell death. In this thesis, we have characterized plant extract and photosensitizer concentrations, minimum treatment durations, and radiant exposure requirements that induce vacuolation of human cells, and we have determined the onset of vacuolation by time-lapse microscopy.

ER vacuolation and paraptosis have been suggested to result from the accumulation of misfolded and unfolded proteins, the efflux of  $\text{Ca}^{2+}$  from the ER and influx into the mitochondria, and the generation of ROS, acting in a feed-forward, self-amplified loop (Yoon et al., 2012; Yoon et al., 2014c; Jeong et al., 2015; Xue et al., 2018). Nuclear envelope vacuolation is thought to occur in response to the absence of or damage to structural proteins involved in membrane spacing and mechanistic forces acting on the nucleus (Crisp et al.,

2006a; Cain et al., 2014). Having characterized the precise onset of vacuolation, which is dependent on photoactivation, we are now able to use *S. occidentalis* extract or Pha and light as a molecular tool. We can measure the events described above at specific timepoints after photoinduction and determine their precise sequence, which remains to be described. Furthermore, study of the relationship between perinuclear vacuolation and damage to structural proteins of the nuclear envelope, such as Sun proteins, lamins and lamin-associated proteins, such as the lamin B receptor may further provide insight into the mechanisms underlying laminopathic diseases, such as Pelger-Huët anomaly. These studies may also provide further insight into porphyria, a group of disorders that result from the buildup of endogenous photosensitizers, such as protoporphyrin IX (Singla et al., 2013; Maitra et al., 2015).

Zwerger et al showed that mutations in the gene coding for the lamin B receptor, which result in the human diseases Pelger-Huët anomaly and Greenberg skeletal dysplasia, induce a vacuolated phenotype in U2OS cells results. Heterozygous Pelger-Huët anomaly is a rare condition (0.01-0.1 % of the world population) is characterized by bilobed neutrophil granulocyte nuclei instead of the normal 3-4 lobes, and by the redistribution of peripheral heterochromatin towards the center of the nucleus (Oosterwijk et al., 2003). Besides that, no other symptoms have been described for the heterozygous phenotype, whereas homozygous Pelger-Huët anomaly is associated with ovoid neutrophil nuclei, skeletal abnormalities and prenatal death. Pelger-Huët anomaly is thought to result from structural abnormalities of the lamin B receptor that is induced by mutations in the N-terminal DNA- and lamin binding domain and the C-terminal sterol reductase domain. The human disease, Greenberg skeletal dysplasia, is another lamin B receptor associated disease, which results exclusively from C-

terminal sterol reductase deficiency of the lamin B receptor in homozygous individuals and is embryonically lethal (Oosterwijk et al., 2003). Hypolobulation has not yet been reported in Greenberg skeletal dysplasia to our knowledge.

Although the mechanism leading to hypolobulation of granulocyte nuclei in Pelger-Huët anomaly is still unknown, it is hypothesized that structural abnormalities in the lamin B receptor lead to altered interactions with peripheral heterochromatin and the nuclear lamina, which is more deformable in granulocytes due to a reduction of lamin A/C levels during differentiation (Olins et al., 2001). There are indications of a connection between the lamin B receptor, lamin A/C and Pelger-Huët anomaly, such as the presence of lamin A in immunoprecipitated lamin B receptor complexes; the partial loss of the lamin B receptor from the nuclear envelope in an Emery-Dreifuss muscular dystrophy patient resulting from mutant lamin A; or the significant elevations of lamin A/C in mature Pelger-Huët anomaly granulocytes as opposed to low levels in normal granulocytes (Simos and Georgatos, 1992; Reichart et al., 2004; Zwerger et al., 2008). Furthermore, the lamin B receptor is one of the first proteins to bind to chromosomes during post-mitotic nuclear formation and is speculated to be involved in nuclear envelope membrane growth (Haraguchi et al., 2000; Olins et al., 2008; Zwerger et al., 2008). Notably, our results showed that *S. occidentalis* extract or Pha and light induced intense lamin A/C staining in treated cells. Thus, these treatment may be used as a molecular tool to study further the connection between lamin B receptor mutations in Pelger-Huët anomaly or Greenberg skeletal dysplasia and lamin A/C. Furthermore, these treatments may also elucidate further the connection between lamin B receptor mutations observed in Pelger-Huët anomaly or Greenberg skeletal dysplasia and the cytoplasmic vacuolation observed by Zwerger et al. 2010, which appeared similar to our vacuolated

phenotype. Although nuclear vacuolation has not yet been reported in Pelger-Huët anomaly granulocytes, nuclear differentiation of lamin B receptor-deficient mouse EPRO cells, a model for granulopoiesis, significantly decreased the distance between the inner- and outer nuclear membrane (Olins et al., 2010). Hence, it would also be of great interest to test *S. occidentalis* extract or Pha in neutrophil granulocytes to determine whether these treatments induce cytoplasmic vacuolation or a decrease the distance between the inner- and outer nuclear membrane, as well.

Notably, we observed ER and nuclear envelope vacuolation in the same phenotype, which is consistent with cells expressing the lamin B receptor mutants and hematoporphyrin derivatives localizing to the nuclear envelope (Tatsuta et al., 1984; Zwerger et al., 2010). It is possible that these observations are due to damage to both organelles concurrently, because the nuclear envelope and the ER are connected through the outer nuclear membrane, or both (Cain et al., 2014). We note that the ER localizing photosensitizers investigated by Gomes da Silva et al. or by Kessel were not reported to induce nuclear envelope vacuolation and that Sun protein knockdown in HeLa cells and *C. elegans* body wall muscle cells did not induce ER vacuolation (Crisp et al., 2006a; Cain et al., 2014). Therefore, this warrants further investigation to determine whether ER and nuclear envelope vacuolation are the same phenotype in *S. occidentalis* or Pha treated cells or whether they can be separated. For example, this could involve lowering the treatment concentration and increasing the radiant exposure, which may elicit one or the other phenotype due to less non-specific localization. For instance, previous reports showed that extracellular concentrations of different pyropheophorbide-a derivatives affected their subcellular localization (MacDonald et al., 1999).

Furthermore, we found that vacuolation was a graded response to increasing radiant exposures that were not immediately toxic to cells. These findings correlate well with the idea that the response of human cells to photodamage varies with the intensity of the treatment, such as photosensitizer concentration or radiant exposure (Piette, 2015). Although Kessel and Gomes da Silva et al. recently demonstrated cytoplasmic vacuolation of the ER as a response to photodamage, they did not specifically demonstrate that it occurs in response to increasing intensity of treatment (Gomes da Silva et al., 2018; Kessel, 2018). We observed that low radiant exposures did not induce any morphological changes, which indicates that cells were likely able to recover from the photodamage by inducing several repair mechanisms, such as ERAD or autophagy. In contrast, high radiant exposures likely induced cell death pathways. Hence, we also propose to co-treatment of human cells with *S. occidentalis* or Pha light as a molecular tool to determine the cellular events and activation of specific pathways that lead to either cell death, vacuolation or survival as radiant light exposures are increased.

## **5.5 Conclusion**

We have found that extracts from *S. occidentalis* or the known photosensitizer Pha induce vacuolation of the ER and the nuclear envelope when cells are co-treated with light. To our knowledge this has not previously been reported for *S. occidentalis*, plant species of the Caprifoliaceae family, or Pha. We reason that vacuolation of the ER and nuclear envelope occurs in response to photodamage to these membranes and membrane-associated proteins. Furthermore, we propose that photodamage to nuclear membrane-associated proteins involved in maintaining the shape of the nuclear envelope, and mechanistic forces acting on the nucleus likely contribute to nuclear envelope vacuolation. We remain to identify the

photoactive compound(s) in *S. occidentalis* and to investigate the exact mechanisms underlying vacuolation of the ER and the nuclear envelope. In particular, we will investigate the connection between nuclear envelope photodamage, lamin accumulation and the expansion of the nuclear envelope. Insight into this connection may be beneficial to the study structural proteins of the nuclear envelope and contribute to studies on cyclic tetrapyrrole-related diseases, such as porphyria, or to laminopathies, such as Pelger-Huët anomaly.

## REFERENCES

- Abrahamse, H., and Hamblin, M. R. (2016). New photosensitizers for photodynamic therapy. *Biochemical Journal*, 473, 347-364.
- Adzhar Kamarulzaman, F., Shaari, K., Siong Hock Ho, A., Haji Lajis, N., Hwang Teo, S., and Boon Lee, H. (2011). Derivatives of pheophorbide - a and pheophorbide - b from photocytotoxic *Piper penangense* extract. *Chemistry & Biodiversity*, 8, 494-502.
- Agostinis, P., Berg, K., Cengel, K. A., Foster, T. H., Girotti, A. W., Gollnick, S. O., Hahn, S. M., Hamblin, M. R., Juzeniene, A., and Kessel, D. (2011). Photodynamic therapy of cancer: an update. *CA: Cancer Journal for Clinicians*, 61, 250-281.
- Ahn, M. Y., Yoon, H. E., Kwon, S. M., Lee, J., Min, S. K., Kim, Y. C., Ahn, S. G., and Yoon, J. H. (2013). Synthesized Pheophorbide a - mediated photodynamic therapy induced apoptosis and autophagy in human oral squamous carcinoma cells. *Journal of Oral Pathology & Medicine*, 42, 17-25.
- Amyot, T. E. (1885). Poisoning by snowberries. *The British Medical Journal*, 1, 986-986.
- Anderson, M. L., and Bailey, A. W. (1979). Effect of fire on a *Symphoricarpos occidentalis* shrub community in central Alberta. *Canadian Journal of Botany*, 57, 2819-2823.
- Anderson, N., and Borlak, J. (2006). Drug-induced phospholipidosis. *FEBS Letters*, 580, 5533-5540.
- Arnason, J., Guerin, B., Kraml, M., Mehta, B., Redmond, R., and Scaiano, J. (1992). Phototoxic and photochemical properties of sanguinarine. *Photochemistry and Photobiology*, 55, 35-38.
- Bacellar, I. O., Oliveira, M. C., Dantas, L. S., Costa, E. B., Junqueira, H. C., Martins, W. K., Durantini, A. M., Cosa, G., Di Mascio, P., and Wainwright, M. (2018). Photosensitized membrane permeabilization requires contact-dependent reactions between photosensitizer and lipids. *Journal of the American Chemical Society*, 140, 9606-9615.
- Baptista, M. S., Cadet, J., Di Mascio, P., Ghogare, A. A., Greer, A., Hamblin, M. R., Lorente, C., Nunez, S. C., Ribeiro, M. S., and Thomas, A. H. (2017). Type I and type II photosensitized oxidation reactions: guidelines and mechanistic pathways. *Photochemistry and Photobiology*, 93, 912-919.
- Barilli, A., Atzeri, C., Bassanetti, I., Ingoglia, F., Dall'Asta, V., Bussolati, O., Maffini, M., Mucchino, C., and Marchiò, L. (2014). Oxidative stress induced by copper and iron complexes with 8-hydroxyquinoline derivatives causes paraptotic death of HeLa cancer cells. *Molecular Pharmaceutics*, 11, 1151-1163.
- Barnaby, A., Duffus, K., and Gupte, S. (2018). Free radical scavenging activity and cytotoxicity assay of *Cissus sicyoides* berries. *Journal of Berry Research*, 8, 1-9.
- Beaubien, E., and Hamann, A. (2011). Spring flowering response to climate change between 1936 and 2006 in Alberta, Canada. *Bioscience*, 61, 514-524.

- Beck, M., Schmidt, A., Malmstroem, J., Claassen, M., Ori, A., Szymborska, A., Herzog, F., Rinner, O., Ellenberg, J., and Aebersold, R. (2011). The quantitative proteome of a human cell line. *Molecular Systems Biology*, 7, 549-557.
- Begum, G., Dube, A., Joshi, P. G., Gupta, P. K., and Joshi, N. B. (2009). Chlorin p6 preferentially localizes in endoplasmic reticulum and Golgi apparatus and inhibits Ca<sup>2+</sup> release from intracellular store. *Journal of Photochemistry and Photobiology B: Biology*, 95, 177-184.
- Ben-Dror, S. (2006). On the correlation between hydrophobicity, liposome binding and cellular uptake of porphyrin sensitizers. *Photochemistry and Photobiology*, 82, 695-701.
- Berg, K., Madslie, K., Bommer Jerry, C., Oftebro, R., Winkelman James, W., and Moan, J. (1991). Light induced relocalization of sulfonated meso-tetraphenylporphines in NHIK 3025 cells and effects of dose fractionation. *Photochemistry and Photobiology*, 53, 203-210.
- Berg, K., and Moan, J. (1994). Lysosomes as photochemical targets. *International Journal of Cancer*, 59, 814-822.
- Berlett, B. S., and Stadtman, E. R. (1997). Protein oxidation in aging, disease, and oxidative stress. *Journal of Biological Chemistry*, 272, 20313-20316.
- Bertrand, R., Solary, E., O'Connor, P., Kohn, K. W., and Pommier, Y. (1994). Induction of a common pathway of apoptosis by staurosporine. *Experimental Cell Research*, 211, 314-321.
- Biertümpfel, R. (2017). Optical Filter Glass Calculation Program (Version 2017.3): SCHOTT AG. Retrieved from [https://www.us.schott.com/advanced\\_optics/english/knowledge-center/technical-articles-and-tools/](https://www.us.schott.com/advanced_optics/english/knowledge-center/technical-articles-and-tools/)
- Bos, A., Li, H., Jean, S., Robichaud, G. A., Johnson, J. A., and Gray, C. A. (2016). Anticancer natural products from traditionally used Canadian medicinal plants. *Planta Medica*, 82, P152.
- Bosco, A. (2017). *A novel anti-mitotic activity on human cells by pulchelloid a, a compound isolated from the prairie plant Gaillardia aristata*. (M.Sc.), University of Lethbridge, Lethbridge, Canada.
- Bowers, M. D., Rosenthal, G., and Berenbaum, M. (1991). *Iridoid glycosides*. Orlando, FL: Academic Press.
- Brandis, A. S., Salomon, Y., and Scherz, A. (2006). Chlorophyll sensitizers in photodynamic therapy *Chlorophylls and Bacteriochlorophylls* (Vol. 25, pp. 461-483): Springer.
- Brasaemle, D. L., Barber, T., Kimmel, A. R., and Londos, C. (1997). Post-translational regulation of perilipin expression Stabilization by stored intracellular neutral lipids. *Journal of Biological Chemistry*, 272, 9378-9387.

- Brunetti, C., George, R. M., Tattini, M., Field, K., and Davey, M. P. (2013). Metabolomics in plant environmental physiology. *Journal of Experimental Botany*, *64*, 4011-4020.
- Buettner, G. R. (1993). The pecking order of free radicals and antioxidants: lipid peroxidation,  $\alpha$ -tocopherol, and ascorbate. *Archives of Biochemistry and Biophysics*, *300*, 535-543.
- Bui-Xuan, N.-H., Tang, P. M.-K., Wong, C.-K., and Fung, K.-P. (2010). Photo-activated pheophorbide-a, an active component of *Scutellaria barbata*, enhances apoptosis via the suppression of ERK-mediated autophagy in the estrogen receptor-negative human breast adenocarcinoma cells MDA-MB-231. *Journal of Ethnopharmacology*, *131*, 95-103.
- Bunjes, R. (2004). Pflanzenvergiftungen im Kindesalter. *Monatsschrift Kinderheilkunde*, *152*, 1055-1061.
- Busch, T., Cengel, K. A., and Finlay, J. (2009). Pheophorbide a as a photosensitizer in photodynamic therapy: in vivo considerations. *Cancer Biology & Therapy*, *8*, 540-542.
- Buytaert, E., Callewaert, G., Hendrickx, N., Scorrano, L., Hartmann, D., Missiaen, L., Vandenheede, J. R., Heirman, I., Grooten, J., and Agostinis, P. (2006a). Role of endoplasmic reticulum depletion and multidomain proapoptotic BAX and BAK proteins in shaping cell death after hypericin-mediated photodynamic therapy. *The FASEB Journal*, *20*, 756-758.
- Buytaert, E., Callewaert, G., Vandenheede, J., and Agostinis, P. (2006b). Deficiency in apoptotic effectors Bax and Bak reveals an autophagic cell death pathway initiated by photodamage to the endoplasmic reticulum. *Autophagy*, *2*, 238-240.
- Buytaert, E., Dewaele, M., and Agostinis, P. (2007). Molecular effectors of multiple cell death pathways initiated by photodynamic therapy. *Biochimica et Biophysica Acta (BBA) - Reviews on Cancer*, *1776*, 86-107.
- Cain, N. E., Tapley, E. C., McDonald, K. L., Cain, B. M., and Starr, D. A. (2014). The SUN protein UNC-84 is required only in force-bearing cells to maintain nuclear envelope architecture. *The Journal of Cell Biology*, *206*, 163-172.
- Castano, A. P., Demidova, T. N., and Hamblin, M. R. (2004). Mechanisms in photodynamic therapy: part one—photosensitizers, photochemistry and cellular localization. *Photodiagnosis and Photodynamic Therapy*, *1*, 279-293.
- Castano, A. P., Demidova, T. N., and Hamblin, M. R. (2005). Mechanisms in photodynamic therapy: part two—cellular signaling, cell metabolism and modes of cell death. *Photodiagnosis and Photodynamic Therapy*, *2*, 1-23.
- Castro-Obregon, S., Del Rio, G., Chen, S., Swanson, R., Frankowski, H., Rao, R., Stoka, V., Vesce, S., Nicholls, D., and Bredesen, D. (2002). A ligand-receptor pair that triggers a non-apoptotic form of programmed cell death. *Cell Death and Differentiation*, *9*, 807-817.

- Celli, J. P., Spring, B. Q., Rizvi, I., Evans, C. L., Samkoe, K. S., Verma, S., Pogue, B. W., and Hasan, T. (2010). Imaging and photodynamic therapy: mechanisms, monitoring, and optimization. *Chemical Reviews*, *110*, 2795-2838.
- Chan, J. Y.-W., Tang, P. M.-K., Hon, P.-M., Au, S. W.-N., Tsui, S. K.-W., Waye, M. M.-Y., Kong, S.-K., Mak, T. C.-W., and Fung, K.-P. (2006). Pheophorbide a, a major antitumor component purified from *Scutellaria barbata*, induces apoptosis in human hepatocellular carcinoma cells. *Planta Medica*, *72*, 28-33.
- Chan, P. S., Koon, H. K., Wu, Z. G., Wong, R. N., Lung, M. L., Chang, C. K., and Mak, N. K. (2009). Role of p38 maps in hypericin photodynamic therapy - induced apoptosis of nasopharyngeal carcinoma cells. *Photochemistry and Photobiology*, *85*, 1207-1217.
- Chavant, L., Combiere, H., and Cros, J. (1975). *Symphoricarpus racemosus* (Michaux): Recherches phytochimiques et etude de la toxicite du fruit. *Plantes Medicinales Et Phytotherapie*, *9*, 267-272.
- Chen, R., Duan, C. Y., Chen, S. K., Zhang, C. Y., He, T., Li, H., Liu, Y. P., and Dai, R. Y. (2013). The suppressive role of p38 MAPK in cellular vacuole formation. *Journal of Cellular Biochemistry*, *114*, 1789-1799.
- Chen, T.-s., Wang, X.-p., Sun, L., Wang, L.-x., Xing, D., and Mok, M. (2008). Taxol induces caspase-independent cytoplasmic vacuolization and cell death through endoplasmic reticulum (ER) swelling in ASTC-a-1 cells. *Cancer Letters*, *270*, 164-172.
- Cheng, H.-H., Wang, H.-K., Ito, J., Bastow, K. F., Tachibana, Y., Nakanishi, Y., Xu, Z., Luo, T.-Y., and Lee, K.-H. (2001). Cytotoxic pheophorbide-related compounds from *Clerodendrum calamitosum* and *C. cyrtophyllum*. *Journal of Natural Products*, *64*, 915-919.
- Cheung, K. K.-Y., Chan, J. Y.-W., and Fung, K.-P. (2013). Antiproliferative effect of pheophorbide a-mediated photodynamic therapy and its synergistic effect with doxorubicin on multiple drug-resistant uterine sarcoma cell MES-SA/Dx5. *Drug and Chemical Toxicology*, *36*, 474-483.
- Chiarini, A., Whitfield, J. F., Pacchiana, R., Armato, U., and Dal Pra, I. (2008). Photoexcited calphostin C selectively destroys nuclear lamin B1 in neoplastic human and rat cells—a novel mechanism of action of a photodynamic tumor therapy agent. *Biochimica et Biophysica Acta (BBA) - Molecular Cell Research*, *1783*, 1642-1653.
- Cho, Y., and Martin, R. (1971). 5, 6-Dehydrolupanine, a new alkaloid, and lupanine from *Thermopsis rhombifolia* (Nutt.) Richards. *Canadian Journal of Chemistry*, *49*, 265-270.
- Choi, B.-h., Ryoo, I.-g., Kang, H. C., and Kwak, M.-K. (2014). The sensitivity of cancer cells to pheophorbide a-based photodynamic therapy is enhanced by Nrf2 silencing. *PLOS ONE*, *9*, e107158.
- Ciechomska, I., Gabrusiewicz, K., Szczepankiewicz, A., and Kaminska, B. (2013). Endoplasmic reticulum stress triggers autophagy in malignant glioma cells undergoing cyclosporine a-induced cell death. *Oncogene*, *32*, 1518-1530.

- Coppola, A., Viggiani, E., Salzarulo, L., and Rasile, G. (1980). Ultrastructural changes in lymphoma cells treated with hematoporphyrin and light. *The American Journal of Pathology*, *99*, 175-193.
- Cordell, G. A., and Colvard, M. D. (2012). Natural products and traditional medicine: Turning on a paradigm. *Journal of Natural Products*, *75*, 514-525.
- Cos, P., Vlietinck, A. J., Berghe, D. V., and Maes, L. (2006). Anti-infective potential of natural products: how to develop a stronger in vitro 'proof-of-concept'. *Journal of Ethnopharmacology*, *106*, 290-302.
- Cragg, G. M., and Newman, D. J. (2013). Natural products: a continuing source of novel drug leads. *Biochimica et Biophysica Acta*, *1830*, 3670-3695.
- Crisp, M., Liu, Q., Roux, K., Rattner, J., Shanahan, C., Burke, B., Stahl, P. D., and Hodzic, D. (2006a). Coupling of the nucleus and cytoplasm: role of the LINC complex. *Journal of Cell Biology*, *172*, 41-53.
- Crisp, M., Liu, Q., Roux, K., Rattner, J., Shanahan, C., Burke, B., Stahl, P. D., and Hodzic, D. (2006b). Coupling of the nucleus and cytoplasm: role of the LINC complex. *J Cell Biol*, *172*, 41-53.
- Dai, J., and Mumper, R. J. (2010). Plant phenolics: extraction, analysis and their antioxidant and anticancer properties. *Molecules*, *15*, 7313-7352.
- Daub, M. (1982). Cercosporin, a photosensitizing toxin from *Cercospora* species. *Phytopathology*, *72*, 370-374.
- Davies, M. J. (2004). Reactive species formed on proteins exposed to singlet oxygen. *Photochemical & Photobiological Sciences*, *3*, 17-25.
- Davies, M. J., and Dean, R. T. (1997). *Radical-mediated protein oxidation: from chemistry to medicine*. New York: Oxford University Press.
- Dechat, T., Pflieger, K., Sengupta, K., Shimi, T., Shumaker, D. K., Solimando, L., and Goldman, R. D. (2008). Nuclear lamins: major factors in the structural organization and function of the nucleus and chromatin. *Genes & Development*, *22*, 832-853.
- Deeg, K., Eichhorn, T., Alexie, G., Kretschmer, N., Andersch, K., Bauer, R., and Efferth, T. (2012). Growth inhibition of human acute lymphoblastic CCRF-CEM leukemia cells by medicinal plants of the West-Canadian Gwich'in Native Americans. *Natural Products and Bioprospecting*, *2*, 35-40.
- Dellinger, M., Ricchelli, F., Moreno, G., and Salet, C. (1994). Hematoporphyrin derivative (Photofrin) photodynamic action on Ca<sup>2+</sup> transport in monkey kidney cells (CV-1). *Photochemistry and Photobiology*, *60*, 368-372.
- Dewick, P. M. (2002). *Medicinal natural products: a biosynthetic approach*. West Sussex, UK: John Wiley and Sons.

- Dewick, P. M. (2009). *Medicinal natural products: a biosynthetic approach* (3 ed.). Chichester, United Kingdom: John Wiley & Sons.
- Di Mascio, P., Devasagayam, T. P., KAISER, S., and SIES, H. (1990). Carotenoids, tocopherols and thiols as biological singlet molecular oxygen quenchers: Portland Press Limited.
- Dias, D. A., Urban, S., and Roessner, U. (2012). A historical overview of natural products in drug discovery. *Metabolites*, 2, 303-336.
- Dobson, P. D., Patel, Y., and Kell, D. B. (2009). 'Metabolite-likeness' as a criterion in the design and selection of pharmaceutical drug libraries. *Drug Discovery Today*, 14, 31-40.
- Doležel, J., Greilhuber, J., and Suda, J. (2007). Estimation of nuclear DNA content in plants using flow cytometry. *Nature Protocols*, 2, 2233-2244.
- Dummin, H., Cernay, T., and Zimmermann, H. (1997). Selective photosensitization of mitochondria in HeLa cells by cationic Zn (II) phthalocyanines with lipophilic side-chains. *Journal of Photochemistry and Photobiology B: Biology*, 37, 219-229.
- Eckhardt, U., Grimm, B., and Hörtensteiner, S. (2004). Recent advances in chlorophyll biosynthesis and breakdown in higher plants. *Plant Molecular Biology*, 56, 1-14.
- Eichwurz, I., Stiel, H., and Röder, B. (2000). Photophysical studies of the pheophorbide a dimer. *Journal of Photochemistry and Photobiology B: Biology*, 54, 194-200.
- Eloff, J. N. (1998). Which extractant should be used for the screening and isolation of antimicrobial components from plants? *Journal of Ethnopharmacology*, 60, 1-8.
- Fabricant, D. S., and Farnsworth, N. R. (2001). The value of plants used in traditional medicine for drug discovery. *Environmental Health Perspectives*, 109, 69-75.
- Feher, M., and Schmidt, J. M. (2003a). Property distributions: differences between drugs, natural products, and molecules from combinatorial chemistry. *Journal of Chemical Information and Computer Sciences*, 43, 218-227.
- Feher, M., and Schmidt, J. M. (2003b). Property distributions: Differences between drugs, natural products, and molecules from combinatorial chemistry. *Journal of Chemical Information and Computer Sciences*, 43, 218-227.
- Fiedor, L., Stasiek, M., Myśliwa-Kurdziel, B., and Strzałka, K. (2003). Phytol as one of the determinants of chlorophyll interactions in solution. *Photosynthesis Research*, 78, 47-57.
- Fombonne, J., Padrón, L., Enjalbert, A., Krantic, S., and Torriglia, A. (2006). A novel paraptosis pathway involving LEI/L-DNaseII for EGF-induced cell death in somatotrope pituitary cells. *Apoptosis*, 11, 367-375.
- Fombonne, J., Reix, S., Rasolonjanahary, R., Danty, E., Thirion, S., Laforge-Anglade, G., Bosler, O., Mehlen, P., Enjalbert, A., and Krantic, S. (2004). Epidermal growth factor

- triggers an original, caspase-independent pituitary cell death with heterogeneous phenotype. *Molecular Biology of the Cell*, *15*, 4938-4948.
- Foote, C. S. (1991). Definition of type I and type II photosensitized oxidation. *Photochemistry and Photobiology*, *54*, 659-659.
- Fuchs, J., and Thiele, J. (1998). The role of oxygen in cutaneous photodynamic therapy. *Free Radical Biology and Medicine*, *24*, 835-847.
- Funakoshi, T., Clever, M., Watanabe, A., and Imamoto, N. (2011). Localization of Pom121 to the inner nuclear membrane is required for an early step of interphase nuclear pore complex assembly. *Molecular Biology of the Cell*, *22*, 1058-1069.
- Garcia-Diaz, M., Huang, Y.-Y., and Hamblin, M. R. (2016). Use of fluorescent probes for ROS to tease apart Type I and Type II photochemical pathways in photodynamic therapy. *Methods*, *109*, 158-166.
- Gerola, A. P., Tsubone, T. M., Santana, A., de Oliveira, H. P., Hioka, N., and Caetano, W. (2011). Properties of chlorophyll and derivatives in homogeneous and microheterogeneous systems. *The Journal of Physical Chemistry B*, *115*, 7364-7373.
- Giannios, I., Chatzantonaki, E., and Georgatos, S. (2017). Dynamics and structure-function relationships of the lamin b receptor (LBR). *PLOS ONE*, *12*, e0169626.
- Giovannetti, R. (2012). The use of spectrophotometry UV-Vis for the study of porphyrins *Macro to Nano Spectroscopy*: InTech.
- Girotti, A. W. (1998). Lipid hydroperoxide generation, turnover, and effector action in biological systems. *Journal of Lipid Research*, *39*, 1529-1542.
- Glinski, J. A., David, E., Warren, T. C., Hansen, G., Leonard, S. F., Pitner, P., Pav, S., Arvigo, R., Balick, M., and Panti, E. (1995). Inactivation of cell surface receptors by pheophorbide a, a green pigment isolated from *Psychotria acuminata*. *Photochemistry and Photobiology*, *62*, 144-150.
- Gomes da Silva, L. C., Zhao, L., Bezu, L., Zhou, H., Sauvat, A., Liu, P., Durand, S., Leduc, M., Souquere, S., Loos, F., Mondragón, L., et al. (2018). Photodynamic therapy with redaporfin targets the endoplasmic reticulum and Golgi apparatus. *The EMBO Journal*, *e98354*, 1-18.
- Gouterman, M. (1959). Study of the effects of substitution on the absorption spectra of porphin. *The Journal of Chemical Physics*, *30*, 1139-1161.
- Gouterman, M. (1961). Spectra of porphyrins. *Journal of Molecular Spectroscopy*, *6*, 138-163.
- Granville, D., Ruehlmann, D., Choy, J., Cassidy, B., Hunt, D., van Breemen, C., and McManus, B. (2001). Bcl-2 increases emptying of endoplasmic reticulum Ca<sup>2+</sup> stores during photodynamic therapy-induced apoptosis. *Cell Calcium*, *30*, 343-350.

- Greenberg, J. T., Guo, A., Klessig, D. F., and Ausubel, F. M. (1994). Programmed cell death in plants: a pathogen-triggered response activated coordinately with multiple defense functions. *Cell*, *77*, 551-563.
- Greenspan, P., Mayer, E. P., and Fowler, S. D. (1985). Nile red: a selective fluorescent stain for intracellular lipid droplets. *The Journal of Cell Biology*, *100*, 965-973.
- Gregory, C. D., and Milner, A. E. (1994). Regulation of cell survival in Burkitt lymphoma: implications from studies of apoptosis following cold - shock treatment. *International Journal of Cancer*, *57*, 419-426.
- Griebel, T., and Zeier, J. (2008). Light regulation and daytime dependency of inducible plant defenses in Arabidopsis: phytochrome signaling controls systemic acquired resistance rather than local defense. *Plant Physiology*, *147*, 790-801.
- Group, E. S. W. (1996). *A national ecological framework for Canada*. Ottawa/Hull: Agriculture and Agri-Food Canada, Research Branch, Centre for Land and Biological Resources Research, and Environment Canada, State of the Environment Directorate, Ecozone Analysis Branch.
- Gubern, A., Barceló-Torns, M., Casas, J., Barneda, D., Masgrau, R., Picatoste, F., Balsinde, J., Balboa, M. A., and Claro, E. (2009). Lipid droplet biogenesis induced by stress involves triacylglycerol synthesis that depends on group VIA phospholipase A2. *Journal of Biological Chemistry*, *284*, 5697-5708.
- Guéraud, F., Atalay, M., Bresgen, N., Cipak, A., Eckl, P. M., Huc, L., Jouanin, I., Siems, W., and Uchida, K. (2010). Chemistry and biochemistry of lipid peroxidation products. *Free Radical Research*, *44*, 1098-1124.
- Hadjadj, D., Denecker, T., Maric, C., Fauchereau, F., Baldacci, G., and Cadoret, J.-C. (2016). Characterization of the replication timing program of 6 human model cell lines. *Genomics Data*, *9*, 113-117.
- Hajduk, P. J., Huth, J. R., and Fesik, S. W. (2005). Druggability indices for protein targets derived from NMR-based screening data. *Journal of Medicinal Chemistry*, *48*, 2518-2525.
- Hajri, A., Coffy, S., Vallat, F., Evrard, S., Marescaux, J., and Aprahamian, M. (1999). Human pancreatic carcinoma cells are sensitive to photodynamic therapy in vitro and in vivo. *British Journal of Surgery*, *86*, 899-906.
- Hajri, A., Wack, S., Meyer, C., Smith, M., Leberquier, C., Kedinger, M., and Aprahamian, M. (2002). In vitro and in vivo efficacy of Photofrin® and pheophorbide a, a bacteriochlorin, in photodynamic therapy of colonic cancer cells. *Photochemistry and Photobiology*, *75*, 140-148.
- Haraguchi, T., Koujin, T., Hayakawa, T., Kaneda, T., Tsutsumi, C., Imamoto, N., Akazawa, C., Sukegawa, J., Yoneda, Y., and Hiraoka, Y. (2000). Live fluorescence imaging reveals early recruitment of emerin, LBR, RanBP2, and Nup153 to reforming functional nuclear envelopes. *Journal of Cell Science*, *113*, 779-794.

- Heaton, J. W., and Marangoni, A. G. (1996). Chlorophyll degradation in processed foods and senescent plant tissues. *Trends in Food Science & Technology*, 7, 8-15.
- Hedner, T., and Everts, B. (1998). The early clinical history of salicylates in rheumatology and pain. *Clinical Rheumatology*, 17, 17-25.
- Hegnauer, R. (1989). *Caprifoliaceae Chemotaxonomie der Pflanzen: Eine Übersicht über die Verbreitung und die Systematische Bedeutung der Pflanzenstoffe*. Basel, Switzerland: Birkhäuser Basel.
- Henderson, B. W., Bellnier, D. A., Greco, W. R., Sharma, A., Pandey, R. K., Vaughan, L. A., Weishaupt, K. R., and Dougherty, T. J. (1997). An in vivo quantitative structure-activity relationship for a congeneric series of pyropheophorbide derivatives as photosensitizers for photodynamic therapy. *Cancer Research*, 57, 4000-4007.
- Henics, T., and Wheatley, D. N. (1999). Cytoplasmic vacuolation, adaptation and cell death: a view on new perspectives and features. *Biology of the Cell*, 91, 485-498.
- Herrmann, H., and Zwerger, M. (2010). The danger of "multi-tasking". *Nucleus*, 1, 319-324.
- Hetzer, M. W., Walther, T. C., and Mattaj, I. W. (2005). Pushing the envelope: structure, function, and dynamics of the nuclear periphery. *Annual Review of Cell and Developmental Biology*, 21, 347-380.
- Hoi, S. W. H., Wong, H. M., Chan, J. Y. W., Yue, G. G. L., Tse, G. M. K., Law, B. K. B., Fong, W. P., and Fung, K. P. (2012). Photodynamic therapy of pheophorbide a inhibits the proliferation of human breast tumour via both caspase - dependent and - independent apoptotic pathways in in vitro and in vivo models. *Phytotherapy Research*, 26, 734-742.
- Hörtensteiner, S., and Kräutler, B. (2011). Chlorophyll breakdown in higher plants. *Biochimica et Biophysica Acta (BBA) - Bioenergetics*, 1807, 977-988.
- Hostettmann, K., and Marston, A. (2002). Twenty years of research into medicinal plants: results and perspectives. *Phytochemistry Reviews*, 1, 275-285.
- Hoye, A. T., Davoren, J. E., Wipf, P., Fink, M. P., and Kagan, V. E. (2008). Targeting mitochondria. *Accounts of Chemical Research*, 41, 87-97.
- Hsiang, Y.-H., Hertzberg, R., Hecht, S., and Liu, L. (1985). Camptothecin induces protein-linked DNA breaks via mammalian DNA topoisomerase I. *Journal of Biological Chemistry*, 260, 14873-14878.
- Hu, X., Makita, S., Schelbert, S., Sano, S., Ochiai, M., Tsuchiya, T., Hasegawa, S. F., Hörtensteiner, S., Tanaka, A., and Tanaka, R. (2015). Reexamination of chlorophyllase function implies its involvement in defense against chewing herbivores. *Plant Physiology*, 167, 660-670.

- Inanami, O., Yoshito, A., Takahashi, K., Hiraoka, W., and Kuwabara, M. (1999). Effects of BAPTA - AM and forskolin on apoptosis and cytochrome c release in photosensitized chinese hamster V79 cells. *Photochemistry and Photobiology*, *70*, 650-655.
- Ishikawa, A., Okamoto, H., Iwasaki, Y., and Asahi, T. (2001). A deficiency of coproporphyrinogen III oxidase causes lesion formation in Arabidopsis. *The Plant Journal*, *27*, 89-99.
- Jacob, R. F., and Mason, R. P. (2005). Lipid peroxidation induces cholesterol domain formation in model membranes. *Journal of Biological Chemistry*, *280*, 39380-39387.
- Jeong, S. A., Kim, I. Y., Lee, A. R., Yoon, M. J., Cho, H., Lee, J.-S., and Choi, K. S. (2015). Ca<sup>2+</sup> influx-mediated dilation of the endoplasmic reticulum and c-FLIPL downregulation trigger CDDO-Me-induced apoptosis in breast cancer cells. *Oncotarget*, *6*, 21173-21192.
- Jong, W. W., Tan, P. J., Kamarulzaman, F. A., Mejin, M., Lim, D., Ang, I., Naming, M., Yeo, T. C., Ho, A. S. H., and Teo, S. H. (2013). Photodynamic activity of plant extracts from Sarawak, Borneo. *Chemistry & Biodiversity*, *10*, 1475-1486.
- Jordan, M. A., Toso, R. J., Thrower, D., and Wilson, L. (1993). Mechanism of mitotic block and inhibition of cell proliferation by taxol at low concentrations. *Proceedings of the National Academy of Sciences*, *90*, 9552-9556.
- Kabe, Y., Ohmori, M., Shinouchi, K., Tsuboi, Y., Hirao, S., Azuma, M., Watanabe, H., Okura, I., and Handa, H. (2006). Porphyrin accumulation in mitochondria is mediated by 2-oxoglutarate carrier. *Journal of Biological Chemistry*, *281*, 31729-31735.
- Kar, R., Singha, P. K., Venkatachalam, M. A., and Saikumar, P. (2009). A novel role for MAP1 LC3 in nonautophagic cytoplasmic vacuolation death of cancer cells. *Oncogene*, *28*, 2556.
- Karchesy, Y. M., Kelsey, R. G., Constantine, G., and Karchesy, J. J. (2016). Biological screening of selected Pacific Northwest forest plants using the brine shrimp (*Artemia salina*) toxicity bioassay. *SpringerPlus*, *5*, 510-519.
- Kariola, T., Brader, G., Li, J., and Palva, E. T. (2005). Chlorophyllase 1, a damage control enzyme, affects the balance between defense pathways in plants. *The Plant Cell*, *17*, 282-294.
- Kaul, A., and Maltese, W. A. (2009). Killing of cancer cells by the photoactivatable protein kinase C inhibitor, calphostin C, involves induction of endoplasmic reticulum stress. *Neoplasia*, *11*, 823-834.
- Keane, K. (2003). *The standing people: Field guide to medicinal plants of the prairie provinces*. Saskatoon, Canada: Root Woman & Dave.
- Kelbauskas, L. (2002). Internalization of aggregated photosensitizers by tumor cells: Subcellular time-resolved fluorescence spectroscopy on derivatives of pyropheophorbide-a

- ethers and chlorin e6 under femtosecond one- and two-photon excitation. *Photochemistry and Photobiology*, 76, 686-694.
- Kemény-Beke, Á., Aradi, J., Damjanovich, J., Beck, Z., Facskó, A., Berta, A., and Bodnár, A. (2006). Apoptotic response of uveal melanoma cells upon treatment with chelidonine, sanguinarine and chelerythrine. *Cancer Letters*, 237, 67-75.
- Kernéis, S., Swift, L. H., Lewis, C. W., Bruyère, C., Oumata, N., Colas, P., Ruchaud, S., Bain, J., and Golsteyn, R. M. (2015). Natural product extracts of the Canadian prairie plant, *Thermopsis rhombifolia*, have anti-cancer activity in phenotypic cell-based assays. *Natural Product Research*, 29, 1026-1034.
- Kerr, J. F. (1965). A histochemical study of hypertrophy and ischaemic injury of rat liver with special reference to changes in lysosomes. *The Journal of Pathology*, 90, 419-435.
- Kessel, D. (2004). Correlation between subcellular localization and photodynamic efficacy. *Journal of Porphyrins and Phthalocyanines*, 8, 1009-1014.
- Kessel, D. (2018). Apoptosis, paraptosis and autophagy: Death and survival pathways associated with photodynamic therapy. *Photochemistry and Photobiology*, 1, 1-7.
- Kessel, D., Luo, Y., Deng, Y., and Chang, C. (1997). The role of subcellular localization in initiation of apoptosis by photodynamic therapy. *Photochemistry and Photobiology*, 65, 422-426.
- Kim, I. Y., Kwon, M., Choi, M.-K., Lee, D., Lee, D. M., Seo, M. J., and Choi, K. S. (2017). Ophiobolin A kills human glioblastoma cells by inducing endoplasmic reticulum stress via disruption of thiol proteostasis. *Oncotarget*, 8, 106740-106752.
- Kim, J.-S., Ohshima, S., Padiaditakis, P., and Lemasters, J. J. (2004). Nitric oxide: a signaling molecule against mitochondrial permeability transition-and pH-dependent cell death after reperfusion. *Free Radical Biology and Medicine*, 37, 1943-1950.
- Kim, S.-A., Lee, M. R., Yoon, J.-H., and Ahn, S.-G. (2016). HOXC6 regulates the antitumor effects of pheophorbide a-based photodynamic therapy in multidrug-resistant oral cancer cells. *International Journal of Oncology*, 49, 2421-2430.
- Kliebenstein, D. (2004). Secondary metabolites and plant/environment interactions: a view through *Arabidopsis thaliana* tinted glasses. *Plant, Cell & Environment*, 27, 675-684.
- Klionsky, D., Herman, P. K., and Emr, S. (1990). The fungal vacuole: composition, function, and biogenesis. *Microbiological Reviews*, 54, 266-292.
- Krammer, B., Hubmer, A., and Hermann, A. (1993). Photodynamic effects on the nuclear envelope of human skin fibroblasts. *Journal of Photochemistry and Photobiology B: Biology*, 17, 109-114.
- Krishnamurthy, P. C., Du, G., Fukuda, Y., Sun, D., Sampath, J., Mercer, K. E., Wang, J., Sosa-Pineda, B., Murti, K. G., and Schuetz, J. D. (2006). Identification of a mammalian mitochondrial porphyrin transporter. *Nature*, 443, 586-589.

- Kroemer, G., Galluzzi, L., Vandenabeele, P., Abrams, J., Alnemri, E. S., Baehrecke, E. H., Blagosklonny, M. V., El-Deiry, W. S., Golstein, P., Green, D. R., Hengartner, M., et al. (2009). Classification of cell death: recommendations of the Nomenclature Committee on Cell Death 2009. *Cell Death and Differentiation*, 16, 3-11.
- Krygowski, T. M., and Stępień, B. T. (2005). Sigma- and pi-electron delocalization: Focus on substituent effects. *Chemical Reviews*, 105, 3482-3512.
- Kuhnlein, H. V., and Turner, N. J. (1991). *Traditional plant foods of Canadian indigenous peoples: nutrition, botany, and use* (Vol. 8). Philadelphia, Pennsylvania: Gordon and Breach Science Publishers.
- Kuijt, J. (1982). *Flora of Waterton Lakes National Park*. Edmonton, Canada: University of Alberta Press.
- Lavi, A., Weitman, H., Holmes, R. T., Smith, K. M., and Ehrenberg, B. (2002). The depth of porphyrin in a membrane and the membrane's physical properties affect the photosensitizing efficiency. *Biophysical Journal*, 82, 2101-2110.
- Lavie, G., Kaplinsky, C., Toren, A., Aizman, I., Meruelo, D., Mazur, Y., and Mandel, M. (1999). A photodynamic pathway to apoptosis and necrosis induced by dimethyl tetrahydroxyhelianthron and hypericin in leukaemic cells: possible relevance to photodynamic therapy. *British Journal of Cancer*, 79, 423-432.
- Lawrence, P., and Brown, W. (1992). Autophagic vacuoles rapidly fuse with pre-existing lysosomes in cultured hepatocytes. *Journal of Cell Science*, 102, 515-526.
- Lee, D., Kim, I. Y., Saha, S., and Choi, K. S. (2016). Paraptosis in the anti-cancer arsenal of natural products. *Pharmacology & Therapeutics*, 162, 120-133.
- Lee, J., and Berg, E. (2013). Neoclassic drug discovery: the case for lead generation using phenotypic and functional approaches. *Journal of Biomolecular Screening*, 18, 1143-1155.
- Lee, J., Homma, T., Kurahashi, T., Kang, E. S., and Fujii, J. (2015a). Oxidative stress triggers lipid droplet accumulation in primary cultured hepatocytes by activating fatty acid synthesis. *Biochemical and Biophysical Research Communications*, 464, 229-235.
- Lee, M.-L., and Schneider, G. (2001). Scaffold architecture and pharmacophoric properties of natural products and trade drugs: application in the design of natural product-based combinatorial libraries. *Journal of Combinatorial Chemistry*, 3, 284-289.
- Lee, W.-J., Chien, M.-H., Chow, J.-M., Chang, J.-L., Wen, Y.-C., Lin, Y.-W., Cheng, C.-W., Lai, G.-M., Hsiao, M., and Lee, L.-M. (2015b). Nonautophagic cytoplasmic vacuolation death induction in human PC-3M prostate cancer by curcumin through reactive oxygen species-mediated endoplasmic reticulum stress. *Scientific Reports*, 10420, 1-14.
- Lee, W.-Y., Lim, D.-S., Ko, S.-H., Park, Y.-J., Ryu, K.-S., Ahn, M.-Y., Kim, Y.-R., Lee, D. W., and Cho, C.-W. (2004). Photoactivation of pheophorbide a induces a mitochondrial-mediated apoptosis in Jurkat leukaemia cells. *Journal of Photochemistry and Photobiology B: Biology*, 75, 119-126.

- Lena, A., Rechichi, M., Salvetti, A., Vecchio, D., Evangelista, M., Rainaldi, G., Gremigni, V., and Rossi, L. (2010). The silencing of adenine nucleotide translocase isoform 1 induces oxidative stress and programmed cell death in ADF human glioblastoma cells. *The FEBS Journal*, 277, 2853-2867.
- Lesperance, A., Tueller, P., and Bohman, V. (1970). Symposium on pasture methods for maximum production in beef cattle: competitive use of the range forage resource. *Journal of Animal Science*, 30, 115-121.
- Leung, H. W. C., Hour, M. J., Chang, W. T., Wu, Y. C., Lai, M. Y., Wang, M. Y., and Lee, H. Z. (2008). P38-associated pathway involvement in apoptosis induced by photodynamic therapy with *Lonicera japonica* in human lung squamous carcinoma CH27 cells. *Food and Chemical Toxicology*, 46, 3389-3400.
- Lewis, W. H. (1979). Snowberry (*Symphoricarpos*) poisoning in children. *The Journal of the American Medical Association*, 242, 2663-2663.
- Li, W.-T., Tsao, H.-W., Chen, Y.-Y., Cheng, S.-W., and Hsu, Y.-C. (2007). A study on the photodynamic properties of chlorophyll derivatives using human hepatocellular carcinoma cells. *Photochemical & Photobiological Sciences*, 6, 1341-1348.
- Lichtenthaler, H. K. (1987). [34] Chlorophylls and carotenoids: pigments of photosynthetic biomembranes *Methods in Enzymology* (Vol. 148, pp. 350-382): Elsevier.
- Lim, Y. C., Yoo, J. O., Park, D., Kang, G., Hwang, B. M., Kim, Y. M., and Ha, K. S. (2009). Antitumor effect of photodynamic therapy with chlorin - based photosensitizer DH - II - 24 in colorectal carcinoma. *Cancer Science*, 100, 2431-2436.
- Looman, J., and Best, K. F. (1979). *Budd's flora of the Canadian prairie provinces*. Hull, Canada: Canadian Government Publishing Centre.
- Lyles, M. B., and Cameron, I. L. (2002). Interactions of the DNA intercalator acridine orange, with itself, with caffeine, and with double stranded DNA. *Biophysical Chemistry*, 96, 53-76.
- MacDonald, I. J., Morgan, J., Bellnier, D. A., Paszkiewicz, G. M., Whitaker, J. E., Litchfield, D. J., and Dougherty, T. J. (1999). Subcellular localization patterns and their relationship to photodynamic activity of pyropheophorbide - a derivatives. *Photochemistry and Photobiology*, 70, 789-797.
- Mach, J. M., Castillo, A. R., Hoogstraten, R., and Greenberg, J. T. (2001). The Arabidopsis-accelerated cell death gene ACD2 encodes red chlorophyll catabolite reductase and suppresses the spread of disease symptoms. *Proceedings of the National Academy of Sciences*, 98, 771-776.
- Maitra, D., Elenbaas, J. S., Whitesall, S. E., Basrur, V., D'Alecy, L. G., and Omary, M. B. (2015). Ambient light promotes selective subcellular proteotoxicity after endogenous and exogenous porphyrinogenic stress. *The Journal of Biological Chemistry*, 290, 23711-23724.

- Makatsori, D., Kourmouli, N., Polioudaki, H., Shultz, L. D., Mclean, K., Theodoropoulos, P. A., Singh, P. B., and Georgatos, S. D. (2004). The inner nuclear membrane protein lamin B receptor forms distinct microdomains and links epigenetically marked chromatin to the nuclear envelope. *Journal of Biological Chemistry*, 279, 25567-25573.
- Mangos, T. J., and Berger, R. G. (1997). Determination of major chlorophyll degradation products. *Zeitschrift für Lebensmitteluntersuchung und Forschung*, 204, 345-350.
- Mann, J. (2000). *Murder, magic, and medicine*. Oxford: Oxford University Press, USA.
- Maplestone, R. A., Stone, M. J., and Williams, D. H. (1992). The evolutionary role of secondary metabolites—a review. *Gene*, 115, 151-157.
- Marshall, I. B., Schut, P. H., and Ballard, M. (1999). *A national ecological framework for Canada: Attribute data*. Ottawa/Hull: Agriculture and Agri-Food Canada, Research Branch, Centre for Land and Biological Resources Research, and Environment Canada, State of the Environment Directorate, Ecozone Analysis Branch.
- Matson, D. R., and Stukenberg, P. T. (2011). Spindle poisons and cell fate: A tale of two pathways. *Molecular Interventions*, 11, 141-150.
- McCutcheon, A., Ellis, S., Hancock, R., and Towers, G. (1992). Antibiotic screening of medicinal plants of the British Columbian native peoples. *Journal of Ethnopharmacology*, 37, 213-223.
- McCutcheon, A., Roberts, T., Gibbons, E., Ellis, S., Babiuk, L., Hancock, R., and Towers, G. (1995). Antiviral screening of British Columbian medicinal plants. *Journal of Ethnopharmacology*, 49, 101-110.
- McCutcheon, A. R., Stokes, R. W., Thorson, L. M., Ellis, S. M., Hancock, R. E. W., and Towers, G. H. N. (1997). Anti-mycobacterial screening of British Columbian medicinal plants. *International Journal of Pharmacognosy*, 35, 77-83.
- McGrath-Hill, C. A., and Vicas, I. M. (1997). Case series of *Thermopsis* exposures. *Journal of Toxicology: Clinical Toxicology*, 35, 659-665.
- Miller, J. S. (2011). The discovery of medicines from plants: a current biological perspective. *Economic Botany*, 65, 396-407.
- Mimnaugh, E. G., Xu, W., Vos, M., Yuan, X., and Neckers, L. (2006). Endoplasmic reticulum vacuolization and valosin-containing protein relocalization result from simultaneous hsp90 inhibition by geldanamycin and proteasome inhibition by velcade. *Molecular Cancer Research*, 4, 667-681.
- Moerman, D. E. (1998). *Native American Ethnobotany*. Portland, OR: Timber Press.
- Moffat, J. G., Vincent, F., Lee, J. A., Eder, J., and Prunotto, M. (2017). Opportunities and challenges in phenotypic drug discovery: an industry perspective. *Nature Reviews Drug Discovery*, 16, 531-543.

- Monel, B., Compton, A. A., Bruel, T., Amraoui, S., Burlaud-Gaillard, J., Roy, N., Guivel-Benhassine, F., Porrot, F., Génin, P., Meertens, L., Sinigaglia, L., et al. (2017). Zika virus induces massive cytoplasmic vacuolization and paraptosis-like death in infected cells. *The EMBO Journal*, *36*, 1653-1668.
- Moss, E. H. (1932). The vegetation of Alberta: Iv. The poplar association and related vegetation of central Alberta. *Journal of Ecology*, *20*, 380-415.
- Moss, E. H., and Packer, J. G. (1983). *Flora of Alberta: a manual of flowering plants, conifers, ferns, and fern allies found growing without cultivation in the Province of Alberta, Canada*. Toronto, Canada University of Toronto Press.
- Mroz, P., Yaroslavsky, A., Kharkwal, G. B., and Hamblin, M. R. (2011). Cell death pathways in photodynamic therapy of cancer. *Cancers*, *3*, 2516-2539.
- Munafó, D. B., and Colombo, M. I. (2001). A novel assay to study autophagy: regulation of autophagosome vacuole size by amino acid deprivation. *Journal of Cell Science*, *114*, 3619-3629.
- Munro, D. B. (2000). Canadian poisonous plants information system. Retrieved from <http://www.cbif.gc.ca/eng/species-bank/canadian-poisonous-plants-information-system/all-plants-scientific-name/symphoricarpos-albus/?id=1370403267021>
- Musacchio, A., and Salmon, E. D. (2007). The spindle-assembly checkpoint in space and time. *Nature Reviews. Molecular Cell Biology*, *8*, 379-393.
- Nakamura, Y., Murakami, A., Koshimizu, K., and Ohigashi, H. (1996). Identification of pheophorbide a and its related compounds as possible anti-tumor promoters in the leaves of *Neptunia oleracea*. *Bioscience, Biotechnology, and Biochemistry*, *60*, 1028-1030.
- Newman, D. J., and Cragg, G. M. (2016). Natural products as sources of new drugs from 1981 to 2014. *Journal of Natural Products*, *79*, 629-661.
- Newman, D. J., Cragg, G. M., and Snader, K. M. (2000). The influence of natural products upon drug discovery. *Natural Product Reports*, *17*, 215-234.
- Ngo, L. T., Okogun, J. I., and Folk, W. R. (2013). 21st century natural product research and drug development and traditional medicines. *Natural Product Reports*, *30*, 584-592.
- Niforou, K. N., Anagnostopoulos, A. K., Vougas, K., Kittas, C., Gorgoulis, V. G., and Tsangaris, G. T. (2008). The proteome profile of the human osteosarcoma U2OS cell line. *Cancer Genomics-Proteomics*, *5*, 63-77.
- Nilapwar, S. M., Nardelli, M., Westerhoff, H. V., and Verma, M. (2011). Chapter four - absorption spectroscopy. In D. Jameson, M. Verma, and H. V. Westerhoff (Eds.), *Methods in Enzymology* (Vol. 500, pp. 59-75): Academic Press.
- Novikoff, A. B., and Essner, E. (1962). Cytolysomes and mitochondrial degeneration. *The Journal of Cell Biology*, *15*, 140.

- Nyman, E. S., and Hynninen, P. H. (2004). Research advances in the use of tetrapyrrolic photosensitizers for photodynamic therapy. *Journal of Photochemistry and Photobiology B: Biology*, 73, 1-28.
- Ochsner, M. (1997). Photophysical and photobiological processes in the photodynamic therapy of tumours. *Journal of Photochemistry and Photobiology B: Biology*, 39, 1-18.
- Olins, A. L., Herrmann, H., Lichter, P., Kratzmeier, M., Doenecke, D., and Olins, D. E. (2001). Nuclear envelope and chromatin compositional differences comparing undifferentiated and retinoic acid- and phorbol ester-treated HL-60 cells. *Experimental Cell Research*, 268, 115-127.
- Olins, A. L., Rhodes, G., Welch, D. B. M., Zwerger, M., and Olins, D. E. (2010). Lamin B receptor. *Nucleus*, 1, 53-70.
- Olins, A. L., Zwerger, M., Herrmann, H., Zentgraf, H., Simon, A. J., Monestier, M., and Olins, D. E. (2008). The human granulocyte nucleus: Unusual nuclear envelope and heterochromatin composition. *European Journal of Cell Biology*, 87, 279-290.
- Ong, C. Y., Ling, S. K., Ali, R. M., Chee, C. F., Samah, Z. A., Ho, A. S. H., Teo, S. H., and Lee, H. B. (2009). Systematic analysis of in vitro photo-cytotoxic activity in extracts from terrestrial plants in Peninsula Malaysia for photodynamic therapy. *Journal of Photochemistry and Photobiology B: Biology*, 96, 216-222.
- Oosterwijk, J., Mansour, S., Van Noort, G., Waterham, H., Hall, C., and Hennekam, R. (2003). Congenital abnormalities reported in Pelger-Huet homozygosity as compared to Greenberg/HEM dysplasia: highly variable expression of allelic phenotypes. *Journal of medical genetics*, 40, 937-941.
- Ott, M., Gogvadze, V., Orrenius, S., and Zhivotovsky, B. (2007). Mitochondria, oxidative stress and cell death. *Apoptosis*, 12, 913-922.
- Pace, N. (1942). The etiology of hypericium, a photosensitivity produced by St. Johnswort. *American Journal of Physiology--Legacy Content*, 136, 650-656.
- Pahl, M., and Smreciu, A. (1999). *Growing native plants of western Canada: Common grasses and wildflowers*. Edmonton: Alberta Agriculture, Food and Rural Development.
- Pathak, M. A. (1984). Mechanisms of psoralen photosensitization reactions. *National Cancer Institute Monograph*, 66, 41-46.
- Pelton, J. (1953). Studies on the life - history of *Symphoricarpos occidentalis* Hook., in Minnesota. *Ecological Monographs*, 23, 17-39.
- Petrillo, S., Chiabrando, D., Genova, T., Fiorito, V., Ingoglia, G., Vinchi, F., Mussano, F., Carossa, S., Silengo, L., Altruda, F., Merlo, G. R., et al. (2018). Heme accumulation in endothelial cells impairs angiogenesis by triggering paraptosis. *Cell Death & Differentiation*, 25, 573-588.

- Piette, J. (2015). Signalling pathway activation by photodynamic therapy: NF- $\kappa$ B at the crossroad between oncology and immunology. *Photochemical & Photobiological Sciences*, *14*, 1510-1517.
- Piette, J., Volanti, C., Vantieghem, A., Matroule, J.-Y., Habraken, Y., and Agostinis, P. (2003). Cell death and growth arrest in response to photodynamic therapy with membrane-bound photosensitizers. *Biochemical Pharmacology*, *66*, 1651-1659.
- Pizzimenti, S., Ciamporcero, E. S., Daga, M., Pettazzoni, P., Arcaro, A., Cetrangolo, G., Minelli, R., Dianzani, C., Lepore, A., and Gentile, F. (2013). Interaction of aldehydes derived from lipid peroxidation and membrane proteins. *Frontiers in Physiology*, *4*, 242.
- Pružinská, A., Tanner, G., Anders, I., Roca, M., and Hörtensteiner, S. (2003). Chlorophyll breakdown: pheophorbide a oxygenase is a Rieske-type iron-sulfur protein, encoded by the accelerated cell death 1 gene. *Proceedings of the National Academy of Sciences*, *100*, 15259-15264.
- Quinn, J. C., Kessell, A., and Weston, L. A. (2014). Secondary plant products causing photosensitization in grazing herbivores: their structure, activity and regulation. *International Journal of Molecular Sciences*, *15*, 1441-1465.
- Radestock, A., Elsner, P., Gitter, B., and Hipler, U.-C. (2007). Induction of apoptosis in HaCaT cells by photodynamic therapy with chlorin e6 or pheophorbide a. *Skin Pharmacology and Physiology*, *20*, 3-9.
- Raffauf, R. F. (1970). *Handbook of alkaloids and alkaloid-containing plants*. New York: Wiley.
- Ram, B. M., and Ramakrishna, G. (2014). Endoplasmic reticulum vacuolation and unfolded protein response leading to paraptosis like cell death in cyclosporine A treated cancer cervix cells is mediated by cyclophilin B inhibition. *Biochimica et Biophysica Acta (BBA) - Molecular Cell Research*, *1843*, 2497-2512.
- Rapozzi, V., Miculan, M., and Xodo, L. (2009). Evidence that photoactivated pheophorbide a causes in human cancer cells a photodynamic effect involving lipid peroxidation. *Cancer Biology & Therapy*, *8*, 1318-1327.
- Rautio, J., Kumpulainen, H., Heimbach, T., Oliyai, R., Oh, D., Järvinen, T., and Savolainen, J. (2008). Prodrugs: design and clinical applications. *Nature Reviews. Drug Discovery*, *7*, 255-270.
- Reichart, B., Klafke, R., Dreger, C., Krüger, E., Motsch, I., Ewald, A., Schäfer, J., Reichmann, H., Müller, C. R., and Dabauvalle, M.-C. (2004). Expression and localization of nuclear proteins in autosomal-dominant Emery-Dreifuss muscular dystrophy with LMNA R377H mutation. *BMC cell biology*, *12*, 1-16.
- Reiners, J. J., Agostinis, P., Berg, K., Oleinick, N. L., and Kessel, D. H. (2010). Assessing autophagy in the context of photodynamic therapy. *Autophagy*, *6*, 7-18.

- Reiners, J. J., Caruso, J., Mathieu, P., Chelladurai, B., Yin, X., and Kessel, D. (2002). Release of cytochrome c and activation of pro-caspase-9 following lysosomal photodamage involves Bid cleavage. *Cell Death and Differentiation*, *9*, 934-944.
- Ricchelli, F. (1995). Photophysical properties of porphyrins in biological membranes. *Journal of Photochemistry and Photobiology B: Biology*, *29*, 109-118.
- Ricchelli, F., Barbato, P., Milani, M., Gobbo, S., Salet, C., and Moreno, G. (1999). Photodynamic action of porphyrin on Ca<sup>2+</sup> influx in endoplasmic reticulum: a comparison with mitochondria. *Biochemical Journal*, *338*, 221-227.
- Ritz, R., Roser, F., Radomski, N., Strauss, W. S., Tatagiba, M., and Gharabaghi, A. (2008). Subcellular colocalization of hypericin with respect to endoplasmic reticulum and Golgi apparatus in glioblastoma cells. *Anticancer Research*, *28*, 2033-2038.
- Roeder, B., Hanke, T., Oelckers, S., Hackbarth, S., and Symietz, C. (2000). Photophysical properties of pheophorbide a in solution and in model membrane systems. *Journal of Porphyrins and Phthalocyanines*, *4*, 37-44.
- Roeder, B., Naether, D., Lewald, T., Braune, M., Nowak, C., and Freyer, W. (1990). Photophysical properties and photodynamic activity in vivo of some tetrapyrroles. *Biophysical Chemistry*, *35*, 303-312.
- Roeder, B., and Wabnitz, H. (1987). Time-resolved fluorescence spectroscopy of hematoporphyrin, mesoporphyrin, pheophorbide a and chlorin e6 in ethanol and aqueous solution. *Journal of Photochemistry and Photobiology B: Biology*, *1*, 103-113.
- Rosenthal, G., and Berenbaum, M. (2012). *Herbivores: their interactions with secondary plant metabolites: ecological and evolutionary processes* (Vol. 2). San Diego: Academic Press Inc.
- Runnels, J., Chen, N., Ortel, B., Kato, D., and Hasan, T. (1999). BPD-MA-mediated photosensitization in vitro and in vivo: cellular adhesion and  $\beta$  1 integrin expression in ovarian cancer cells. *British Journal of Cancer*, *80*, 946.
- Saczko, J., Mazurkiewicz, M., Chwiłkowska, A., Kulbacka, J., Kramer, G., Ługowski, M., Snietura, M., and Banaś, T. (2007). Intracellular distribution of Photofrin in malignant and normal endothelial cell lines. *Folia Biologica*, *53*, 7-12.
- Saenz, C., Cheruku, R. R., Ohulchansky, T. Y., Joshi, P., Tabaczynski, W. A., Missert, J. R., Chen, Y., Pera, P., Tracy, E., Marko, A., Rohrbach, D., et al. (2017). Structural and epimeric isomers of HPPH [3-devinyl 3-{1-(1-hexyloxy) ethyl}pyropheophorbide-a]: Effects on uptake and photodynamic therapy of cancer. *ACS Chemical Biology*, *12*, 933-946.
- Sanchez, R., Williams, C., Daza, J. L., Dan, Q., Xu, Q., Chen, Y., Delgado, C., Arpajirakul, N., Jeffes, E. W. B., Kim, R. C., Douglass, T., et al. (2002). T9 glioma cells expressing membrane-macrophage colony stimulating factor produce CD4<sup>+</sup> T cell-associated protective immunity against T9 intracranial gliomas and systemic immunity against different syngeneic gliomas. *Cellular Immunology*, *215*, 1-11.

- Sasaki, D. T., Dumas, S. E., and Engleman, E. G. (1987). Discrimination of viable and non - viable cells using propidium iodide in two color immunofluorescence. *Cytometry Part A*, 8, 413-420.
- Sasidharan, S., Chen, Y., Saravanan, D., Sundram, K., and Latha, L. Y. (2011). Extraction, isolation and characterization of bioactive compounds from plants' extracts. *African Journal of Traditional, Complementary and Alternative Medicines*, 8, 1-10.
- Schlothauer, J., Hackbarth, S., and Röder, B. (2008). A new benchmark for time-resolved detection of singlet oxygen luminescence—revealing the evolution of lifetime in living cells with low dose illumination. *Laser Physics Letters*, 6, 216.
- Semeraro, P., Chimienti, G., Altamura, E., Fini, P., Rizzi, V., and Cosma, P. (2018). Chlorophyll a in cyclodextrin supramolecular complexes as a natural photosensitizer for photodynamic therapy (PDT) applications. *Materials Science and Engineering: C*, 85, 47-56.
- Serturmer, F. (1805). Darstellung der reinen Mohnsaure (Opiumsauce) nebst einer chemischen Untersuchung des Opiums unter vorzuglicher Hinsicht auf einen darin neu entdeckten Stoff und die dahin gehorigen Bemerkungen. *Journal Der Pharmacie*, 14, 47-93.
- Settembre, C., Fraldi, A., Medina, D. L., and Ballabio, A. (2013). Signals from the lysosome: a control centre for cellular clearance and energy metabolism. *Nature Reviews Molecular Cell Biology*, 14, 283.
- Sharman, W. M., Allen, C. M., and van Lier, J. E. (2000). [35] Role of activated oxygen species in photodynamic therapy *Methods in Enzymology* (Vol. 319, pp. 376-400): Academic Press.
- Shioi, Y., Watanabe, K., and Takamiya, K.-i. (1996). Enzymatic conversion of pheophorbide a to the precursor of pyropheophorbide a in leaves of *Chenopodium album*. *Plant and Cell Physiology*, 37, 1143-1149.
- Shubin, A. V., Demidyuk, I. V., Komissarov, A. A., Rafieva, L. M., and Kostrov, S. V. (2016). Cytoplasmic vacuolization in cell death and survival. *Oncotarget*, 7, 55863-55889.
- Simos, G., and Georgatos, S. D. (1992). The inner nuclear membrane protein p58 associates in vivo with a p58 kinase and the nuclear lamins. *The EMBO Journal*, 11, 4027-4036.
- Singla, A., Griggs, N. W., Kwan, R., Snider, N. T., Maitra, D., Ernst, S. A., Herrmann, H., and Omary, M. B. (2013). Lamin aggregation is an early sensor of porphyria-induced liver injury. *Journal of Cell Science*, 126, 3105-3112.
- Skalkos, D., Hampton, J. A., Keck, R. W., Wagoner, M., and Selman, S. H. (1994). Iminium salt benzochlorins: structure - activity relationship studies. *Photochemistry and Photobiology*, 59, 175-181.

- Smith, M. H., Ploegh, H. L., and Weissman, J. S. (2011). Road to ruin: targeting proteins for degradation in the endoplasmic reticulum. *Science*, 334, 1086-1090.
- Smolenski, S., Silinis, H., and Farnsworth, N. R. (1974). Alkaloid screening V. *Lloydia*, 37, 506-536.
- Sowemimo, A., van de Venter, M., Baatjies, L., Koekemoer, T., Adesanya, S., and Lin, W. (2012). Cytotoxic compounds from the leaves of *Combretum paniculatum* Vent. *African Journal of Biotechnology*, 11, 4631-4635.
- Sperandio, S., de Belle, I., and Bredesen, D. E. (2000). An alternative, nonapoptotic form of programmed cell death. *Proceedings of the National Academy of Sciences*, 97, 14376-14381.
- Spickett, C. M., Wiswedel, I., Siems, W., Zarkovic, K., and Zarkovic, N. (2010). Advances in methods for the determination of biologically relevant lipid peroxidation products. *Free Radical Research*, 44, 1172-1202.
- Stermitz, F. R., Tawara-Matsuda, J., Lorenz, P., Mueller, P., Zenewicz, L., and Lewis, K. (2000). 5'-methoxyhydnocarpin-d and pheophorbide a: *Berberis* species components that potentiate berberine growth inhibition of resistant *Staphylococcus aureus*. *Journal of Natural Products*, 63, 1146-1149.
- Sun, Q., Chen, T., Wang, X., and Wei, X. (2010). Taxol induces paraptosis independent of both protein synthesis and MAPK pathway. *Journal of Cellular Physiology*, 222, 421-432.
- Sun, X., and Leung, W. (2002). Photodynamic Therapy with Porphyrin - a Methyl Ester in Human Lung Carcinoma Cancer Cell: Efficacy, Localization and Apoptosis. *Photochemistry and Photobiology*, 75, 644-651.
- Swinney, D. C., and Anthony, J. (2011). How were new medicines discovered? *Nature Reviews Drug Discovery*, 10, 507.
- Szafer-Hajdrych, M., and Goslinska, O. (2004). The quantitative determination of phenolic acids and antimicrobial activity of *Symphoricarpos albus* (L.) Blake. *Acta Poloniae Pharmaceutica*, 61, 69-74.
- Szafer, M., Kowalewski, Z., and Phillipson, J. D. (1978). Chelidonine from *Symphoricarpos albus*. *Phytochemistry*, 17, 1446-1447.
- Szokalska, A., Makowski, M., Nowis, D., Wilczyński, G. M., Kujawa, M., Wójcik, C., Młynarczyk-Biały, I., Salwa, P., Bil, J., Janowska, S., Agostinis, P., et al. (2009). Proteasome inhibition potentiates antitumor effects of photodynamic therapy in mice through induction of ER stress and unfolded protein response. *Cancer Research*, 69, 4235-4243.
- Tabas, I., and Ron, D. (2011). Integrating the mechanisms of apoptosis induced by endoplasmic reticulum stress. *Nature Cell Biology*, 13, 184-190.

- Tajiri, H., Hayakawa, A., Matsumoto, Y., Yokoyama, I., and Yoshida, S. (1998). Changes in intracellular Ca<sup>2+</sup> concentrations related to PDT-induced apoptosis in photosensitized human cancer cells. *Cancer Letters*, *128*, 205-210.
- Takemura, T., Ohta, N., Nakajima, S., and Sakata, I. (1989). Critical importance of the triplet lifetime of photosensitizer in photodynamic therapy of tumor. *Photochemistry and Photobiology*, *50*, 339-344.
- Takeuchi, Y., Kurohane, K., Ichikawa, K., Yonezawa, S., Nango, M., and Oku, N. (2003). Induction of intensive tumor suppression by antiangiogenic photodynamic therapy using polycation - modified liposomal photosensitizer. *Cancer*, *97*, 2027-2034.
- Tan, P. J., Ong, C. Y., Danial, A., Yusof, H. M., Neoh, B. K., and Lee, H. B. (2011). Cyclic tetrapyrrolic photosensitisers from the leaves of *Phaeanthus ophthalmicus*. *Chemistry Central Journal*, *5*, 32.
- Tang, P. M.-K., Bui-Xuan, N.-H., Wong, C.-K., Fong, W.-P., and Fung, K.-P. (2010). Pheophorbide a-mediated photodynamic therapy triggers HLA class I-restricted antigen presentation in human hepatocellular carcinoma. *Translational Oncology*, *3*, 114-122.
- Tang, P. M.-K., Chan, J. Y.-W., Au, S. W.-N., Kong, S.-K., Tsui, S. K.-W., Waye, M. M.-Y., Mak, T. C.-W., Fong, W.-P., and Fung, K.-P. (2006). Pheophorbide a, an active compound isolated from *Scutellaria barbata*, possesses photodynamic activities by inducing apoptosis in human hepatocellular carcinoma. *Cancer Biology & Therapy*, *5*, 1111-1116.
- Tang, P. M.-K., Liu, X.-Z., Zhang, D.-M., Fong, W.-P., and Fung, K.-P. (2009a). Pheophorbide a based photodynamic therapy induces apoptosis via mitochondrial-mediated pathway in human uterine carcinosarcoma. *Cancer Biology & Therapy*, *8*, 533-539.
- Tang, P. M.-K., Zhang, D.-M., Xuan, N.-H. B., Tsui, S. K.-W., Waye, M. M.-Y., Kong, S.-K., Fong, W.-P., and Fung, K.-P. (2009b). Photodynamic therapy inhibits p-glycoprotein mediated multidrug resistance via JNK activation in human hepatocellular carcinoma using the photosensitizer pheophorbide a. *Molecular Cancer*, *8*, 56-68.
- Tannas, K. (2003). *Common plants of the western rangelands: Trees and shrubs* (Vol. 2). Edmonton, Canada: Alberta Agriculture, Food and Rural Development.
- Tatsuta, M., Yamamoto, R., Yamamura, H., Iishi, H., Noguchi, S., Ichii, M., and Okuda, S. (1984). Photodynamic effects of exposure to hematoporphyrin derivatives and dye-laser radiation on human gastric adenocarcinoma cells. *Journal of the National Cancer Institute*, *73*, 59-67.
- Teiten, M., Bezdetnaya, L., Morliere, P., Santus, R., and Guillemin, F. (2003a). Endoplasmic reticulum and Golgi apparatus are the preferential sites of Foscan® localisation in cultured tumour cells. *British Journal of Cancer*, *88*, 146-152.
- Teiten, M. H., Marchal, S., D'Hallewin, M., Guillemin, F., and Bezdetnaya, L. (2003b). Primary photodamage sites and mitochondrial events after Foscan® photosensitization of MCF - 7 human breast cancer cells. *Photochemistry and Photobiology*, *78*, 9-14.

- Thiers, R., Margoshers, M., and Vallee, B. (1959). Simple ultraviolet photometer. *Analytical Chemistry*, *31*, 1258-1261.
- Thomé, M. P., Filippi-Chiela, E. C., Villodre, E. S., Migliavaca, C. B., Onzi, G. R., Felipe, K. B., and Lenz, G. (2016). Ratiometric analysis of acridine orange staining in the study of acidic organelles and autophagy. *Journal of Cell Science*, *129*, 4622-4632.
- Tsai, P.-L., Zhao, C., Turner, E., and Schlieker, C. (2016). The Lamin B receptor is essential for cholesterol synthesis and perturbed by disease-causing mutations. *eLife*, *5*, 1-26.
- Uprety, Y., Asselin, H., Dhakal, A., and Julien, N. (2012). Traditional use of medicinal plants in the boreal forest of Canada: review and perspectives. *Journal of Ethnobiology and Ethnomedicine*, *8*, 7.
- Vasquez, R. J., Howell, B., Yvon, A., Wadsworth, P., and Cassimeris, L. (1997). Nanomolar concentrations of nocodazole alter microtubule dynamic instability in vivo and in vitro. *Molecular Biology of the Cell*, *8*, 973-985.
- Velázquez, A. P., and Graef, M. (2016). Autophagy regulation depends on ER homeostasis controlled by lipid droplets. *Autophagy*, *12*, 1409-1410.
- Venkatesan, T., Jeong, M.-J., Choi, Y.-W., Park, E.-J., El-Desouky, S. K., and Kim, Y.-K. (2016). Deoxyrhapontigenin, a natural stilbene derivative isolated from *Rheum undulatum* L. Induces endoplasmic reticulum stress-mediated apoptosis in human breast cancer cells. *Integrative Cancer Therapies*, *15*, 44-52.
- Verma, A., Facchina, S. L., Hirsch, D. J., Song, S.-Y., Dillahey, L. F., Williams, J. R., and Snyder, S. H. (1998). Photodynamic tumor therapy: mitochondrial benzodiazepine receptors as a therapeutic target. *Molecular Medicine*, *4*, 40-45.
- Villacorta, R. B., Roque, K. F. J., Tapang, G. A., and Jacinto, S. D. (2017). Plant extracts as natural photosensitizers in photodynamic therapy: in vitro activity against human mammary adenocarcinoma MCF-7 cells. *Asian Pacific Journal of Tropical Biomedicine*, *7*, 358-366.
- Walter, P., and Ron, D. (2011). The unfolded protein response: from stress pathway to homeostatic regulation. *Science*, *334*, 1081-1086.
- Wang, C., and Chen, T. (2012). Intratumoral injection of taxol in vivo suppresses A549 tumor showing cytoplasmic vacuolization. *Journal of Cellular Biochemistry*, *113*, 1397-1406.
- Wang, L., Gundelach, J. H., and Bram, R. J. (2017). Cycloheximide promotes paraptosis induced by inhibition of cyclophilins in glioblastoma multiforme. *Cell Death & Disease*, *8*, 1-11.
- Wang, Y., Li, X., Wang, L., Ding, P., Zhang, Y., Han, W., and Ma, D. (2004). An alternative form of paraptosis-like cell death, triggered by TAJ/TROY and enhanced by PDCD5 overexpression. *Journal of Cell Science*, *117*, 1525-1532.

- Wang, Y., Wei, Q., Yang, L., and Liu, Z.-L. (2003). Iridoid glucosides from Chinese herb *Lonicera chrysantha* and their antitumor activity. *Journal of Chemical Research*, 2003, 676-677.
- Wei, T., Kang, Q., Ma, B., Gao, S., Li, X., and Liu, Y. (2015). Activation of autophagy and paraptosis in retinal ganglion cells after retinal ischemia and reperfusion injury in rats. *Experimental and Therapeutic Medicine*, 9, 476-482.
- Whitehead, S. R., and Bowers, M. D. (2013). Iridoid and secoiridoid glycosides in a hybrid complex of bush honeysuckles (*Lonicera* spp., Caprifoliaceae): Implications for evolutionary ecology and invasion biology. *Phytochemistry*, 86, 57-63.
- Wilkinson, F., Helman, W. P., and Ross, A. B. (1995). Rate constants for the decay and reactions of the lowest electronically excited singlet state of molecular oxygen in solution. An expanded and revised compilation. *Journal of Physical and Chemical Reference Data*, 24, 663-677.
- Wink, M. (1993). The plant vacuole: a multifunctional compartment. *Journal of Experimental Botany*, 231-246.
- Wongsinkongman, P., Brossi, A., Wang, H.-K., Bastow, K. F., and Lee, K.-H. (2002). Antitumor agents. Part 209: Pheophorbide-a derivatives as photo-Independent cytotoxic agents. *Bioorganic & Medicinal Chemistry*, 10, 583-591.
- Woodburn, K., Vardaxis, N., Hill, J., Kaye, A., and Phillips, D. (1991). Subcellular localization of porphyrins using confocal laser scanning microscopy. *Photochemistry and Photobiology*, 54, 725-732.
- Wyld, L., Reed, M., and Brown, N. (2001). Differential cell death response to photodynamic therapy is dependent on dose and cell type. *British Journal of Cancer*, 84, 1384.
- Xodo, L., Rapozzi, V., Zacchigna, M., Drioli, S., and Zorzet, S. (2012). The chlorophyll catabolite pheophorbide a as a photosensitizer for the photodynamic therapy. *Current Medicinal Chemistry*, 19, 799-807.
- Xue, J., Li, R., Zhao, X., Ma, C., Lv, X., Liu, L., and Liu, P. (2018). Morusin induces paraptosis-like cell death through mitochondrial calcium overload and dysfunction in epithelial ovarian cancer. *Chemico-Biological Interactions*, 283, 59-74.
- Yang, L., Munck, M., Swaminathan, K., Kapinos, L. E., Noegel, A. A., and Neumann, S. (2013). Mutations in *lmna* modulate the laminin - nesprin-2 interaction and cause LINC complex alterations. *PLOS ONE*, 8, 1-12.
- Yeh, C.-J. G., Hsi, B.-L., and Faulk, W. P. (1981). Propidium iodide as a nuclear marker in immunofluorescence. II. Use with cellular identification and viability studies. *Journal of Immunological Methods*, 43, 269-275.

- Yoo, J.-O., Lee, C.-H., Hwang, B.-M., Kim, W. J., Kim, Y.-M., and Ha, K.-S. (2009). Regulation of intracellular Ca<sup>2+</sup> in the cytotoxic response to photodynamic therapy with a chlorin-based photosensitizer. *Journal of Porphyrins and Phthalocyanines*, *13*, 811-817.
- Yoon, H.-E., Oh, S.-H., Kim, S.-A., Yoon, J.-H., and Ahn, S.-G. (2014a). Pheophorbide a-mediated photodynamic therapy induces autophagy and apoptosis via the activation of MAPKs in human skin cancer cells. *Oncology Reports*, *31*, 137-144.
- Yoon, M., Kang, Y., Lee, J., Kim, I., Kim, M., Lee, Y., Park, J., Lee, B., Kim, I., and Kim, H. (2014b). Stronger proteasomal inhibition and higher CHOP induction are responsible for more effective induction of paraptosis by dimethoxycurcumin than curcumin. *Cell Death & Disease*, *5*, e1112.
- Yoon, M. J., Kim, E. H., Kwon, T. K., Park, S. A., and Choi, K. S. (2012). Simultaneous mitochondrial Ca<sup>2+</sup> overload and proteasomal inhibition are responsible for the induction of paraptosis in malignant breast cancer cells. *Cancer Letters*, *324*, 197-209.
- Yoon, M. J., Lee, A. R., Jeong, S. A., Kim, Y.-S., Kim, J. Y., Kwon, Y.-J., and Choi, K. S. (2014c). Release of Ca(2+) from the endoplasmic reticulum and its subsequent influx into mitochondria trigger celastrol-induced paraptosis in cancer cells. *Oncotarget*, *5*, 6816-6831.
- Yumnam, S., Hong, G. E., Raha, S., Saralamma, V. V. G., Lee, H. J., Lee, W. S., Kim, E. H., and Kim, G. S. (2016). Mitochondrial dysfunction and Ca<sup>2+</sup> overload contributes to hesperidin induced paraptosis in hepatoblastoma cells, HepG2. *Journal of Cellular Physiology*, *231*, 1261-1268.
- Yumnam, S., Hong Gyeong, E., Raha, S., Saralamma Venu Venkatarama, G., Lee Ho, J., Lee, W. S., Kim, E. H., and Kim Gon, S. (2015). Mitochondrial dysfunction and Ca<sup>2+</sup> overload contributes to hesperidin induced paraptosis in hepatoblastoma cells, HEPG2. *Journal of Cellular Physiology*, *231*, 1261-1268.
- Yung, H.-w., Korolchuk, S., Tolkovsky, A. M., Charnock-Jones, D. S., and Burton, G. J. (2007). Endoplasmic reticulum stress exacerbates ischemia-reperfusion-induced apoptosis through attenuation of Akt protein synthesis in human choriocarcinoma cells. *The FASEB Journal*, *21*, 872-884.
- Zheng, W., Thorne, N., and McKew, J. C. (2013). Phenotypic screens as a renewed approach for drug discovery. *Drug Discovery Today*, *18*, 1067-1073.
- Zheng, X., Morgan, J., Pandey, S. K., Chen, Y., Tracy, E., Baumann, H., Missert, J. R., Batt, C., Jackson, J., and Bellnier, D. A. (2009). Conjugation of 2-(1'-hexyloxyethyl)-2-devinylpyropheophorbide-a (HPPH) to carbohydrates changes its subcellular distribution and enhances photodynamic activity in vivo. *Journal of medicinal chemistry*, *52*, 4306-4318.
- Zigler, J., Lepe-Zuniga, J., Vistica, B., and Gery, I. (1985). Analysis of the cytotoxic effects of light-exposed HEPES-containing culture medium. *In Vitro Cellular & Developmental Biology*, *21*, 282-287.

Zupanska, A., Dziembowska, M., Ellert-Miklaszewska, A., Gaweda-Walerych, K., and Kaminska, B. (2005). Cyclosporine a induces growth arrest or programmed cell death of human glioma cells. *Neurochemistry International*, 47, 430-441.

Zwerger, M., Herrmann, H., Gaines, P., Olins, A. L., and Olins, D. E. (2008). Granulocytic nuclear differentiation of lamin B receptor-deficient mouse EPRO cells. *Experimental hematology*, 36, 977-987.

Zwerger, M., Kolb, T., Richter, K., Karakesisoglou, I., and Herrmann, H. (2010). Induction of a massive endoplasmic reticulum and perinuclear space expansion by expression of lamin B receptor mutants and the related sterol reductases TM7SF2 and DHCR7. *Molecular Biology of the Cell*, 21, 354-368.